UNIVERSITE DE LORRAINE
2015

FACULTE DE PHARMACIE

T H E S E

Présentée et soutenue publiquement

Le 02 octobre 2015, sur un sujet dédié à :

Apport de la nanotechnologie dans le domaine de l'antibiothérapie

pour obtenir

le Diplôme d'Etat de Docteur en Pharmacie

par
Roudayna DIAB
Née le 18 janvier 1977 au LIBAN

Membres du Jury

Président : Monsieur Bertrand RIHN, Professeur des Universités, Faculté de Pharmacie

Directeur de thèse : Monsieur Raphaël DUVAL, Professeur des Universités, Faculté de Pharmacie

Juges : Madame Andreea PASC, Maître de Conférences, Faculté des Sciences et Technologies
Madame Béatrice DEMORE, Maître de Conférences, Faculté de Pharmacie et Praticien Hospitalier, Centre Hospitalier Régional et Universitaire de Nancy
Madame Véronique MEYER, Pharmacien d'officine

UNIVERSITÉ DE LORRAINE
FACULTÉ DE PHARMACIE
Année universitaire 2014-2015

DOYEN
Francine PAULUS
Vice-Doyen
Béatrice FAIVRE
Directeur des Etudes
Virginie PICHON
Conseil de la Pédagogie
Président, Brigitte LEININGER-MULLER
Collège d'Enseignement Pharmaceutique Hospitalier
Président, Béatrice DEMORE
Commission Prospective Facultaire
Président, Christophe GANTZER
Vice-Président, Jean-Louis MERLIN
Commission de la Recherche
Président, Raphaël DUVAL

Responsable de la filière Officine	Béatrice FAIVRE
Responsables de la filière Industrie	Isabelle LARTAUD, Jean-Bernard REGNOUF de VAINS
Responsable de la filière Hôpital	Béatrice DEMORE
Responsable Pharma Plus ENSIC	Jean-Bernard REGNOUF de VAINS
Responsable Pharma Plus ENSAIA	Raphaël DUVAL
Responsable de la Communication	Marie-Paule SAUDER
Responsable de la Cellule de Formation Continue et individuelle	Béatrice FAIVRE
Responsable de la Commission d'agrément des maîtres de stage	Béatrice FAIVRE
Responsables des échanges internationaux	Bertrand RIHN
Responsable ERASMUS	Mihayl VARBANOV

DOYENS HONORAIRES

Chantal FINANCE
Claude VIGNERON

PROFESSEURS EMERITES

Jeffrey ATKINSON
Max HENRY
Gérard SIEST
Claude VIGNERON

PROFESSEURS HONORAIRES

Roger BONALY
Pierre DIXNEUF
Marie-Madeleine GALTEAU
Thérèse GIRARD
Michel JACQUE
Pierre LABRUDE
Lucien LALLOZ
Pierre LECTARD
Vincent LOPPINET
Marcel MIRJOLET
Maurice PIERFITTE
Janine SCHWARTZBROD
Louis SCHWARTZBROD

MAITRES DE CONFERENCES HONORAIRES

Monique ALBERT
Mariette BEAUD
Gérald CATAU
Jean-Claude CHEVIN
Jocelyne COLLOMB
Bernard DANGIEN
Marie-Claude FUZELLIER
Françoise HINZELIN
Marie-Hélène LIVERTOUX
Bernard MIGNOT
Jean-Louis MONAL
Blandine MOREAU
Dominique NOTTER

Christine PERDICAKIS

Marie-France POCHON

ASSISTANTS HONORAIRES

Anne ROVEL
Maria WELLMAN-ROUSSEAU

Marie-Catherine BERTHE
Annie PAVIS

ENSEIGNANTS	*Section CNU**	*Discipline d'enseignement*
PROFESSEURS DES UNIVERSITES - PRATICIENS HOSPITALIERS		
Danièle BENSOUSSAN-LEJZEROWICZ	*82*	*Thérapie cellulaire*
Chantal FINANCE	*82*	*Virologie, Immunologie*
Jean-Louis MERLIN	*82*	*Biologie cellulaire*
Alain NICOLAS	*80*	*Chimie analytique et Bromatologie*
Jean-Michel SIMON	*81*	*Economie de la santé, Législation pharmaceutique*
PROFESSEURS DES UNIVERSITES		
Jean-Claude BLOCK	*87*	*Santé publique*
Christine CAPDEVILLE-ATKINSON	*86*	*Pharmacologie*
Raphaël DUVAL	*87*	*Microbiologie clinique*
Béatrice FAIVRE	*87*	*Biologie cellulaire, Hématologie*
Luc FERRARI	*86*	*Toxicologie*
Pascale FRIANT-MICHEL	*85*	*Mathématiques, Physique*
Christophe GANTZER	*87*	*Microbiologie*
Frédéric JORAND	*87*	*Eau, Santé, Environnement*
Isabelle LARTAUD	*86*	*Pharmacologie*
Dominique LAURAIN-MATTAR	*86*	*Pharmacognosie*
Brigitte LEININGER-MULLER	*87*	*Biochimie*
Pierre LEROY	*85*	*Chimie physique*
Philippe MAINCENT	*85*	*Pharmacie galénique*
Alain MARSURA	*32*	*Chimie organique*
Patrick MENU	*86*	*Physiologie*
Jean-Bernard REGNOUF de VAINS	*86*	*Chimie thérapeutique*
Bertrand RIHN	*87*	*Biochimie, Biologie moléculaire*
MAITRES DE CONFÉRENCES DES UNIVERSITÉS - PRATICIENS HOSPITALIERS		
Béatrice DEMORE	*81*	*Pharmacie clinique*
Julien PERRIN	*82*	*Hématologie biologique*
Marie SOCHA	*81*	*Pharmacie clinique, thérapeutique et biotechnique*
Nathalie THILLY	*81*	*Santé publique*
MAITRES DE CONFÉRENCES		
Sandrine BANAS	*87*	*Parasitologie*
Xavier BELLANGER	*87*	*Parasitologie, Mycologie médicale*
Emmanuelle BENOIT	*86*	*Communication et Santé*
Isabelle BERTRAND	*87*	*Microbiologie*
Michel BOISBRUN	*86*	*Chimie thérapeutique*
François BONNEAUX	*86*	*Chimie thérapeutique*
Ariane BOUDIER	*85*	*Chimie Physique*
Cédric BOURA	*86*	*Physiologie*
Igor CLAROT	*85*	*Chimie analytique*
Joël COULON	*87*	*Biochimie*
Sébastien DADE	*85*	*Bio-informatique*
Dominique DECOLIN	*85*	*Chimie analytique*
Roudayna DIAB	*85*	*Pharmacie galénique*

Natacha DREUMONT	*87*	*Biochimie générale, Biochimie clinique*
Joël DUCOURNEAU	*85*	*Biophysique, Acoustique*

ENSEIGNANTS (suite)	*Section CNU**	*Discipline d'enseignement*
Florence DUMARCAY	*86*	*Chimie thérapeutique*
François DUPUIS	*86*	*Pharmacologie*
Adil FAIZ	*85*	*Biophysique, Acoustique*
Anthony GANDIN	*87*	*Mycologie, Botanique*
Caroline GAUCHER	*85/86*	*Chimie physique, Pharmacologie*
Stéphane GIBAUD	*86*	*Pharmacie clinique*
Thierry HUMBERT	*86*	*Chimie organique*
Olivier JOUBERT	*86*	*Toxicologie, Sécurité sanitaire*
Francine KEDZIEREWICZ	*85*	*Pharmacie galénique*
Alexandrine LAMBERT	*85*	*Informatique, Biostatistiques*
Julie LEONHARD	*86*	*Droit en Santé*
Faten MERHI-SOUSSI	*87*	*Hématologie*
Christophe MERLIN	*87*	*Microbiologie environnementale*
Maxime MOURER	*86*	*Chimie organique*
Coumba NDIAYE	*86*	*Epidémiologie et Santé publique*
Francine PAULUS	*85*	*Informatique*
Caroline PERRIN-SARRADO	*86*	*Pharmacologie*
Virginie PICHON	*85*	*Biophysique*
Sophie PINEL	*85*	*Informatique en Santé (e-santé)*
Anne SAPIN-MINET	*85*	*Pharmacie galénique*
Marie-Paule SAUDER	*87*	*Mycologie, Botanique*
Rosella SPINA	*86*	*Pharmacognosie*
Gabriel TROCKLE	*86*	*Pharmacologie*
Mihayl VARBANOV	*87*	*Immuno-Virologie*
Marie-Noëlle VAULTIER	*87*	*Mycologie, Botanique*
Emilie VELOT	*86*	*Physiologie-Physiopathologie humaines*
Mohamed ZAIOU	*87*	*Biochimie et Biologie moléculaire*
Colette ZINUTTI	*85*	*Pharmacie galénique*

PROFESSEUR ASSOCIE

Anne MAHEUT-BOSSER	*86*	*Sémiologie*

PROFESSEUR AGREGE

Christophe COCHAUD	*11*	*Anglais*

**<u>Disciplines du Conseil National des Universités</u> :*

80 : Personnels enseignants et hospitaliers de pharmacie en sciences physico-chimiques et ingénierie appliquée à la santé

81 : Personnels enseignants et hospitaliers de pharmacie en sciences du médicament et des autres produits de santé

82 : Personnels enseignants et hospitaliers de pharmacie en sciences biologiques, fondamentales et cliniques

85 ; Personnels enseignants-chercheurs de pharmacie en sciences physico-chimiques et ingénierie appliquée à la santé

86 : Personnels enseignants-chercheurs de pharmacie en sciences du médicament et des autres produits de santé

87 : Personnels enseignants-chercheurs de pharmacie en sciences biologiques, fondamentales et cliniques

32 : Personnel enseignant-chercheur de sciences en chimie organique, minérale, industrielle

11 : Professeur agrégé de lettres et sciences humaines en langues et littératures anglaises et anglo-saxonnes

SERMENT DES APOTHICAIRES

Je jure, en présence des maîtres de la Faculté, des conseillers de l'ordre des pharmaciens et de mes condisciples :

D' honorer ceux qui m'ont instruit dans les préceptes de mon art et de leur témoigner ma reconnaissance en restant fidèle à leur enseignement.

D'exercer, dans l'intérêt de la santé publique, ma profession avec conscience et de respecter non seulement la législation en vigueur, mais aussi les règles de l'honneur, de la probité et du désintéressement.

De ne jamais oublier ma responsabilité et mes devoirs envers le malade et sa dignité humaine ; en aucun cas, je ne consentirai à utiliser mes connaissances et mon état pour corrompre les mœurs et favoriser des actes criminels.

Que les hommes m'accordent leur estime si je suis fidèle à mes promesses.

Que je sois couvert d'opprobre et méprisé de mes confrères si j'y manque.

« LA FACULTE N'ENTEND DONNER AUCUNE APPROBATION, NI IMPROBATION AUX OPINIONS EMISES DANS LES THESES, CES OPINIONS DOIVENT ETRE CONSIDEREES COMME PROPRES A LEUR AUTEUR ».

Remerciements

À Monsieur Bertrand Rihn,
Je vous suis reconnaissante pour votre soutien, vos conseils et votre accueil. Veuillez trouver dans cet ouvrage le témoignage de mon respect et de ma gratitude.

À Monsieur Raphaël Duval,
Merci d'avoir accepté de diriger cette thèse et pour tous les échanges scientifiques que nous avons eus à travers les projets multidisciplinaires. Tu trouveras dans cet écrit toute ma gratitude et mon amitié.

À Madame Béatrice Démoré,
Merci d'avoir accepté de juger cette thèse, pour tes conseils pour le stage hospitalier et pour ta disponibilité. Tu trouveras dans ce manuscrit toute ma reconnaissance.

À Madame Andreea Pasc,
Merci d'avoir accepté de juger cette thèse malgré ton emploi du temps très chargé.
Merci pour ton accueil et ta bonne humeur.
Tu trouveras dans ce manuscrit toute mes plus sincères remerciements et mon amitié.

À Madame Véronique Meyer,
Merci d'avoir accepté de juger cette thèse. Soyez assurée de mon respect et ma gratitude.

À tous mes collègues enseignants-chercheurs, personnels administratifs et étudiants à la faculté de pharmacie,
Je vous adresse mes remerciements les plus sincères. Sans votre gentillesse et disponibilité, je n'aurais pas pu réussir cette expérience unique !

Table des matières

Liste des abréviations

Alginate lyase	AlgL
Aerodynamic diameter	AED
Alveolar macrophages	AM
Colony-forming units	CFU
Confocal laser scanning microscopy	CLSM
Cystic fibrosis	CF
Dichloromethane	DCM
Dimethyl sulfoxide	DMSO
Dimyristoylphosphatidylglycerol	DMPG
Dipalmitoyphosphatidylcholine	DPPC
Dipalmitoyphosphatidylglycerol	DPPG
Dioleylphosphatidylethanolamine	DOPE
Distearylphosphatidylethanolamine	DSPE
Encapsulation efficiency	EE
Ethidium bromide	EtBr
Ethylene diamine tetra-acetate	EDTA
Gram-negative bacteria	GNB
Gram-positive bacteria	GPB
Hexagonal II phase	HII
Hydrogenated soybean phosphatidylcholine	HSPC
Isosorbide mononitrate	ISMN
Lipopolysaccharides	LPS
Lipoteichoic acids	LTA
Mass median aerodynamic diameter	MMAD
Mesoporous silica nanoparticles	MSN
Methicillin-resistant *Staphylococcus aureus*	MRSA
Microspheres	MS
Minimum bactericidal concentration	MBC
Minimum inhibitory concentration	MIC
Multi-drug resistance	MDR
Multilamellar vesicles	MLV
Nanoparticles (nanoparticules)	NP
Nile Red	NR
Oil/water	O/W
Oleoyl chitosan nanoparticles	OCNP
Phosphatidic acid	PA
Phosphatidylcholine	PC
Phosphatidylethanolamine	PE
Phosphatidylglycerol	PG
Phosphatidylinositol	PI

Phosphatidylserine	PS
Polydispersity index	PDI
Polyethylene glycol	PEG
Polylactic acid	PLA
Poly(lactide-co-glycolide) acid	PLGA
Polyvinyl alcohol	PVA
Nitric oxide	NO
Quaternary ammonium compounds	QAC
Reactive nitrogen species	RNS
Reactive oxygen species	ROS
Rifampicin	RIF
Stearylamine	SA
Sterically stabilized anionic liposomes	SSAL
Sterically stabilized cationic liposomes	SSCL
Sterically-stabilized liposomes	SSL
Solid lipid nanoparticles	SLN
S-nitrosoglutathione	GSNO
Teichoic acids	TA
Transmission electron microscopy	TEM
Vancomycin	Van
zinc oxide nanoparticles	ZnO-NP

Introduction générale

La chimiothérapie des maladies infectieuses a révolutionné le 20ème siècle. Des millions de vies humaines ont été épargnées grâce aux antibiotiques. Toutefois, ces derniers semblent être les victimes de leur propre succès. L'utilisation massive des antibiotiques dans le monde a engendré une pression de sélection, ce qui a favorisé l'apparition des souches résistantes au traitement.

Le besoin de renouveler l'arsenal thérapeutique croît sans cesse. Grâce à la chimie organique, de nouvelles molécules actives contre les bactéries multi-résistantes voient le jour, avec la crainte d'apparition prochaine de souches résistantes.

Les cliniciens tentent de trouver une issue à cette impasse en proposant des associations non conventionnelles d'antibiotiques. Ces nouvelles associations visent à élargir le spectre thérapeutique et/ou de contourner la résistance bactérienne. La réintroduction d'anciennes molécules, jadis abandonnées en raison de leur toxicité sévère, telles que la colistine et le chloramphénicol, constitue parfois l'option clinique de dernier recours pour traiter les infections récalcitrantes.

Le développement de vecteurs non viraux capables de piloter l'antibiotique et de franchir les barrières biologiques bactériennes ou celles de l'hôte, est une approche qui séduit de plus en plus de chercheurs dans le monde. Le premier avantage est que cette approche peut intégrer toutes les autres stratégies proposées jusque-là pour combattre la résistance bactérienne, comme nous le schématisons dans la figure 1.

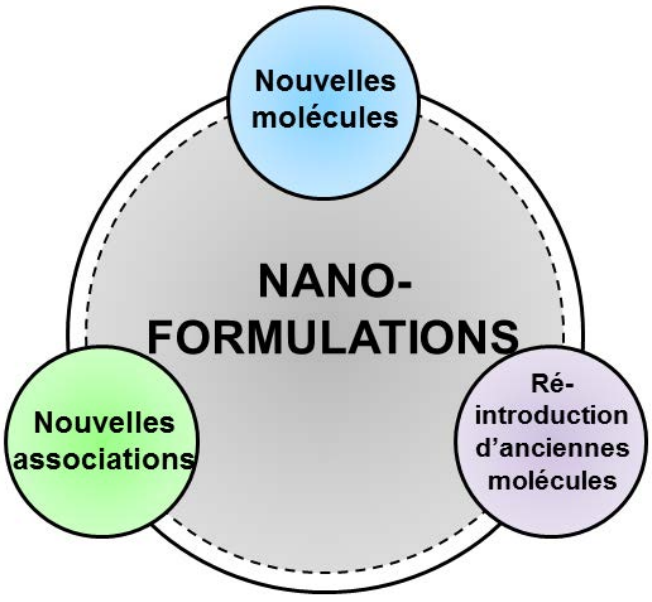

Figure 1. Les principales stratégies connues à ce jour visant à combattre la résistance bactérienne aux antibiotiques.

Les nouvelles molécules issues de la synthèse organique peuvent être nanoencapsulées dans le but de corriger les caractéristiques physico-chimiques non favorables à une administration

optimale, telles que la faible solubilité aqueuse et/ou la faible stabilité, qui constituent des obstacles majeurs à leur développement comme futurs médicaments.

La nanotechnologie offre aussi la possibilité de co-formuler deux ou plusieurs molécules dans le même vecteur et les dresser contre une cible commune. De plus, les anciennes molécules retirées du marché en raison de leur toxicité sévère, peuvent être vectorisées dans le but de limiter leur action hors cible. Autrement dit, la nanotechnologie permet de diminuer considérablement la toxicité d'antibiotiques en ciblant principalement l'organe, le tissue ou les cellules infectées.

Le second grand avantage de la vectorisation d'antibiotiques est que les vecteurs peuvent être conçus de façon à produire une cinétique de libération qui s'accorde avec la pharmacodynamie de l'antibiotique encapsulé. Ainsi, les antibiotiques dont l'activité est temps-dépendante, peuvent être formulés dans des particules à profil de libération prolongée ; tandis que les nanoparticules permettant une libération contrôlée et, si possible, sélective de la cible seront mieux adaptées aux antibiotiques dont l'activité est dose-dépendante. Ce point est traité en détails dans le chapitre 1, section 4.2.

Le troisième avantage se traduit par l'interaction spécifique nanoparticule-bactérie. Une fois maîtrisée, cette interaction apporterait une solution radicale à la résistance bactérienne au traitement. C'est pourquoi, le premier chapitre de ce manuscrit est dédié à l'analyse de ces interactions.

Dans cette thèse, nous avons associé recherche bibliographique et travail expérimental pour aborder quelques aspects de l'apport important de la nanotechnologie dans le domaine de l'antibiothérapie. Ainsi, le premier chapitre constitue une synthèse de 98 articles scientifiques traitant l'encapsulation d'antibiotiques dans des vecteurs non viraux, leurs mécanismes d'interactions avec les bactéries et leurs modes d'action pour contourner la résistance bactérienne.

Les deuxième et troisième chapitres présentent des travaux originaux de vectorisation d'antibiotiques. Le deuxième chapitre présente, donc, l'élaboration des nanoliposomes chargés en une nouvelle molécule avec potentiel anti-infectieux, le *S*-nitrosoglutathion (GSNO), un donneur endogène de l'oxyde nitrique, comme une nouvelle thérapeutique antibactérienne. L'objectif principal de l'encapsulation est de réaliser une libération sélective du GSNO dans les macrophages afin de renforcer ses capacités de défense, surtout dans le cas des infections causées par des bactéries multi-résistantes. Gardons à l'esprit que la libération non contrôlée de l'oxyde nitrique peut être néfaste, vu son fort potentiel pro-inflammatoire.
Le troisième et dernier chapitre de ce manuscrit traite la microencapsulation d'un antituberculeux commercialisé depuis plusieurs années, la rifampicine. Cette fois-ci, l'objectif est de cibler les macrophages, siège de l'infection intracellulaire causée par les mycobactéries, mais aussi de formuler une poudre pour inhalation permettant une administration pulmonaire de la rifampicine ; une forme galénique de la rifampicine qui n'existe pas sur le marché et qui n'est pourtant pas sans intérêts directs.

Chapitre 1

Interactions nanoparticule-bactérie: de nouveaux horizons pour combattre la résistance aux antibiotiques

"Insights in Nanoparticle- Bacterium interactions: New Frontiers to Bypass Bacterial Resistance to Antibiotics"

Ce chapitre est rédigé sous forme d'une revue de la littérature scientifique, actuellement sous presse dans le journal « *Current Pharmaceutical Design* ».

Current Pharmaceutical Design, 2015, *21*, 000-000 1

Insights in Nanoparticle-Bacterium Interactions: New Frontiers to Bypass Bacterial Resistance to Antibiotics

R. Diab[a,b]†, B. Khameneh[c], O. Joubert[d] and R.E. Duval[a,b,e]

[a]*CNRS, UMR 7565, SRSMC, Vandœuvre-lès-Nancy, F-54506, France;* [b]*Université de Lorraine, UMR 7565, SRSMC, Nancy, F-54001, France;* [c]*Department of Food and Drug Control, Students Research Committee, Mashhad University of Medical Sciences, Mashhad, Iran;* [d]*Université de Lorraine, CITHEFOR, EA 3452, Faculté de Pharmacie, Nancy, France;* [e]*ABC Platform®, Nancy, F-54001, France*

Abstract: Nanotechnology has been revealed as a fundamental approach for antibiotics delivery. In this paper, recent findings demonstrating the superiority of nanocarried-antibiotics over "naked" ones and the ways by which nanoparticles can help to overwhelm bacterial drug resistance are reviewed. The second part of this paper sheds light on nanoparticle-bacterium interaction patterns. Finally, key factors affecting the effectiveness of nanoparticles interactions with bacteria are discussed.

Keywords: Antibiotic, controlled-release, liposome, nanoparticle, resistance, targeting.

Cette revue est une tentative de répondre à la première question posée dans cette thèse : comment la nanotechnologie peut-elle améliorer l'activité antibactérienne des antibiotiques voire contourner la résistance bactérienne ?

Les différentes facettes des antibiotiques nano-encapsulés sont, donc, présentées à travers de récents travaux de recherche, à savoir : le pouvoir pénétrant à travers les biofilms bactériens (Meers *et al.*,2008) ; (Alipour *et al.*,2008) ; la stabilité face aux attaques enzymatiques (Alipour *et al.*,2009) ; (Wright,2005) ; la capacité d'agir sur les bactéries intracellulaires confinées dans les macrophages (Abed &Couvreur,2014) ; le ciblage d'organes voire de tissus qui a permis d'améliorer considérablement la tolérance de l'hôte aux antibiotiques (Xiong *et al.*,2014). De plus, certains types de nanoparticules, comme les nanoparticules inorganiques (Pati *et al.*,2014), ont une action bactéricide intrinsèque pour laquelle aucune forme de résistance n'est connue à ce jour.

En outre, la nanoencapsulation permet d'associer les antibiotiques dans le même vecteur dans le but d'obtenir une action synergique. Cette stratégie a montré une capacité à déjouer la résistance bactérienne en inhibant la pompe d'efflux de la paroi bactérienne, comme il a été démontré pour les nanoliposomes contenant la pipérine (Khameneh *et al.*,2015) ; ou alors en inhibant la formation des biofilms et/ou en éradiquant les biofilms déjà formés, comme c'est le cas des nanoparticules libérant l'oxyde nitrique (Jardeleza *et al.*,2011).

Malheureusement, la nano- et la micro-encapsulation des antibiotiques sont réalisées *via* des procédés qui s'avèrent plus ou moins efficaces en fonction du type d'antibiotique et du type du vecteur visé. Il est évident que l'efficacité d'encapsulation affecte directement l'activité bactérienne du vecteur ainsi conçu.

Il est important de noter que l'encapsulation s'est montrée, parfois, néfaste quant à l'activité de l'antibiotique encapsulé, surtout pour ceux qui agissent sur la membrane bactérienne. A titre d'exemple, le méropénème encapsulé dans des Fluidosomes® a montré une diminution de

son activité antibactérienne de 4 à 16 fois, sur les différentes souches bactériennes testées (Drulis-Kawa *et al.*,2006).

Toutes ces remarques conduisent à la deuxième grande question posée dans cette thèse : quelles sont donc les mécanismes d'interactions entre les trois acteurs, à savoir, l'antibiotique, le vecteur et la bactérie ? Et, quelles sont les facteurs qui régissent ces interactions ?

Afin de répondre à ces questions, une analyse des données de la littérature a été réalisée et constitue la deuxième partie de la revue. La figure 2 présente un aperçu général des facteurs régissant les interactions nanoparticule-bactérie. La compréhension des interactions qui s'opèrent entre la bactérie, la nanoparticule et l'antibiotique encapsulée permettrait, sans doute, de guider le choix de vecteurs et de formulation en fonction de l'antibiotique et du type de la bactérie visée.

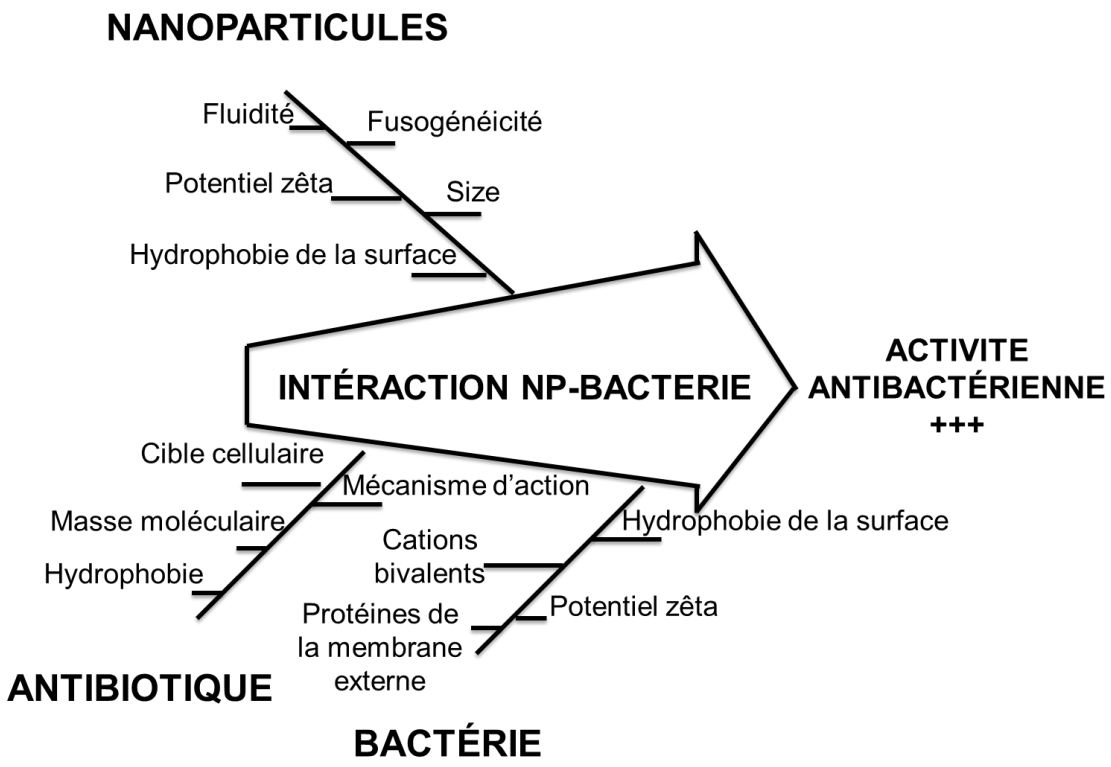

Figure 2. Les principaux facteurs régissant les interactions nanoparticule-bactérie, présentés sous forme d'un diagramme d'Ishikawa.

Insights in nanoparticle- bacterium interactions: new frontiers to bypass bacterial resistance to antibiotics

R. Diab[a,b]†, B. Khameneh[c], O. Joubert[d] and R.E. Duval[a,b,e]

[a] *CNRS, UMR 7565, SRSMC, Vandœuvre-lès-Nancy, F-54506, France*
[b] *Université de Lorraine, UMR 7565, SRSMC, Nancy, F-54001, France*
[c] *Department of Food and Drug Control, Students Research Committee, Mashhad University of Medical Sciences, Mashhad, Iran*
[d] *Université de Lorraine, CITHEFOR, EA 3452, Faculté de Pharmacie, Nancy, France*
[e] *ABC Platform®, Nancy, F-54001, France*

† To whom correspondence should be directed

Dr. Roudayna Diab

SRSMC, UMR 7565, CNRS-Université de Lorraine,
Faculté de Pharmacie, Université de Lorraine
5, rue Albert Lebrun, BP 80403
54001 Nancy Cedex
France
Tel +33 3 83 68 22 74
Fax +33 3 83 68 23 01
E. mail: roudayna.diab@univ-lorraine.fr

A b s t r a c t
Nanotechnology has been revealed as a fundamental approach for antibiotics delivery. In this paper, recent findings demonstrating the superiority of nanocarried-antibiotics over "naked" ones and the ways by which nanoparticles can help to overwhelm bacterial drug resistance are reviewed. The second part of this paper sheds light on nanoparticle-bacterium interaction patterns. Finally, key factors affecting the effectiveness of nanoparticles interactions with bacteria are discussed.

Key words*: antibiotic, controlled-release, liposome, nanoparticle, resistance, targeting.*

1 . I n t r o d u c t i o n

Antibiotics, drugs that saved millions of lives in the twentieth century, seem to be of a decreasing efficacy nowadays. Recalcitrant infections threaten people lives, inflicting heavy burdens on the society. Common solutions are: developing new molecules [1]; [2]; re-introducing some abundant molecules [3]; using plant polyphenolic compounds [4], etc. Unfortunately, in the long run, all of these solutions could have lesser or even null efficacy because of the emergence of resistant strains. Today, there is a growing need of a radical approach enabling to short-circuit the bacterial resistance. This approach is supposed to help antibiotics to bypass the multiples bacterial barriers in order to reach their therapeutic targets.
Barriers could mainly be summarized by bacterial biofilms, cell walls and destructive enzymes (Fig. 1). The viscous mucus surrounding the bacterial foci could also be considered as an additional barrier.
Generally speaking, antibiotics are ineffective against biofilms due to their inability to cross such a complex matrix. Biofilms are composed of a wide variety of extracellular biopolymers such as polysaccharides, proteins, glycoproteins and glycolipids and in some cases they contain amounts of extracellular DNA [5]. Besides, biofilms shelter bacterial cells called "persisters" that represent the most resistant phenotype [6]. Bacteria embedded in biofilms are characterized by a slow metabolism which reinforces their resistance against antibiotics, especially those acting by inhibiting cell wall or protein synthesis [6]. In addition, in biofilms the hypoxic and acidic environment may deactivate pH-sensitive antibiotics [7].
Bacterial cell wall is another obstacle to the effective delivery of antibiotics, owing to its electrical charge and special architecture. Both Gram-negative (GNB) and Gram-positive bacteria (GPB) are negatively-charged. Their wall contains several anionic components, such as teichoic (TA), lipoteichoic acids (LTA) (in GPB), lipopolysaccharides (LPS) (in GNB), peptidoglycan layers and phospholipids (in both types). Therefore, permeation of anionic antibiotics, *e.g.* β-lactams, across the bacterial wall in both types would be restricted [8].
Moreover, with regard to the wall architecture, GPB's wall is simply composed of an outer hydrophilic thick layer of peptidoglycan covered by TA and LTA, and a cytoplasmic membrane [9]. On the other hand, GNB have a complex wall organized in outer lipophilic layer mainly composed of LPS and proteins, followed by an aqueous periplasmic space and then by an internal peptidoglycan wall that directly covers the cytoplasmic membrane [9].
The GNB wall's outer membrane is crossed by tiny aqueous channels called porins enabling small hydrophilic molecules to permeate. Consistently, porins characteristics such as size, structure and expression level considerably affect the antibacterial spectrum of hydrophilic

antibiotics [10]. This can explain, in part, why GNB are intrinsically resistant to hydrophilic antibiotics of high molecular weight, *e.g.* glycopeptides, which are only effective against GPB [10]; [11].

Furthermore, the enzymatic barrier represented by a number of virulence factors produced by opportunistic bacteria jeopardizes antibiotic effectiveness. *Pseudomonas aeruginosa, Staphylococcus aureus* and *Escherichia coli* have all the enzymatic weapons causing damage to both administered antibiotics and host cells [12]. For instance, *P. aeruginosa* produces a myriad of enzymes, such as elastase, chitinase, lipase, and proteases, that are destructive for host tissues; in addition to metallo-β-lactamases and aminoglycoside acetyltransferase that can deactivate the most effective antibiotics [13]; [14]; [15].

In some contexts, the situation could be more complex. For instance in cystic fibrosis (CF), the, abundantly secreted viscous mucus creates an additional physico-chemical barrier to antibiotics. This mucus contains abnormally high concentrations of neutrophil-derived DNA and filamentous actin, which are produced as a result of the inflammatory response to bacterial virulence factors. These former interact with glycoproteins, *e.g.* mucin, resulting in viscous sputa covering the epithelial surface, and thus favoring the bacterial adherence and subsequently biofilm production [16].

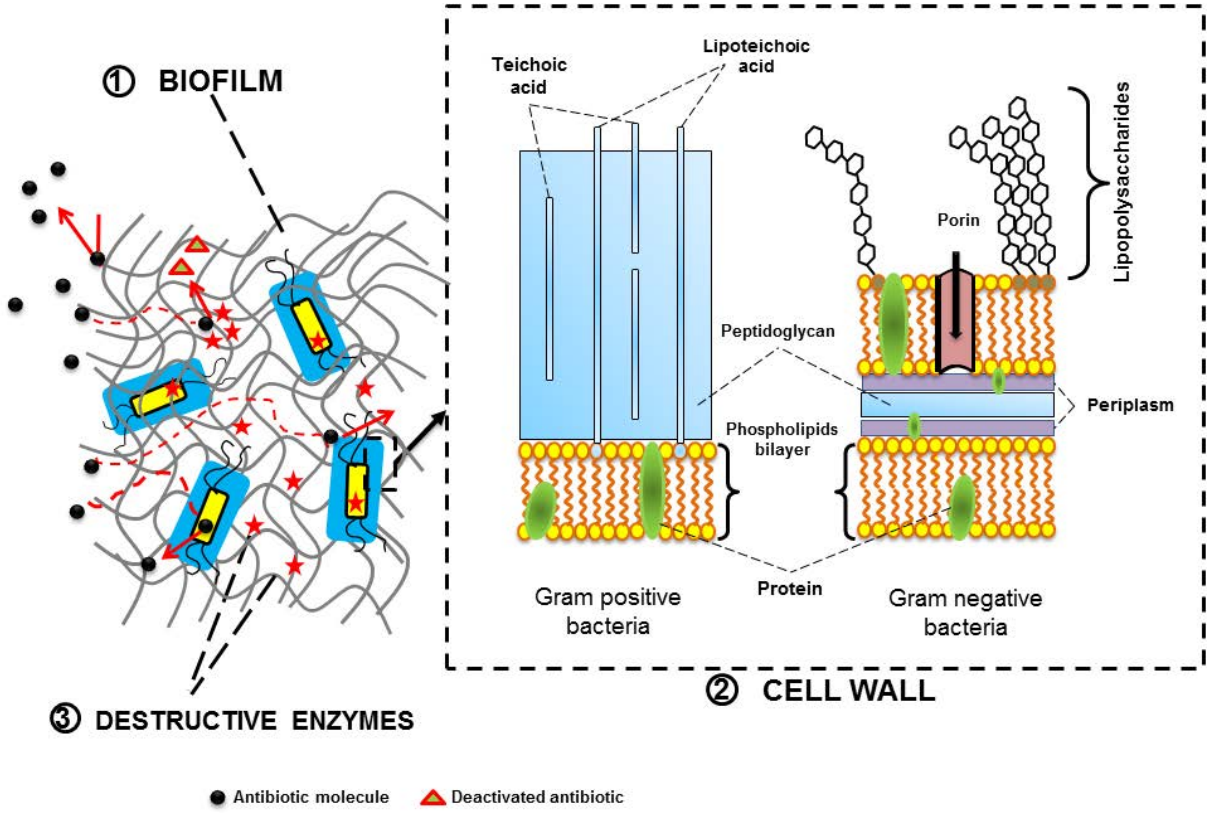

Fig. 1. The main potential barriers to antibiotic delivery.

Nanotechnology has been revealed as a fundamental approach for antibiotics delivery allowing the above mentioned barriers to be overcome. In this paper, recent findings pointing out the superiority of nanocarried-antibiotics over "naked" ones and the ways by which nanoparticles (NP) can help to overwhelm bacterial drug resistance are reviewed. The second part of this paper sheds light on NP-bacterium interaction patterns. Finally, key factors affecting the effectiveness of NP interaction with bacteria are discussed.

2. How can nanoparticles help to bypass bacterial drug resistance?

All over the world, researchers developed different nanotechnology- based approaches with the aim to overcome the currently-known bacterial resistance mechanisms to antibiotics. Some revealed promising findings and led to clinical trials. Today, several "nano-antibiotics" are clinically-approved for human use. For instance, **AX-Tobra™** is an inhalable liposomal tobramycin based on Fluidosomes® technology, claimed for the treatment of *Pseudomonas aeruginosa* pulmonary infections in cystic fibrosis. It is developed and commercialized by Axentis pharma (Zurich, Swizerland). **Pulmaquin™** and **Lipoquin™** are two inhalable liposomal dosage forms of ciprofloxacin for the treatment of serious infectious diseases encountered in cystic fibrosis or in non-cystic fibrosis bronchiectasis. They are developed and commercialized by Grifols, S.A. and Aradigm Corporation (Hayward, CA, USA). These novel formulations were recently reviewed and discussed in details [17]; [18]. **Arikace®** is an inhaled liposomal dosage form of amikacin developed for the treatment of cystic fibrosis-associated pulmonary infections caused by *P. aeruginosa* [19]. Now, it is undergoing phase III clinical trials.

Numerous approaches are still under investigation. They are reviewed hereafter.

2.1. Alteration of bacteria's efflux pump activity

In this regard, recently-reported advances could be mentioned. Khameneh *et al.* developed piperine-containing nanoliposomes as a vector for gentamicin. The liposomal formulation was specifically developed to fight methicillin-resistant *Staphylococcus aureus* (MRSA), an antibiotic-resistant bacteria which is widely recognized as a nosocomial pathogen [20].

The encapsulation of gentamicin in classical nanoliposomes or piperine-containing nanoliposomes resulted in a dramatic decrease of minimum inhibitory concentration (MIC) values of 16- and 32 folds, respectively. Similarly, minimum bactericidal concentration (MBC) values were also reduced 4- and 8- folds for encapsulated gentamicin in classical nanoliposomes or piperine-containing nanoliposomes, respectively. These hopeful results were attributed to the piperine inhibiting effect on the bacterial efflux pump. This argument was confirmed using ethidium bromide (EtBr) fluorescence assay. The fluorescence of this compound occurs only when it is bound to nucleic acid. Accordingly, bacterial suspension was incubated with EtBr for 30 min in the presence of: i) bare nanoliposomes (without piperine), ii) piperine-containing nanoliposomes or iii) piperine in its free form. After centrifugation and washing of bacteria, the loss of fluorescence was checked in order to investigate the efflux of EtBr outside bacterial cells. Consistently, a gradual decrease of fluorescence during the assay period was observed in the first case, *i.e.* in the absence of piperine. However, in the presence of piperine the fluorescence was significantly enhanced indicating a significant inhibition of the efflux pump [20]. Therefore, the enhanced antibacterial activity of gentamicin encapsulated in piperine-containing nanoliposomes is likely to be the consequence of an increase in its intracellular concentration. It is of note that piperine in its free form was less effective in inhibiting the efflux pump than the liposomal one, as demonstrated by the EtBr fluorescence assay.

2.2. Antibiofilm activity

Nitric oxide (NO)-releasing NP were found to prevent the formation of bacterial biofilms and to eradicate already formed biofilms. Some examples of recent breakthroughs in this domain are presented hereafter.

Jardeleza *et al.* encapsulated isosorbide mononitrate (ISMN), as NO donor into different liposomal formulations with the purpose to enhance the antibiofilm activity against *Staphylococcus aureus*'s biofilms [21]. NO-releasing multilamellar vesicles (MLV) efficiently eliminated *S. aureus*'s biofilms *in vitro*. A five min-exposure to 60 mg/mL ISMN-loaded MLV induced an almost complete eradication of the biofilms. Paradoxically, the authors observed that at low concentrations NO-releasing MLV enhanced the formation of biofilms, which is in accordance with previously obtained results [22].

Duong *et al.* developed nanoparticulate NO-core cross-linked star polymers as new therapeutics able to combating biofilms that are frequently formed during long exposure of the body to medical devices and catheters [23]. These systems were found to release NO in a controlled and slowed-down manner in bacterial cultures and showed great efficacy in preventing both cell attachment and biofilm formation in *P. aeruginosa* over time. This study unveiled, in part, the inherent mechanisms of NO's antibiofilm activity. Accordingly, NO-releasing NP inhibit the switch of planktonic cells in contact with a surface to the biofilm form by continuously stimulating phosphodiesterase activity. Thus, NO-releasing NP maintained low intracellular concentrations of cyclic di-guanosine monophosphate (c-di-GMP) in the growing bacterial population, thereby confining growth to an unattached free-swimming mode [23].

The dual delivery of two antibiotics *via* their co-encapsulation in nanoliposomes is another proposed strategy to bypass resistance mediated by biofilm formation. For instance, Moghadas-Sharif proposed vancomycin/rifampin-co-loaded nanoliposomes as a new therapeutic against *Staphylococcus epidermidis* [24]. This strategy was based on two points. First, combination therapy of vancomycin and rifampicin helps avoid the emergence of rifampin-resistant strains. Indeed, numerous studies have already reported the antibiofilm activities of rifampin in combinations with other antibiotics [25]; [26]; [27]. Second, rifampicin fails alone to eradicate bacterial biofilm [28]. Nevertheless, the developed liposomal combination was ineffective to eradicate *S. epidermidis*'s biofilm. The authors attributed this result to the lack of liposomal adsorption or low penetration into the bacterial biofilm [24]. A more adjusted formulation with enhanced penetration behavior into the biofilm may lead to the initially expected effect.

2.3. Enhanced penetration through biofilms

Several research papers reported the improved penetration across bacterial biofilms as a plausible reason behind the enhanced antibacterial activity of encapsulated antibiotics against resistant bacteria. For instance, liposomal encapsulation of polymyxin B was first described by Alipour and co-authors as a strategy to enhance its antibacterial activity against *P. aeruginosa* resistant strains [29]. As they expected, lower MIC values were observed for liposomal formulations with respect to that of the free drug. In an attempt to elucidate the involved mechanisms, the researchers focused on the drug uptake and more precisely on its

penetration across the biofilm formed by the polymyxin B-resistant *P. aeruginosa* strain. They used a coupled immunocytochemistry-transmission electron microscopy (TEM) imaging technique. Accordingly, a clinical strain of *P. aeruginosa* resistant to polymyxin B was incubated either with free or liposomal polymyxin B at sub-MIC concentrations (*i.e.* 64 and 16 µg/mL, respectively). Untreated bacteria were used as control. Penetration efficiency into biofilms was checked at predetermined intervals of 0, 4, 8 and 16 h at 37°C. TEM studies showed that the uptake of polymyxin B-loaded liposomes by the resistant strain was higher than that of the free drug [29]. It is important to mention that the treatment with both free drug and empty liposomes did not display a superior effectiveness with regard to the free drug indicating that the enhanced activity can only be attributed to the entrapped form.

Furthermore, the superiority of liposomal aminoglycosides was demonstrated on *in vivo* chronic *Pseudomonas* infection model [30]. Consistently, mucoid *P. aeruginosa*-containing agar beads were instilled intratracheally to Sprague-Dawley female rats. After the establishment of infection, animals were treated by inhalation over 14 days. Two treatment regimens were used; tri-weekly dosing schedule with free or liposomal amikacin at 6 mg/kg per dose and compared with the classical aminoglycoside regimen, *i.e.* a twice daily dosing of free tobramycin at the same dose (6 mg/kg/day). Finally, animals were killed and lungs were homogenized. Homogenates were subsequently cultured on agar plates. Then, colony-forming units (CFU) were counted in order to assess the effectiveness of the treatment. The researchers found that "free amikacin was relatively ineffective in the reduction of CFU under these conditions, while bacteria were undetectable in a large proportion of the group treated with liposomal amikacin" [30]. Interestingly, the thrice-weekly treatment with the liposomal amikacin was as effective as the twice-daily treatment with free tobramycin. Although, tobramycin showed a lower MIC value than amikacin against the planktonic form of *P. aeruginosa* [30]. The authors explained the observed enhanced effectiveness of liposomal amikacin by the enhanced penetration through biofilm and by the drug sustained-release pattern. The researchers have demonstrated the drug sustained-release profile from liposomes in CF-patients 'sputa [30]. They also checked biofilm penetration on *in vitro* 4 days- grown biofilms produced by a mucoid form of PA01, prepared using rat lung models with chronic infections. For this aim, fluorescently-labeled liposomal amikacin was used and biofilm penetration was imaged by confocal laser scanning microscopy (CLSM) [30].

2.4. Protection against enzymatic degradation and inactivation by polyanionic compounds

Nanoparticulate delivery systems provide a physical barrier shielding the entrapped antibiotic from aggregation and inactivation with polyanionic compounds, such as bacterial endotoxins *e.g.* LPS and LTA. Additionally, encapsulation may protect antibiotics against enzymatic degradation by β-lactamases, macrolide esterases and other bacterial enzymes [31].

Two decades ago, Lagacé *et al.* demonstrated that liposomal encapsulation of ticarcillin or tobramycin reverse the resistance of *P. aeruginosa* strains towards these both antibiotics [32]. Growth inhibition of ticarcillin- and tobramycin- resistant strains was achieved using ticarcillin and tobramycin liposomal formulations at 2 % and 20 % of their respective MIC. Liposomal formulations were as effective against the β-lactamase -producing strains as β-lactamase -non producing ones.

Recently, Alipour *et al.* demonstrated the versatility of liposomal encapsulation in protecting tobramycin or polymyxin B from inhibition by LPS, LTA, neutrophil-derived DNA, actin filaments (F-actin) and glycoproteins *e.g.* mucin, common components in the CF-patients 'sputa [33]. Being polycationic, tobramycin and polymyxin B can bind to these polyanionic compounds and thereby have their bioactivity reduced. The authors postulated that "liposomes are able to reduce the antibiotic contact with polyanionic factors in the sputum and to enhance bacteria-antibiotic interactions" [33]. *In vitro* stability studies revealed that liposomal formulations were stable after an 18 h-incubation at 37°C with i) a supernatant of biofilm-forming *P. aeruginosa*, ii) a combination of DNA, F-actin, LPS and LTA or iii) an intact or an autoclaved patient's sputum. No significant differences with respect to control (before incubation) were observed. Furthermore, the antibacterial potency of liposomal antibiotics were checked after both short (3 h) and prolonged (18 h) exposure to a combination of DNA/F-actin or LPS/LTA at different concentrations. It was found that for both free and liposomal drugs the antibioactivity was reduced in a concentration-dependent manner. However, much higher concentrations (100 to 1000 mg/L) and (500 to 100 mg/L) of LPS/LTA and DNA/F-actin, respectively, were needed to inhibit liposomal forms in comparison to free drugs. The authors explained this finding by the increased viscoelasticity induced by the high concentrations of polyanionic elements that may hinder the interaction of liposomes with bacteria. Indeed, the early leakage of antibiotics from liposomes cannot be used as a plausible cause of the inactivation of liposomal antibiotic because *in vitro* stability studies showed that liposomal vesicles were not disrupted [33].

To further confirm the superiority of liposomal forms, the authors studied the bactericidal activity of liposomal formulations *versus* free forms against *P. aeruginosa* found in CF-patients' sputa. The antibacterial activities of liposomal formulations were 4-fold higher when compared to the free drugs, despite the presence of different bacterial strains in the patient's sputum. It is of note that liposomal tobramycin reduced growth at a high concentration (128 mg/L), whereas liposomal polymyxin B did it at a markedly lower concentration (8 mg/L). The dissimilar activities of tobramycin and polymyxin B was attributed to their different sites of action. The different behaviors of liposomal formulations as a function of the encapsulated drug will be discussed thoroughly in the following sections of this review.

The same research group conducted a meticulously detailed study confirming the inhibiting effect of the polyanionic compounds in CF-patients 'sputa, *i.e.* neutrophil-derived DNA, mucoid *P. aeruginosa*-produced alginates and mucins, on the antibacterial activities of free and liposomal aminoglycosides [34]. It was found that bactericidal concentrations of aminoglycosides were increased by 8- to 256-folds against biofilm-forming strain, while the treatment with alginate lyase (AlgL) improved the eradication of this latter. The activity of the tested aminoglycosides, *i.e.* tobramycin, gentamicin and amikacin, was significantly increased by the concomitant use of recombinant human DNase or AlgL. However, liposomal antibiotic formulations did not display an additional effectiveness with respect to the free drugs, unless used in combination with AlgL.

These non-conclusive results could be explained by the fact that the authors compared free and liposomal antibiotics at high concentration (512 mg/L). Very often, the superiority of the liposomal formulation over the free form was easier to be demonstrated at low tested

concentrations, *i.e.* 1 mg/L for liposomal amikacin [30], 8 mg/L for liposomal tobramycin [35], 1.7 mg/L for liposomal mupirocin [36].

2.5. Intracellular bacterial killing

Obviously, the intracellular location reinforces bacterial resistance as it shields them from both humoral and cellular host defenses and also from the action of therapeutic agents. Indeed, intracellular bacteria, such as *Mycobacterium tuberculosis* and *Listeria monocytogenes,* use cells of the innate immune system, not only as reservoirs to launch recurrent infections but even more as vectors enabling them to invade other sites of the body [37]. On the other hand, most of antibiotics, *e.g.* aminoglycosides, β-lactams and glycopeptides, have restricted cellular penetration while others can readily diffuse, *e.g.* fluoroquinolones and macrolides. Unfortunately, these latter suffer from low intracellular retention [38]. Accordingly, a small number of available antibiotics are effective against intracellular infections. To fight intracellular infections, NP are promising vectors allowing antibiotics to target macrophages and to reach bacteria located in intracellular compartments. In this field, a recent review article has already highlighted the role of NP for targeting intracellular infections [39].

Furthermore, engineered NP enable to keep their loaded antibiotics intact. We recently demonstrated that sterically-stabilized liposomes (SSL) loaded with S-nitrosoglutathione could be good candidates for macrophage targeting (unpublished data). We found that SSL are predominantly internalized by caveolae-dependent endocytosis which is the preferred pathway for drug delivery systems as it avoids the fusion with lysosomes and the subsequent drug degradation in its highly acidic environments.

2.6. Specific targeting and sustained-release

Inherent toxicity of antibiotics is a crucial drawback that led to limit or even to stop the use of some of them, such as aminoglycosides and lipopeptides known for their neuro- and nephrotoxicity [40]. Therefore, specific targeting to bacteria would counteract drug toxicity, since it enables to avoid non-selective and uncontrolled delivery to host cells.

To date, few works reported the design of NP with a specific targeting to bacteria for therapeutic purposes. Some examples are presented hereafter. Qi *et al.* elaborated mesoporous silica NP (MSN) as nanocarriers of vancomycin (Van) in order to specifically target GPB over macrophage-like cells [41]. The specific recognition was based on hydrogen bonding interactions of Van with the terminal D-alanyl-D-alanine moieties of GPB. Cell viability assay showed a good biocompatibility of Van-MSN with human embryonic kidney and human hepatocytes.

Tang *et al.* have recently described the design of a nanoparticulate carrier loaded with a fluorescent dye, and called it “nanoprobe” for diagnostic purposes [42]. The surface of the nanoprobe was grafted with a bacterial ligand, *i.e.* concanavalin A, and therefore displayed a high affinity to bacteria. The developed nanoprobe was shown to rapidly detect and quantify the extent of bacterial colonization on wounds and catheters in real time.

Prolonged or sustained release of the loaded antibiotic is of great importance for antibiotics with time-dependent action, such as lipoproteins, β-lactams, glycopeptides and some fluoroquinolones. The importance of the sustained-release profile was highlighted by Meers *et*

al. [30]. Thanks to the prolonged release of amikacin from liposomes, this latter was as effective, when administered tri-weekly, as free tobramycin administered twice-daily and despite the fact that MIC of tobramycin is lower than that of amikacin. Additional examples of antibiotic-loaded polymeric NP were recently reviewed [43].

2.7. Down-regulation of bacteria' oxidative-stress resistance genes

Bacterial adaptation to oxidative and nitrosative stress could be considered as a resistance mechanism to host defenses [44]. Indeed, innate immune cells generate reactive oxygen species (ROS) and reactive nitrogen species (RNS) such as superoxide and peroxynitrite, respectively, in order to kill phagocyted bacteria [45]. Consistently, pathogenic bacteria resist to host-mediated oxidative stress by up-regulating the expression of their antioxidant enzymes [46]. Importantly, it was claimed that many antibiotics exert their bactericidal effects *via* the production of hydroxyl radicals, regardless of their molecular targets [47].

Recently, it was found that metal NP, namely zinc oxide-NP (ZnO-NP), exert by themselves bactericidal effects on GPB and GNB [48]. A synergistic killing effect on acid fast bacteria (*i.e. Mycobacterium bovis*-BCG) was also observed for ZnO-NP when used in combination with rifampicin [48]. Moreover, ZnO-NP effectively killed MRSA clinical strains [48].

Several mechanisms were found to be involved in ZnO-NP antibacterial activities. Most importantly, ZnO-NP were found to down-regulate the transcription of oxidative stress resistance genes in *S. aureus*. Strictly speaking, the treatment with 300 µg/mL of ZnO-NP decreased the transcription of peroxide stress regulon *katA* and *perR* genes by 10- and 3.1-folds, respectively, when compared to untreated bacteria [48]. These results highlight the importance of ZnO-NP in fighting drug-resistant bacteria.

It is of note that ZnO-NP induced oxidative stress response on macrophages, as ROS and NO production was markedly increased, thus reinforcing their bacterial killing capacity [48].

Generally speaking, metal NP, such gold or silver NP, are known to induce oxidative stress in host cells, which is considered as one of mechanisms involved in their toxic effects [49]; [50]. However, to the best of our knowledge, Pati *et al.* were the first to demonstrate the opposite effect on bacterial cells [48].

3. Mechanisms of nanoparticle- bacterium interactions

NP interactions with bacterial cells or biofilms are ruled by two types of driving forces, *i.e.* electrostatic and hydrophobic. Evidences of electrostatic NP interactions with bacteria are multiple. For instance, positively-charged NP, especially those with zeta potential above +40 mV, are known to alter the bacterial cell membrane permeability by acting as detergents, causing an osmotic damage finally leading to cell death. This effect is weakened or nonexistent for NP with low positive potential or negatively-charged ones, respectively [8]. It is noteworthy that such interactions are unlikely to be overcome by bacterial adaptive resistance based on a single gene mutation, since bacterial membrane is highly evolutionarily conserved [51].

Hydrophobic interactions were reported in numerous research papers dealing with the antibacterial efficacy of quaternary ammonium compounds (QAC) micelles or QAC-containing micelles [52]; [53]; [54]. It was found that the antibacterial efficacy of these latter

vary as a function of the QAC's alkyl chain length. The optimal activity was observed for the more hydrophobic ones, *i.e.* containing C12 to C16 alkyl chain, when compared to those with short carbon chain (< C12) [52]. This was attributed to a stronger adherence to bacterial biofilms of QAC with longer alkyl chains [53].

Moreover, Cottenye *et al*. reported that hydrophobic interactions play an important role in liposome adherence to biofilms [54]. This is on the basis of their observation that only the fluorescent dye encapsulated in liposomes was tracked while the bare one was readily washed out of the biofilms. Accordingly, they concluded that the bound liposomes remained intact in the biofilms and no drastic reorganization in the liposomal wall occurred due to hydrophobic interactions with the biofilms [54].

During the last decades, researchers attempted to gain deep insights in NP interactions with bacterial cell-wall. The involved mechanisms are likely to be directly dependent on nanoparticle type and structural composition. The main interaction patterns are discussed hereafter.

3.1. Internalization mechanism of liposomes

3.1.1. Passive fusion "stalk mechanism"

Taking into account the barriers and the interaction driving forces, NP were designed in order to give rise to different types of interaction with bacteria or their biofilms. Passive fusion is the commonly described interaction mechanism with the bacterial cell-wall for NP in general but also particularly for fusogenic liposomes. The formulation of fusogenic liposomes is based on the combined use of lipids forming hexagonal II (HII) phase and lipids forming lamellar phase [55]. The lipids forming HII phase, such as phosphatidylethanolamine (PE), phosphatidylserine (PS) or phosphatidic acid (PA), have a small polar head showing a cone shaped-molecule. When used in formulation, the negative curvature stress leads to the spontaneous formation of inverted micelles (HII phase) [56]. In contrast, lipids with similar packing ratios for the polar head and the hydrophobic queue, such as phosphatidylcholine (PC), phosphatidylglycerol (PG) or phosphatidylinositol (PI), have a cylindric shape and produce a small or no curvature stress. They form lamellar phases [57].

The principal fusion mechanism as identified by Markin *et al.* was called the stalk mechanism [58]. The approaching membranes form an hourglass-shaped structure, called stalk, generating a local stress and spontaneous curvature in these membranes followed by bilayer reorganization. The stalk formation is promoted by an HII forming lipids since they stabilize the hemi-fusion intermediate structures. This hypothesized mechanism was subsequently confirmed thanks to TEM. The intermediate structure consisting in lamellar/HII transition phase was observed in a mixture of PC/PE after dehydration [59].

It is of note that there is a category of lipids called lysolipids, characterized by a bully polar head, molecularly shaped as inverted cone and so form hexagonal I (HI) phase. They produce a positive curvature stress in the membranes and inhibit the stalk formation of approaching membranes and thereby their fusion [60]. Accordingly, the design of fusogenic liposomes requires a careful qualitative and quantitative choice of phospholipids as it directly influences the stability of lamellar/HII transition phase [55].

3.1.2. Chemically triggered fusion

Passive fusion of liposomes with biological membranes could be considered as a drawback preventing a specific delivery of their loaded drugs. Thus, another generation of liposomes has been developed by grafting a hydrophilic polymer, *i.e.* polyethylene glycol (PEG), that confers a higher stability to liposomal wall and inhibiting its spontaneous fusion with biological membranes. Hence, liposomes containing PEG-lipid conjugates are called sterically-stabilized liposomes (SSL). Nonetheless, in order to restore the fusiogenecity in the vicinity of the site of action, *e.g.* biofilms or bacterial cell membrane, Kirpotin *et al.* elaborated liposomes containing pH-sensitive fusogenic phospholipid, *i.e.* dioleylphosphatidylethanolamine (DOPE), and a small percentage of a disulfide-linked PEG conjugate with distearylphosphatidylethanolamine (mPEG-DTP-DSPE) [61]. The authors demonstrated that the thiolytic cleavage of the disulfide bridge resulted in the detachment of PEG from DOPE-containing liposomes, and subsequently liposomal fusion occurred at pH 5.5 accompanied with the leakage of the entrapped dye.

3.1.3. Fusion triggered by specific "ligand-receptor" recognition

In an attempt to target a specific type of bacteria, researchers focused on the outer membrane composition of the considered bacterium. This is with the aim to find a membrane component that specifically interacts with a ligand grafted on NP surface. Accordingly, Bardonnet *et al.* took benefit of the fact that some strains of *Helicobacter pylori* has an outer membrane protein (BabA2 adhesin) that binds with the fucosylated Lewis b (Leb) histo-blood group antigen expressed by human gastric epithelial cells [62]. Based on this phenomenon, Bardonnet *et al.* elaborated liposomes containing a synthesized glycolipid (Fuc-E4-Chol) composed of cholesterol as an anchor part, four ethylene glycol residues as a linker, and fucose as an exposed part at the surface of liposomes [63]. These liposomes were used as delivery systems for ampicillin and metronidazole and were found to be effective against both the spiral and the coccoid bacterial forms.

In this study, the authors attributed the interactions *H. pylori*-liposomes to four events [63]. The first one is the incorporation cholesterol in the formulation of liposomes which enhances their interaction with *H. pylori*, because of the specific affinity of this latter to this steroid. The second phenomenon is the electrostatic interaction as *H. pylori* is negatively-charged. The authors found that liposomes exhibiting a lower negative zeta-potential (between -2.9 and -4.3 mV) were more efficient than those with a higher one (between -12.2 and -20 mV). The third phenomenon is the specific interaction of fucosylated liposomes-BabA2 adhesin, since better results were obtained with liposomes grafted with the synthesized glycolipid Fuc-E4-Chol. Finally, the fourth important point was the age of the bacterial culture or, in other words, the bacterium phenotype. During aging, the morphology of *H. pylori* evolves from the spiral to the coccoid resistant form. Fucosylated liposomes were found to interact with both phenotypes, whereas analogous ones without Fuc-E4-Chol were only able to interact with *H. pylori* spiral form. Consistently, the authors supposed that both phenotypes express BabA2 adhesin on the outer membrane [63].

3.2. Internalization mechanisms of polymeric and inorganic nanoparticles

Internalization of inorganic/polymeric NP by viable bacteria was previously demonstrated. Kumar *et al.* evidenced the uptake of inorganic NP, sizing from 30 to 50 nm, by viable bacteria using flow cytometry [64]. The researchers exposed *E. coli* to high concentrations of ZnO NP and TiO_2 NP, up to 80 µg/ml, for periods ranging from 30 to 90 min. it was shown that NP were taken up in a concentration-dependent manner. It is of note that over the longest incubation period, cell death did not exceed 13.3%.

Recently, Curia *et al.* reported the internalization of polyurethane NP by *S. aureus* by a "Trojan horse" mechanism [65]. Polyurethane NP were naturally generated from the bacterial action on plastic materials. Generated NP was covered by a protein corona and were shown to be taken up by a dynamic movement of the bacterial membrane. The authors tried to explain this phenomenon, usually observed in Eukaryote and not in Prokaryote, by the fact that NP covering with a protein corona modified the electromagnetic parameters of engineered NP-bacterium interactions.

Little is known about the exact mechanisms of the interaction of inorganic or polymeric NP with bacterial walls and membranes. LPS, phospholipids seem to be the target sites for inorganic NP action; whereas phospholipids and outer membrane proteins could be the sites of action for polymeric NP. Jiang *et al.* studied the interaction of Al_2O_3 NP with micelles and vesicles formed of LPS/PE extracted from *E. coli*, as bacterial membrane models [66]. A strong attachment of NP with LPS/PE vesicles and micelles was evidenced by atomic force microsocopy. After an exposure of 24 h, it was observed that LPS vesicles were coated with NP that formed a layer of tens of nanometer; while the exposure to NP disturbed the stability of PE vesicles that became larger with thicker walls.

These observations are consistent with previous findings, reported by Fortunellai and Monti [67]. The researchers studied the interaction of three phospholipids (DOPC, DOPS, DMTAP) with TiO_2 surfaces. They showed that interactions influenced the conformation properties of phospholipids and reduced the mobility of lipid bilayers. Phosphate or carbonyl oxygens of the lipids constituted the target sites of interactions [67].

Xi *et al*. studied the interaction of OCNP, polymeric NP that are formed of oleoyl-chitosan, with *S. aureus* and *E. coli* as models of GPB and GNB, respectively [68]. This work focused on the role of membrane proteins and phospholipids in NP-bacterium interactions. The change in membrane protein conformation was investigated by measuring the fluorescence of a protein residue, tyrosine (Tyr). Tyr is normally located in both sides of the bacterial membrane. If the NP interacted with membrane proteins, the conformation of these latter would be altered, and Tyr residues located inside the membrane would be exposed to the surface and thus increasing the fluorescence intensity. Accordingly, it was found that for both *S. aureus* and *E. coli* the fluorescence intensity of Tyr residues was increased after a 1 h-incubation with OCNP, in a concentration-dependent manner. The authors deduced that "*OCNP influenced the structure of cell membranes by interacting with proteins on the cell membrane of the bacteria*" [68].

Phospholipids were also evaluated as a potential target for OCNP. Toward this aim, OCNP were treated with yolk lecithin in order to simulate the effect of membrane phospholipids. The treated on non-treated OCNP were incubated with *S. aureus* or with *E. coli* for 24 h. The role of lecithin in NP-bacterium interaction was appreciated by comparing the growth inhibition

rate of treated and non-treated NP. Results showed that phospholipids do not affect the interaction of OCNP with the GNB model. In contrast, the antibacterial activity of OCNP on the GPB model was significantly decreased when NP were pre-treated with lecithin [68].
Moreover, the specific uptake of NP represent another potential mechanism. Bismuth NP are discussed as a given example [69]. Bismuth NP surface was modified by grafting polyclonal antibody in order to specifically interact with multi-drug resistant (MDR) *Pseudomonas aeruginosa*. Encouraging results were obtained; after an exposure to a low dose of X-rays for 20 min, 90% of MDR *P. aeruginosa* were killed *versus* around 15%, with or without incubation with antibody-modified bismuth NP, respectively. Furthermore, the combined use of antibody-modified bismuth NP and X-ray irradiation did not result in any notable damage on host cells (Hela and MG-63 cells).
It is of note that neither X-rays at low dose nor antibody-modified bismuth NP showed a significant bactericidal effect when used alone [69]. These results were attributed to the dose enhancement of the radiosensitizer, *i.e.* bismuth, in the vicinity of bacterial cells. To confirm that the specific targeting was the cause of the enhanced bactericidal results, unmodified NP were used and compared with antibody-modified ones under the same treatment conditions. As expected, bacterial eradication was 10 times higher when antibody-modified NP were used [69].

4. Factors affecting nanoparticle- bacterium interaction

4.1. Nanoparticle-related factors

4.1.1. Size and surface hydrophobicity

The size is a key factor to be considered in the design of NP intended to overcome the bacterial first barrier, *i.e.* the biofilm. Keeping in mind that the effective pore size in bacterial biofilms is about few tens of nanometers, hydrophilic NP, *e.g.* dextran-based NP, with large diameter (>100 nm) cannot diffuse through pores and would be excluded. Even more, it was found that the penetration of those whose diameter > 50 nm in biofilms was limited [70]. It is of note that in this study, particle diffusion was measured in dense bacterial microcolonies where biofilms are highly viscous.
In contrast, several research papers reported a good diffusion of liposome whose sizes ranged between 100 and 350 nm through bacterial biofilms [29], or through CF-patients 'sputa [30]. Liposomes of larger sizes (> 400 nm) showed a restricted diffusion through biofilms [71].
NP-bacterium interaction could be revealed by the antibacterial enhanced efficiency. For instance, large hydrophobic NP, *e.g.* 500 nm-sized ZnO-NP, exhibited a quite efficient bacterial killing which was, in some cases, higher than that of 50 nm-sized NP [48]. In contrast, NP with hydrophilic surface, *e.g.* polyethylene glycol-capped ZnO-NP, showed a strong inverse relationship between size and antibacterial activity [72]. A similar behavior was reported for silver-NP, where only very small NP (1-10 nm) presented a direct interaction with bacteria [73].
Furthermore, the interaction with the second bacterial barrier, *i.e.* LPS, was found to be affected by the surface hydrophobicity of NP. Given the fact that LPS consist on hydrophobic (*i.e.* lipid A) and hydrophilic (*i.e.* O-specific polysaccharide, core oligosaccharide) components, complex interactions including both hydrophobic and hydrogen bonds could take

place. Naberezhnykh *et al.* demonstrated a direct relationship between NP -surface hydrophobicity and the LPS-binding efficiency [74]. The authors found that liposomes coated with hydrophobic chitosan derivatives show higher LPS-binding than liposomes coated with chitosan. The latter showed higher LPS-binding than did free liposomes. The increased LPS-binding was attributed to the hydrophobic interactions in addition to hydrogen and ionic bonds formation between chitosan molecule and LPS [74].

4.1.2. Zeta potential

The aforementioned electrostatic NP-bacterium interactions make it easy to predict that NP's zeta potential would be influent on these interactions. One would imagine that cationic particles can strongly adhere to the negatively-charged bacterial biofilms to the detriment of effective penetration; whereas anionic particles would be repulsed and neutral, *e.g.* PEG-surface grafted, particles would more readily pass. This reasoning is supported by the research papers of Ahmed *et al.* [75]; [76]. The authors found that pegylation of cationic liposomes decreased their adsorption to the bacterial biofilms. Furthermore, Meers *et al.* used zwitterionic lipids to prepare amikacin-loaded neutral liposomes, that showed a quite efficient penetration in both *P. aeruginosa*'s biofilms and CF-patients' sputa. This was explained, in part, by the reduced ionic interactions [30].

Seen from a different angle, the strong adhesion of cationic particles to bacterial biofilms would be advantageous when biofilm targeting is aimed. Consistently, Kim & Jones reported the effectiveness of cationic liposomes to deliver penicillin G to *S. aureus*' s biofilm as demonstrated by the higher bacterial growth inhibiting effect with respect to the free drug [77].

McAllister *et al.* studied the role of surface charge in liposomal interactions with bacterial cells in planktonic form [78]. The authors found that only positively-charged liposomes exhibited a significantly enhanced antibacterial activity with respect to the free drug. Both anionic and neutral liposomes showed similar activities to that of the free drug. These results were attributed to a stronger cell association due to attractive electrostatic interactions, as bacterial cell-wall is negatively-charged.

Similar results were reported for polymeric nanocapsules. Fernandes *et al.* developed nanocapsules based on two different chemically-modified biopolymers with improved cationic character (*i.e.* aminocellulose and thiolated chitosan) [8]. In this study, interactions between nanocapsules and a model of bacterial membrane were studied using Langmuir monolayers and liposomal bilayers composed of *E. coli*-extracted α-phosphatidylglycerol. It was found that the membrane disturbing capacity was directly proportional to the nanocapsules cationic charges. Supporting results provided by killing studies were also reported [8].

4.1.3. Fusogenicity, fluidity and lamellarity

All these factors involve lipid-based nanocapsules and in particular liposomes. Indeed, fusogenicity was found to be dependent on the constituting lipids characteristics and more precisely on their intrinsic curvature. Phospholipids exhibiting negative-curvature, *e.g.* PE, PA and PS promote fusogenicity, as they stabilize the hemi-fusion intermediate structures; whereas lipids with no curvature stress, *e.g.* as PC, PG and PI, do not (see section 3.1).

Ma *et al.* elaborated tobramycin-loaded nanoliposomes containing DOPE and dimyristoylphospholipids with different polar head groups: PA, PS, PG and PI [79]. The liposome-bacterium fusion studies showed that the highest degree of fusion was obtained with PA and the lowest one was obtained with PI. As expected, the fusogenicity was dramatically enhanced with the increase of DOPE content.

It is worth mentioning that the content of negative curvature- displaying lipids is higher in bacterial membranes than in eukaryotic membranes, which may contribute in the selective fusional interaction with bacteria rather than with host cells. This feature was already demonstrated for methacrylate co-polymers [80].

In addition, the fusion with bacteria is favored by the fluidity of the liposomal membrane. This latter is generally assessed indirectly by measuring the gel-to-liquid phase transition temperature (Tc). The higher the Tc values of the lipid mixture is, the higher the membrane rigidity and the higher liposomal stability will be [81]. It is well-established that cholesterol increases the Tc value of the lipid mixture. Hence, higher rigidity is obtained accompanied with increased *in vitro* stability [82].

Unfortunately, the increased rigidity was found to unfavorably influence the liposome-bacterium fusion. Ma *et al.* reported that a cholesterol content as high as 50% almost completely inhibited the liposomal fusion with *P. aeruginosa* [79]. In the same vein, lipids with long and saturated hydrocarbon chains and thus exhibiting high Tc values would negatively influence the membrane fluidity and thereby the liposome-bacterium fusion.

Accordingly, tobramycin-loaded liposomes called Fluidosomes® were designed from a mixture of dipalmitoyphosphatidylcholine (DPPC) and dimyristoylphosphatidylglycerol (DMPG) at a ratio of 18/1 w/w displaying an overall Tc < 37°C [83]. The authors demonstrated the efficient fusion of Fluidosomes® with *P. aeruginosa* using different techniques, namely lipid-mixing studies, flow cytometry analysis and immunocytochemistry-coupled TEM (Fig. 2) [84]. The highest fusion rate was observed after about 5 h for the resistant strain and after much shorter time for the sensitive strain. These results suggest that Fluidosomes® are good candidates to combat impermeability-related bacterial resistance [84]. Today, tobramycin-loaded Fluidosomes® are produced by Axentis pharma (Zurich, Switzerland) and marketed as AX-TOBRA™.

Lamellarity seems not to play a crucial role in liposomal interaction with bacteria and/or their biofilms. Jardeleza *et al.* reported that at short exposure time, *i.e.* 5 min, stronger anti-biofilm effects of MLV were observed in comparison to unilamellar vesicles (ULV) [21]. Nevertheless, the authors mentioned that this difference were not statistically significant. In this study, MLV displaying the same drug encapsulation efficiency as ULV were shown to produce comparable anti- *S. aureus* biofilm effects. Likewise, Ma *et al.* did not observed a significant influence of lamellarity on liposomes-bacterium fusion level [79].

4.2. Antibiotic-related factors

4.2.1. Cellular target and activity pattern

In literature, different behaviors were sometimes reported for similarly-formulated nanoparticulate delivery systems as a function of the loaded antibiotic. Indeed, the encapsulation of antibiotics exerting their effect on bacterial membranes, *e.g.* β-lactams, and glycopeptides, may hamper their binding to their target. However, with those exerting their

effects on internal cell organelles, *e.g.* aminoglycosides, macrolides and fluoroquinolones, the encapsulation would help to increase their intracellular concentration and thus their availability in the vicinity of their targets.

For instance, meropenem, a β-lactame antibiotic, entrapped in Fluidosomes® showed 4- to 16-folds higher MICs for *P. aeruginosa* sensitive and resistant strains than did the free drug [85]. Even though, the fusional interaction between Fluidosomes® and *P. aeruginosa* was previously demonstrated [84]. In contrast, tobramycin, an aminoglycoside antibiotic, loaded in Fluidosomes® showed a superior antibacterial activity in both *in vitro* and *in vivo* studies against *P. aeruginosa* strains with respect to the free drug [86].

Furthermore, the antibiotic's activity pattern is fundamental in the choice of NP release profile. NP exhibiting sustained-release profile could be more interesting than fusogenic liposomes for the delivery of β-lactams or glycopeptides, whose antibacterial activity is mainly time-dependent. This reasoning is supported by several published investigations.

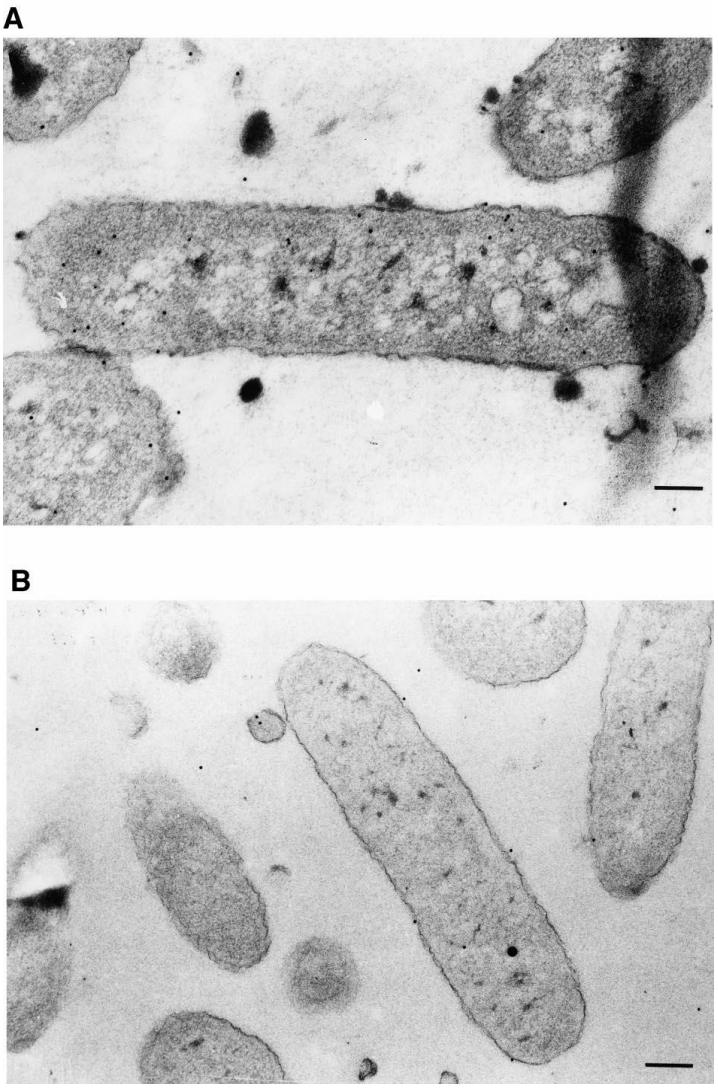

Fig. 2. Detection of tobramycin inside bacterial cells by immunogold labeling. (A) *Pseudomonas aeruginosa* 429 incubated 6 h with Fluidosomes. (B) Pseudomonas aeruginosa 429 incubated 6 h with free tobramycin. Magnification: A, × 41126; B, × 36720. This figure was published in [84], Copyright Elsevier 2000.

Nadakumar *et al.* developed a sustained-release nanoparticulate delivery system using poly(lactide-co-glycolide) acid (PLGA) with high glycolic acid ratio (10:90) or polylactic acid (PLA) for meropenem delivery [87]. Both systems released meropenem over 30 days with a faster and greater release from PLGA-NP. It was found that PLGA-NP induced 2-folds reduction of *Escherichia coli* growth than did PLA-NP. The enhanced efficacy may be explained by the greater drug amount released from the former. In agreement with this rationale, a correlation between the drug released amount and the CFU count was found for both systems.

Vancomycin, a glycopeptide antibiotic, entrapped in SLN produced greater antibacterial effectiveness against both *S. aureus* and MRSA after 18 h as compared to the bare drug. This was explained in part by the ability of SLN to maintain therapeutic concentrations for an extended period of time [88].

The same tendency was also noted for antibiotics whose activity is mainly dose-dependent such as aminoglycosides and fluoroquinolones. For instance, Abdelghany *et al.* developed gentamicin-loaded PLGA-NP achieving a sustained-release profile [89]. These latter exhibited significantly improved antibacterial activities against *P. aeruginosa* PA01 strain in both planktonic and biofilm forms with respect to the free drug [89].

Imbuluzqueta *et al.* used prodrug and nanoencapsulation approaches in order to achieve a sustained-release of gentamicin [90]. In this work, a hydrophobic derivative of gentamicin, *i.e.* gentamicin bis(2-ethylhexyl) sulfosuccinate, was synthesized and then entrapped in PLGA-NP. The developed NP enabled to maintain an antibiotic therapeutic concentration for up to 4 days in both liver and spleen. Consequently, only 4 doses were sufficient to eliminate the splenic infection from 50% of the infected mice, while 14 doses of the free drug did not produce a significant difference when compared to untreated animals.

4.2.2. Hydrophobicity and molecular weight

Hydrophobicity and molecular weight of antibiotics have a strong influence on their performance and their activity spectrum. For instance, vancomycin is hydrophilic (log P -3.1) and displays a high molecular weight (1485.7 g/mole). Consequently, it is impermeable through GNB's wall, and its high molecular weight hampers its permeation through the aqueous porine channels. Thus, vancomycin's activity spectrum is restricted to GPB. This reasoning is confirmed by the fact that vancomycin' s spectrum was broadened to include GNB when encapsulated in fusogenic liposomes [10]. In other words, the encapsulation helped to bypass the impermeability limiting-factor. Conversely, hydrophobic antibiotics readily permeate through GNB's wall.

Indeed, once encapsulated, the drug's physico-chemical properties are expected to be of minor significance, instead those of the nanocarriers would have the main influence. Despite this, these former have to be taken into account. Both hydrophobicity and molecular weight of the entrapped drug would directly affect the achieved loading efficiency. It was well-established that highly hydrophilic drugs with low molecular weight do not enable high loadings to be reached [91]. In turn, the drug loading directly impacts the efficiency of drug delivery to the target, *e.g.* the affected organ, the infection foci or even bacterial cells.

For instance, daptomycin, an amphiphilic lipopeptide antibiotic, was entrapped in nanoliposomes with an efficiency as high as 88 %. This result explain, in part, the achieved

enhanced delivery to the infection site in the derma where effective therapeutic concentrations were maintained for several hours [92]. Higher encapsulation efficiencies (> 95%) were achieved for clarithromycin, a hydrophobic antibiotic (log P 3.16), which is encouraging to consider clinical applications of the liposomal form [93].
Inversely, gentamicin, a polycationic antibiotic, highly hydrophilic (log P -4.1) with a relatively low molecular weight (477.5 g/mole), enabled low encapsulation efficiencies to be achieved in liposomal formulations (< 10%) [94]. Higher encapsulation efficiencies of gentamicin in liposomes were reported recently, but not exceeding 30% [20].

4.3. Bacterium-related factors

Obviously, surface hydrophobicity and zeta potential of the bacterial cell-wall tune the NP-bacterium non-specific interactions. However, specific components, *e.g.* outer-membrane proteins, such as those involved in the efflux pump system, probably play a decisive role in these interactions. This question was addressed by Drulis-Kawa *et al.* [95]. The authors studied thoroughly the interaction of 100 nm-sized cationic liposomes with a GNB, *i.e. P. aeruginosa*, in attempt to determine the most relevant bacterial structure or wall properties [95]. They shed light on different potential factors; namely surface hydrophobicity, electrostatic potential, outer membrane's proteins and LPS. Toward this purpose, fluorescently-labelled liposomes and different bacterial strains were used. Zeta potential of the tested strains varied between -3.9 and -15.0 mV, while surface hydrophobicity was in the range of 0.5 to 34.0%.
All the tested strains showed interaction with liposomes. Although, no correlation between zeta potential or hydrophobicity with liposome-bacterium fusion level could be noted.
With regard to LPS, the tested strains presented different O-antigen lengths, including short- and fast-migrating LPS. Unexpectedly, it was found that strains presenting the same LPS molecular patterns showed different fusion levels.
Finally, the outer-membrane proteins of the tested strains were analysed. Importantly, it was noted that a strong interaction with liposomes occurred for all the strains possessing the 18 kDa protein bands. The strongest interaction was noted for strains exhibiting the highest amount 18 kDa proteins. No visible interaction occurred for strains that lacked for the 18 kDa protein.
Another important factor is the divalent cation level, *e.g.* Ca^{2+} and Mg^{2+}, was reported to be a key factor determining the NP-bacterium fusion level. Divalent cations play the role of binding sites on the bacterial cell-wall and thus favor the interaction of negatively-charged NP [96]. Recently, Ma *et al.* measured the liposomes-bacterium degree of fusion in presence of different concentration of additional Ca^{2+} [79]. As expected, a high fusion level up to 90% was recorded in the presence of 5 mM- Ca^{2+} concentration. The fusion was almost completely inhibited in the absence of Ca^{2+}.
Similarly, the electrostatic and hydrophobic properties of biofilms should be taken into account for NP design. The majority of bacterial biofilms are negatively charged with few exceptions such as the biofilms of *S. aureus* and *S. epidermidis* which are positively-charged because of the partially deacetylated *N*-acetylglycosaminoglycan [97]. Consequently, cationic NP generally interact more efficiently than anionic ones.

Furthermore, for a given bacterium, biofilms hydrophobic properties may vary as a function of the studied sub-train and thus alter NP-interaction effectiveness. For instance, cationic liposomes showed different behaviors in *S. epidermidis*‘ s biofilms produced by different sub-strains defined as hydrophobic, hydrophilic or mutant m3 [98].

Conflicts of interest

The authors declare no conflict of interest.

Acknowledgment

Financial support was provided by the French Ministry of Higher Education and Research.

R e f e r e n c e s

[1] Fuse S, Tsukamoto H, Yuan Y, Wang TA, Zhang Y, Bolla M *et al*. Functional and structural analysis of a key region of the cell wall inhibitor moenomycin. ACS Chem Biol 2010;5: 701-11.

[2] Nakayama K, Kawato H, Watanabe J, Ohtsuka M, Yoshida K, Yokomizo Yet al.. MexAB-OprM specific efflux pump inhibitors in *Pseudomonas aeruginosa*. Part 3: Optimization of potency in the pyridopyrimidine series through the application of a pharmacophore model. Bioorg Med Chem Lett 2004;14: 475-9.

[3] Li J, Nation RL, Turnidge JD, Milne RW, Coulthard K, Rayner CRet al.. Colistin: the re-emerging antibiotic for multidrug-resistant Gram-negative bacterial infections. Lancet Infect Dis 2006;6: 589-601.

[4] Yanagawa Y, Yamamoto Y, Hara Y & Shimamura T. A combination effect of epigallocatechin gallate, a major compound of green tea catechins, with antibiotics on Helicobacter pylori growth *in vitro*. Curr Microbiol 2003;47: 244-9.

[5] Flemming H & Wingender J. The biofilm matrix. Nat Rev Microbiol 2010;8: 623-33.

[6] Taylor EN, Kummer KM, Dyondi D, Webster TJ & Banerjee R. Multi-scale strategy to eradicate Pseudomonas aeruginosa on surfaces using solid lipid nanoparticles loaded with free fatty acids. Nanoscale 2014;6: 825-32.

[7] Bjarnsholt T, Ciofu O, Molin S, Givskov M & Høiby N. Applying insights from biofilm biology to drug development - can a new approach be developed?. Nat Rev Drug Discov 2013;12: 791-808.

[8] Fernandes MM, Francesko A, Torrent-Burgués J, Carrión-Fité FJ, Heinze T & Tzanov T. Sonochemically processed cationic nanocapsules: efficient antimicrobials with membrane disturbing capacity. Biomacromolecules 2014;15: 1365-74.

[9] Cabeen MT & Jacobs-Wagner C. Bacterial cell shape. Nat Rev Microbiol 2005;3: 601-10.

[10] Nicolosi D, Scalia M, Nicolosi VM & Pignatello R. Encapsulation in fusogenic liposomes broadens the spectrum of action of vancomycin against Gram-negative bacteria. Int J Antimicrob Agents 2010;35: 553-8.

[11] Rumbo C, Gato E, López M, Ruiz de Alegría C, Fernández-Cuenca F, Martínez-Martínez Let al.. Contribution of efflux pumps, porins, and β-lactamases to multidrug resistance in clinical isolates of *Acinetobacter baumannii*. Antimicrob Agents Chemother 2013;57: 5247-57.

[12] Casadevall A & Pirofski L. Virulence factors and their mechanisms of action: the view from a damage-response framework. J Water Health 2009;7 Suppl 1: S2-S18.
[13] Davies J & Davies D. Origins and evolution of antibiotic resistance. Microbiol Mol Biol Rev 2010;74: 417-33.
[14] John S & Balagurunathan R. Metallo beta lactamase producing *Pseudomonas aeruginosa* and *Acinetobacter baumannii*. Indian J Med Microbiol 2011;29: 302-4.
[15] Poole K. Aminoglycoside resistance in *Pseudomonas aeruginosa*. Antimicrob Agents Chemother 2005;49: 479-87.
[16] Rubin BK. Mucus structure and properties in cystic fibrosis. Paediatr Respir Rev 2007;8: 4-7.
[17] Cipolla D, Gonda I & Chan H. Liposomal formulations for inhalation. Ther Deliv 2013;4: 1047-72.
[18] Cipolla D, Shekunov B, Blanchard J & Hickey A. Lipid-based carriers for pulmonary products: preclinical development and case studies in humans. Adv Drug Deliv Rev 2014;75: 53-80.
[19] Clancy JP, Dupont L, Konstan MW, Billings J, Fustik S, Goss CHet al.. Phase II studies of nebulised Arikace in CF patients with *Pseudomonas aeruginosa* infection. Thorax 2013;68: 818-25.
[20] Khameneh B, Iranshahy M, Ghandadi M, Ghoochi Atashbeyk D, Fazly Bazzaz BS & Iranshahi M. Investigation of the antibacterial activity and efflux pump inhibitory effect of co-loaded piperine and gentamicin nanoliposomes in methicillin-resistant *Staphylococcus aureus*. Drug Dev Ind Pharm 2014;20: 1-6.
[21] Jardeleza C, Rao S, Thierry B, Gajjar P, Vreugde S, Prestidge CAet al.. Liposome-encapsulated ISMN: a novel nitric oxide-based therapeutic agent against *Staphylococcus aureus* biofilms. PLoS One 2014;9: e92117.
[22] Jardeleza C, Foreman A, Baker L, Paramasivan S, Field J, Tan LWet al.. The effects of nitric oxide on *Staphylococcus aureus* biofilm growth and its implications in chronic rhinosinusitis. Int Forum Allergy Rhinol 2011;1: 438-44.
[23] Duong HTT, Jung K, Kutty SK, Agustina S, Adnan NNM, Basuki JSet al.. Nanoparticle (star polymer) delivery of nitric oxide effectively negates *Pseudomonas aeruginosa* biofilm formation. Biomacromolecules 2014;10: 1195-208.
[24] Moghadas-Sharif N, Fazly Bazzaz BS, Khameneh B & Malaekeh-Nikouei B. The effect of nanoliposomal formulations on *Staphylococcus epidermidis* biofilm. Drug Dev Ind Pharm 2014; Epub ahead of print.
[25] Peck KR, Kim SW, Jung S, Kim Y, Oh WS, Lee JYet al.. Antimicrobials as potential adjunctive agents in the treatment of biofilm infection with *Staphylococcus epidermidis*. Chemotherapy 2003;49: 189-93.
[26] Mihailescu R, Furustrand Tafin U, Corvec S, Oliva A, Betrisey B, Borens Oet al.. High activity of Fosfomycin and Rifampin against methicillin-resistant *Staphylococcus aureus* biofilm *in vitro* and in an experimental foreign-body infection model. Antimicrob Agents Chemother 2014;58: 2547-53.
[27] Szczuka E & Kaznowski A. Antimicrobial activity of tigecycline alone or in combination with rifampin against *Staphylococcus epidermidis* in biofilm. Folia Microbiol (Praha) 2014;59: 283-8.

[28] Reiter KC, Sambrano GE, Villa B, Paim TGDS, de Oliveira CF & d'Azevedo PA. Rifampicin fails to eradicate mature biofilm formed by methicillin-resistant *Staphylococcus aureus*. Rev Soc Bras Med Trop 2012;45: 471-4.
[29] Alipour M, Halwani M, Omri A & Suntres ZE. Antimicrobial effectiveness of liposomal polymyxin B against resistant Gram-negative bacterial strains. Int J Pharm 2008;355: 293-8.
[30] Meers P, Neville M, Malinin V, Scotto AW, Sardaryan G, Kurumunda Ret al.. Biofilm penetration, triggered release and in vivo activity of inhaled liposomal amikacin in chronic *Pseudomonas aeruginosa* lung infections. J Antimicrob Chemother 2008;61: 859-68.
[31] Wright GD. Bacterial resistance to antibiotics: enzymatic degradation and modification. Adv Drug Deliv Rev 2005;57: 1451-70.
[32] Lagacé J, Dubreuil M & Montplaisir S. Liposome-encapsulated antibiotics: preparation, drug release and antimicrobial activity against *Pseudomonas aeruginosa*. J Microencapsul 1991;8: 53-61.
[33] Alipour M, Suntres ZE, Halwani M, Azghani AO & Omri A. Activity and interactions of liposomal antibiotics in presence of polyanions and sputum of patients with cystic fibrosis. PLoS One 2009a;4: e5724.
[34] Alipour M, Suntres ZE & Omri A. Importance of DNase and alginate lyase for enhancing free and liposome encapsulated aminoglycoside activity against *Pseudomonas aeruginosa*. J Antimicrob Chemother 2009b;64: 317-25.
[35] Alipour M, Suntres ZE, Lafrenie RM & Omri A. Attenuation of *Pseudomonas aeruginosa* virulence factors and biofilms by co-encapsulation of bismuth-ethanedithiol with tobramycin in liposomes. J Antimicrob Chemother 2010;65: 684-93.
[36] Hurler J, Sørensen KK, Fallarero A, Vuorela P & Škalko-Basnet N. Liposomes-in-hydrogel delivery system with mupirocin: *in vitro* antibiofilm studies and in vivo evaluation in mice burn model. Biomed Res Int 2013;2013: 498485.
[37] Rosenberger CM & Finlay BB. Phagocyte sabotage: disruption of macrophage signalling by bacterial pathogens. Nat Rev Mol Cell Biol 2003;4: 385-96.
[38] Vazifeh D, Bryskier A & Labro MT. Mechanism underlying levofloxacin uptake by human polymorphonuclear neutrophils. Antimicrob Agents Chemother 1999;43: 246-52.
[39] Abed N & Couvreur P. Nanocarriers for antibiotics: A promising solution to treat intracellular bacterial infections. Int J Antimicrob Agents 2014;43: 485-96.
[40] Sorlí L, Luque S, Grau S, Berenguer N, Segura C, Montero MMet al.. Trough colistin plasma level is an independent risk factor for nephrotoxicity: a prospective observational cohort study. BMC Infect Dis 2013;13: 380.
[41] Qi G, Li L, Yu F & Wang H. Vancomycin-modified mesoporous silica nanoparticles for selective recognition and killing of pathogenic Gram-positive bacteria over macrophage-like cells. ACS Appl Mater Interfaces 2013;5: 10874-81.
[42] Tang EN, Nair A, Baker DW, Hu W & Zhou J. *In vivo* imaging of infection using a bacteria-targeting optical nanoprobe. J Biomed Nanotechnol 2014;10: 856-63.
[43] Xiong M, Bao Y, Yang X, Zhu Y & Wang J. Delivery of antibiotics with polymeric particles. Adv Drug Deliv Rev 2014;: doi: 10.1016.
[44] Hassett DJ & Cohen MS. Bacterial adaptation to oxidative stress: implications for pathogenesis and interaction with phagocytic cells. FASEB J 1989;3: 2574-82.

[45] Fang FC. Antimicrobial reactive oxygen and nitrogen species: concepts and controversies. Nat Rev Microbiol 2004;2: 820-32.
[46] Tu WY, Pohl S, Summpunn P, Hering S, Kerstan S & Harwood CR. Comparative analysis of the responses of related pathogenic and environmental bacteria to oxidative stress. Microbiology 2012;158: 636-47.
[47] Hassett DJ & Imlay JA. Bactericidal antibiotics and oxidative stress: a radical proposal. ACS Chem Biol 2007;2: 708-10.
[48] Pati R, Mehta RK, Mohanty S, Padhi A, Sengupta M, Vaseeharan B *et al.* Topical application of zinc oxide nanoparticles reduces bacterial skin infection in mice and exhibits antibacterial activity by inducing oxidative stress response and cell membrane disintegration in macrophages. Nanomedicine 2014;10: 1195-208.
[49] Khan A, Abdelhalim A, Al-Ayed S & Alhomida S. Effect of gold nanoparticles on glutathione and malondialdehyde levels in liver, lung and heart of rats. Saudi J Biol Sci 2012;19: 461-4.
[50] Xin L, Wang J, Wu Y, Guo S & Tong J. Increased oxidative stress and activated heat shock proteins in human cell lines by silver nanoparticles. Hum Exp Toxicol 2014; Epub ahead of print.
[51] Brogden KA. Antimicrobial peptides: pore formers or metabolic inhibitors in bacteria?. Nat Rev Microbiol 2005;3: 238-50.
[52] Gilbert P & Moore LE. Cationic antiseptics: diversity of action under a common epithet. J Appl Microbiol 2005;99: 703-15.
[53] Sandt C, Barbeau J, Gagnon M & Lafleur M. Role of the ammonium group in the diffusion of quaternary ammonium compounds in *Streptococcus mutans* biofilms. J Antimicrob Chemother 2007;60: 1281-7.
[54] Cottenye N, Cui Z, Wilkinson KJ, Barbeau J & Lafleur M. Interactions between non-phospholipid liposomes containing cetylpyridinium chloride and biofilms of *Streptococcus mutans*: modulation of the adhesion and of the biodistribution. Biofouling 2013;29: 817-27.
[55] Allen TM, Hong K & Papahadjopoulos D. Membrane contact, fusion, and hexagonal (HII) transitions in phosphatidylethanolamine liposomes. Biochemistry 1990;29: 2976-85.
[56] Siegel DP. The modified stalk mechanism of lamellar/inverted phase transitions and its implications for membrane fusion. Biophys J 1999;76: 291-313.
[57] Kent B, Garvey CJ, Cookson D & Bryant G. The inverse hexagonal - inverse ribbon - lamellar gel phase transition sequence in low hydration DOPC:DOPE phospholipid mixtures. Chem Phys Lipids 2009;157: 56-60.
[58] Markin VS, Kozlov MM & Borovjagin VL. On the theory of membrane fusion. The stalk mechanism. Gen Physiol Biophys 1984;3: 361-77.
[59] Yang L & Huang HW. Observation of a membrane fusion intermediate structure. Science 2002;297: 1877-9.
[60] Chernomordik LV & Kozlov MM. Mechanics of membrane fusion. Nat Struct Mol Biol 2008;15: 675-83.
[61] Kirpotin D, Hong K, Mullah N, Papahadjopoulos D & Zalipsky S. Liposomes with detachable polymer coating: destabilization and fusion of dioleoylphosphatidylethanolamine vesicles triggered by cleavage of surface-grafted poly(ethylene glycol). FEBS Lett 1996;388: 115-8.

[62] Ilver D, Arnqvist A, Ogren J, Frick IM, Kersulyte D, Incecik ET *et al. Helicobacter pylori* adhesin binding fucosylated histo-blood group antigens revealed by retagging. Science 1998;279: 373-7.
[63] Bardonnet P, Faivre V, Boullanger P, Piffaretti J & Falson F. Pre-formulation of liposomes against *Helicobacter pylori*: characterization and interaction with the bacteria. Eur J Pharm Biopharm 2008;69: 908-22.
[64] Kumar A, Pandey AK, Singh SS, Shanker R & Dhawan A. A flow cytometric method to assess nanoparticle uptake in bacteria. Cytometry A 2011;79: 707-12.
Curia, R., Milani, M., Didenko, L., Avtandilov, G., Shevlyagina, N. & Smirnova, T. (2014). Beyond the biodestruction of polyurethane: S. aureus uptake of nanoparticles is a challenge for toxicology. Formatex Research Center.
[66] Jiang W, Ghosh S, Song L, Vachet RW & Xing B. Effect of Al_2O_3 nanoparticles on bacterial membrane amphiphilic biomolecules. Colloids Surf B Biointerfaces 2013;102: 292-9.
[67] Fortunelli A & Monti S. Simulations of lipid adsorption on TiO_2 surfaces in solution. Langmuir 2008;24: 10145-54.
[68] Xing K, Chen XG, Liu CS, Cha DS & Park HJ. Oleoyl-chitosan nanoparticles inhibit *Escherichia coli* and *Staphylococcus aureus* by damaging the cell membrane and putative binding to extracellular or intracellular targets. Int J Food Microbiol 2009;132: 127-33.
[69] Luo Y, Hossain M, Wang C, Qiao Y, An J, Ma Let al.. Targeted nanoparticles for enhanced X-ray radiation killing of multidrug-resistant bacteria. Nanoscale 2013;5: 687-94.
[70] Peulen T & Wilkinson KJ. Diffusion of nanoparticles in a biofilm. Environ Sci Technol 2011;45: 3367-73.
[71] Messiaen A, Forier K, Nelis H, Braeckmans K & Coenye T. Transport of nanoparticles and tobramycin-loaded liposomes in Burkholderia cepacia complex biofilms. PLoS One 2013;8: e79220.
[72] Nair S, Sasidharan A, Divya Rani VV, Menon D, Nair S, Manzoor Ket al.. Role of size scale of ZnO nanoparticles and microparticles on toxicity toward bacteria and osteoblast cancer cells. J Mater Sci Mater Med 2009;20 Suppl 1: S235-41.
[73] Morones JR, Elechiguerra JL, Camacho A, Holt K, Kouri JB, Ramírez JTet al.. The bactericidal effect of silver nanoparticles. Nanotechnology 2005;16: 2346-53.
[74] Naberezhnykh GA, Gorbach VI, Likhatskaya GN, Bratskaya SY & Solov'eva TF. Interaction of N-acylated and N-alkylated chitosans included in liposomes with lipopolysaccharide of Gram-negative bacteria. Biochemistry (Mosc) 2013;78: 301-8.
[75] Ahmed K, Gribbon PN & Jones MN. The application of confocal microscopy to the study of liposome adsorption onto bacterial biofilms. J Liposome Res 2002;12: 285-300.
[76] Ahmed K & Jones MN. The effect of shear on the desorption of liposomes adsorbed to bacterial biofilms. J Liposome Res 2003;13: 187-97.
[77] Kim H & Jones MN. The delivery of benzyl penicillin to *Staphylococcus aureus* biofilms by use of liposomes. J Liposome Res 2004;14: 123-39.
[78] McAllister SM, Alpar HO & Brown MR. Antimicrobial properties of liposomal polymyxin B. J Antimicrob Chemother 1999;43: 203-10.

[79] Ma Y, Wang Z, Zhao W, Lu T, Wang R, Mei Qet al.. Enhanced bactericidal potency of nanoliposomes by modification of the fusion activity between liposomes and bacterium. Int J Nanomedicine 2013;8: 2351-60.
[80] Wei G, Liu X, Yuan L, Ju X, Chu L & Yang L. Lipid composition influences the membrane-disrupting activity of antimicrobial methacrylate co-polymers. J Biomater Sci Polym Ed 2011;22: 2041-61.
[81] Papahadjopoulos D, Jacobson K, Nir S & Isac T. Phase transitions in phospholipid vesicles. Fluorescence polarization and permeability measurements concerning the effect of temperature and cholesterol. Biochim Biophys Acta 1973;311: 330-48.
[82] Tseng L, Liang H, Chung T, Huang Y & Liu D. Liposomes incorporated with cholesterol for drug release triggered by magnetic field. J Med Biol Eng 2007;27: 29-34.
[83] Beaulac C, Clément-Major S, Hawari J & Lagacé J. Eradication of mucoid Pseudomonas aeruginosa with fluid liposome-encapsulated tobramycin in an animal model of chronic pulmonary infection. Antimicrob Agents Chemother 1996;40: 665-9.
[84] Sachetelli S, Khalil H, Chen T, Beaulac C, Sénéchal S & Lagacé J. Demonstration of a fusion mechanism between a fluid bactericidal liposomal formulation and bacterial cells. Biochim Biophys Acta 2000;1463: 254-66.
[85] Drulis-Kawa Z, Gubernator J, Dorotkiewicz-Jach A, Doroszkiewicz W & Kozubek A. In vitro antimicrobial activity of liposomal meropenem against *Pseudomonas aeruginosa* strains. Int J Pharm 2006;315: 59-66.
[86] Sachetelli S, Beaulac C, Riffon R & Lagacé J. Evaluation of the pulmonary and systemic immunogenicity of Fluidosomes, a fluid liposomal-tobramycin formulation for the treatment of chronic infections in lungs. Biochim Biophys Acta 1999;1428: 334-40.
[87] Nandakumar V, Geetha V, Chittaranjan S & Doble M. High glycolic poly (DL lactic co glycolic acid) nanoparticles for controlled release of meropenem. Biomed Pharmacother 2013;67: 431-6.
[88] Kalhapure RS, Mocktar C, Sikwal DR, Sonawane SJ, Kathiravan MK, Skelton Aet al.. Ion pairing with linoleic acid simultaneously enhances encapsulation efficiency and antibacterial activity of vancomycin in solid lipid nanoparticles. Colloids Surf B Biointerfaces 2014;117: 303-11.
[89] Abdelghany SM, Quinn DJ, Ingram RJ, Gilmore BF, Donnelly RF, Taggart CC *et al.* Gentamicin-loaded nanoparticles show improved antimicrobial effects towards *Pseudomonas aeruginosa* infection. Int J Nanomedicine 2012;7: 4053-63.
[90] Imbuluzqueta E, Gamazo C, Lana H, Campanero MÁ, Salas D, Gil AGet al.. Hydrophobic gentamicin-loaded nanoparticles are effective against *Brucella melitensis* infection in mice. Antimicrob Agents Chemother 2013;57: 3326-33.
[91] Vrignaud S, Benoit J & Saulnier P. Strategies for the nanoencapsulation of hydrophilic molecules in polymer-based nanoparticles. Biomaterials 2011;32: 8593-604.
[92] Li C, Zhang X, Huang X, Wang X, Liao G & Chen Z. Preparation and characterization of flexible nanoliposomes loaded with daptomycin, a novel antibiotic, for topical skin therapy. Int J Nanomedicine 2013;8: 1285-92.
[93] Liu X, Sun W, Zhang B, Tian B, Tang X, Qi Net al.. Clarithromycin-loaded liposomes offering high drug loading and less irritation. Int J Pharm 2013;443: 318-27.

[94] Lutwyche P, Cordeiro C, Wiseman DJ, St-Louis M, Uh M, Hope MJ *et al*. Intracellular delivery and antibacterial activity of gentamicin encapsulated in pH-sensitive liposomes. Antimicrob Agents Chemother 1998;42: 2511-20.
[95] Drulis-Kawa Z, Dorotkiewicz-Jach A, Gubernator J, Gula G, Bocer T & Doroszkiewicz W. The interaction between *Pseudomonas aeruginosa* cells and cationic PC:Chol:DOTAP liposomal vesicles *versus* outer-membrane structure and envelope properties of bacterial cell. Int J Pharm 2009;367: 211-9.
[96] Düzgünes N, Nir S, Wilschut J, Bentz J, Newton C, Portis A *et al*. Calcium- and magnesium-induced fusion of mixed phosphatidylserine/phosphatidylcholine vesicles: effect of ion binding. J Membr Biol 1981;59: 115-25.
[97] Otto M. Staphylococcal biofilms. Curr Top Microbiol Immunol 2008;322: 207-28.
[98] Sanderson NM, Guo B, Jacob AE, Handley PS, Cunniffe JG & Jones MN. The interaction of cationic liposomes with the skin-associated bacterium *Staphylococcus epidermidis*: effects of ionic strength and temperature. Biochim Biophys Acta 1996;1283: 207-14.

Chapitre 2

Développement des liposomes stabilisés stériquement comme vecteurs du S-nitrosoglutathion pour cibler les macrophages

"Elaboration of Sterically Stabilized Liposomes for S-nitrosoglutathione Targeting to Macrophage"

Le chapitre 2 représente un travail original traitant le développement des nanoliposomes encapsulant le *S*-nitrosoglutathion (GSNO), un donneur endogène de l'oxyde nitrique, comme une nouvelle thérapeutique antibactérienne. Ce travail est publié dans le *Journal of Biomedical Nanotechnology*.

Article

Journal of
Biomedical Nanotechnology
Vol. 11, 1–14, 2015
www.aspbs.com/jbn

Elaboration of Sterically Stabilized Liposomes for *S*-Nitrosoglutathione Targeting to Macrophages

R. Diab[1,*], A. S. Virriat[1], C. Ronzani[1], S. Fontanay[2], S. Grandemange[3], A. Elaissari[4], B. Foliguet[5], P. Maincent[1], P. Leroy[1], R. E. Duval[2], B. H. Rihn[1], and O. Joubert[1]

[1] *Université de Lorraine, CITHEFOR, EA 3452, Faculté de Pharmacie, Nancy, France*
[2] *CNRS, SRSMC, UMR 7565, Vandœuvre-lès-Nancy, France, Université de Lorraine, UMR 7565, Nancy, France ABC Platform®, Nancy, France*
[3] *CNRS, CRAN, UMR 7039, Vandœuvre-lès-Nancy, France Université de Lorraine, CRAN, UMR 7039, Vandœuvre-lès-Nancy, France*
[4] *CNRS, LAGEP, UMR 5007, Villeurbanne, France Université de Lyon, LAGEP, UMR 5007, Villeurbanne, France*
[5] *Université de Lorraine, Faculté de Médecine, Vandœuvre-lès-Nancy, France*

S-nitrosoglutathione (GSNO) is a potential therapeutic for infectious disease treatment because of its pivotal role in macrophage-mediated inflammatory responses and host defense in addition to direct antibacterial activities. In this study, sterically stabilized cationic liposomes (SSCL) and sterically stabilized anionic liposomes (SSAL) were developed as nanocarriers for macrophage targeting. Elaborated liposomes were characterized in terms of size, zeta potential, morphology, encapsulation efficiency, *in vitro* drug release behavior and cytotoxicity. Their versatility in targeting monocytes/macrophages was determined by confocal laser scanning microscopy and transmission electron microscopy. Flow cytometry revealed that cellular uptake of both SSCL and SSAL was governed by several endocytic clathrin- and caveolae-dependent mechanisms. Quantitative assessments of intracellular nitric oxide demonstrated highly efficient uptake of GSNO-loaded SSCL that was twenty-fold higher than that of GSNO-free molecules. GSNO-loaded SSCL displayed strong bacteriostatic effects on *Staphylococcus aureus* and *Pseudomonas aeruginosa*, which can be involved in pulmonary infectious diseases. These results reveal the potential of liposomal GSNO as an anti-infective therapeutic due to its macrophage targeting capacity and direct antibacterial effects.

KEYWORDS: *Antibacterial, Liposomes, Macrophages, Nitric Oxide, S-Nitrosoglutathione, Sustained Release, Targeting.*

L'oxyde nitrique (NO) est un médiateur biologique intervenant dans la défense innée, notamment dans la réponse inflammatoire médiée par les macrophages contre les attaques bactériennes et virales. L'objectif principal de la nanoencapsulation du GSNO est de réaliser une libération ciblée sélective dans les macrophages et/ou les cellules bactériennes.

Dans la cellule, le GSNO et le NO (libéré après clivage enzymatique de la liaison S-N) permettrait de renforcer les capacités de défense innée des macrophages mais aussi d'exercer un effet bactéricide direct. L'internalisation des nanoliposomes se ferait grâce à l'interaction fusionnelle de leur bicouche phospholipidique avec la membrane plasmique des macrophages ou avec la paroi bactérienne.

La nanoencapsulation permettrait donc de contrôler la libération de son cargo et d'empêcher ainsi une libération massive du NO, ce qui peut générer des effets délétères sur les tissus environnants suite à la formation d'espèces réactives de l'azote. En outre, l'encapsulation du GSNO permettrait d'augmenter sa stabilité physico-chimique, sachant qu'il s'agit d'une molécule extrêmement fragile, présentant une sensibilité à la chaleur, à la lumière et aux métaux lourds, même si la concentration de ces derniers est de quelques ppm.

La première partie de ce travail consiste en la mise au point du procédé d'encapsulation et des différentes techniques de caractérisation physico-chimique des nanoliposomes élaborés. La seconde partie se focalise sur l'interaction nanoliposome-macrophage et les mécanismes d'internalisation potentiels mis en jeu. La dernière partie concerne l'évaluation de l'activité antibactérienne directe des nanoliposomes sur différentes souches bactériennes.

La plupart des hypothèses émises au départ du projet, ont été vérifiées. D'une façon très intéressante, les nanoliposomes développés se sont montrés capables de cibler les macrophages et d'y réaliser une concentration intracellulaire en NO 20 fois plus élevées, par rapport à la molécule libre (non encapsulée). De plus, une forte activité bactériostatique a été observée sur *Staphyloccocus aureus* et *Pseudomonas aeruginosa*, des souches bactériennes impliquées dans les infections nosocomiales récalcitrantes.

Elaboration of Sterically Stabilized Cationic and Anionic Liposomes for *S*-nitrosoglutathione Targeting to Macrophages

R. Diab[a]†, A. S. Virriat[a], C. Ronzani[a], S. Fontanay[b], S. Grandemange[c], A. Elaissari[d], B. Foliguet[e], P. Maincent[a], P. Leroy[a], R. E. Duval[b], B. H. Rihn[a] and O. Joubert[a]

[a] *Université de Lorraine, CITHEFOR, EA 3452, Faculté de Pharmacie, Nancy, France*

[b] *CNRS, SRSMC, UMR 7565, Vandœuvre-lès-Nancy, France*
Université de Lorraine, UMR 7565, Nancy, France
ABC Platform®, Nancy, France

[c] *CNRS, CRAN, UMR 7039, Vandœuvre-lès-Nancy, France*
Université de Lorraine, CRAN, UMR 7039, Vandœuvre-lès-Nancy, France

[d] *CNRS, LAGEP, UMR 5007, Villeurbanne, France*
Université de Lyon, LAGEP, UMR 5007, Villeurbanne, France

[e] *Université de Lorraine, Faculté de Médecine, Vandœuvre-lès-Nancy, France*

† **To whom correspondence should be directed**
Dr. Roudayna Diab
CITHEFOR, EA 3452, Faculty of Pharmacy
University of Lorraine
5, rue Albert Lebrun, BP 80403
54001 Nancy Cedex
E. mail: roudayna.diab@univ-lorraine.fr

A b s t r a c t

S-nitrosoglutathione (GSNO) is a potential therapeutic for infectious disease treatment because of its pivotal role in macrophage-mediated inflammatory responses and host defense in addition to direct antibacterial activities. In this study, sterically stabilized cationic liposomes (SSCL) and sterically stabilized anionic liposomes (SSAL) were developed as nanocarriers for macrophage targeting. Elaborated liposomes were characterized in terms of size, zeta potential, morphology, encapsulation efficiency, *in vitro* drug release behavior and cytotoxicity. Their versatility in targeting monocytes/macrophages was determined by confocal laser scanning microscopy and transmission electron microscopy. Flow cytometry revealed that cellular uptake of both SSCL and SSAL was governed by several endocytic clathrin- and caveolae-dependent mechanisms. Quantitative assessments of intracellular nitric oxide demonstrated highly efficient uptake of GSNO-loaded SSCL that was twenty-fold higher than that of GSNO-free molecules. GSNO-loaded SSCL displayed strong bacteriostatic effects on *Staphylococcus aureus* and *Pseudomonas aeruginosa*, which can be involved in pulmonary infectious diseases. These results reveal the potential of liposomal GSNO as an anti-infective therapeutic due to its macrophage targeting capacity and direct antibacterial effects.

Key words: *antibacterial, liposomes, macrophages, nitric oxide, S-nitrosoglutathione, sustained release, targeting.*

1 . I n t r o d u c t i o n

Macrophages are therapeutic targets of increasing importance because they are situated at the crossroads of several pathological pathways. Their central roles in the pathogenesis of numerous diseases, including cancer [1], infectious [2], inflammatory [3] and autoimmune [4] diseases, atherosclerosis [5] and metabolic disorders [6], have been well established. Macrophage-targeted therapeutics have potentially significant treatment benefits. Macrophages could be considered secondary drug reservoirs that are able to disseminate in the body and selectively deliver drug cargo to sites of action [7]. Macrophages are the immune system's first line of defense. They act as reservoirs for viruses [8], bacteria [9] and parasites [10] and are involved in the pathogenesis of many deadly infectious diseases. Macrophages have been increasingly attractive therapeutic targets for various anti-infective agents. Micro- and nanoparticulate systems have been developed to enable enhanced efficacy of the loaded drug. For instance, rifampicin-loaded microspheres developed for the treatment of tuberculosis achieved an intra-macrophage drug concentration that was seven-fold higher compared to the free drug concentration [11]. More recently, liposomal formulations of polyene macrolide antibiotics have proven to be more effective in treating systemic mycosis by targeting circulating monocytes/macrophages and transporting them to infection sites [12].

S-nitrosoglutathione (GSNO) is an endogenously occurring reservoir and transporter of nitric oxide (NO), playing a pivotal role in physiological processes such as pulmonary function regulation, macrophage-mediated inflammatory response and host defense [13]. GSNO contributes to the bactericidal activities of macrophages and neutrophils. NO (released from GSNO) interacts with other free radicals, including superoxide ions produced by macrophages, and leads to formation of reactive nitrogen species (RNS) such as peroxynitrite,

a powerful oxidant species capable of inducing lipid peroxidation and cellular damage [14, 15]. Moreover, GSNO has been shown to display direct antibacterial activities [16]. It can interact directly or indirectly via NO-donating, with thiol groups in proteins and metal-containing enzymes of the respiratory cycle and the DNA synthetic pathway, thereby blocking bacterial respiration and DNA replication, respectively [17].

Achieving high local and sustained intracellular concentrations in macrophages is thought to potentiate GSNO antibacterial activities, particularly against infections caused by multidrug resistance bacteria, which constitutes a public health concern. Due to its crucial involvement in the inflammatory process, targeting the mononuclear phagocytic system represents a key endpoint in the treatment of deadly disease-associated infections, including those arising from chronic obstructive pulmonary disease, asthma and cystic fibrosis in which the inflammatory process is a key driver of both disease progression and pathogenesis [18]. Taking into account the well-elucidated role of GSNO in down-regulating the inflammatory process [19, 20, 21], the development of GSNO-based therapeutics for targeting macrophages could improve treatment of such diseases.

Liposomes are the leading drug delivery systems for targeting macrophages because of their natural recognition by the mononuclear phagocytic system, particularly macrophages. Furthermore, targeting macrophages could be enhanced by adjusting liposome physicochemical properties, such as size, zeta potential and lipid composition [18]. Unfortunately, available data regarding optimal vesicle size are controversial. Some studies have reported that liposomes smaller than 100 nm showed increased cellular uptake compared to larger liposomes [22, 23], whereas other studies suggest enhanced liposomal uptake with increasing size [24, 25].

With regard to their zeta potential, both cationic and anionic liposomes have been used for targeting macrophages. Cationic liposomes have been shown to be particularly efficient for intracellular trafficking and are commonly used for gene delivery. They have been used for targeting different cell types, including macrophages [26] and endothelial cells from angiogenic tumor vasculature [27, 28]. Nevertheless, some issues concerning toxicity aspects inherent to cationic liposomes have been raised. Recent findings showed that electrostatic interactions between cationic lipids in liposomes and proteoglycan at the cell surface appear to trigger apoptosis by activating protein kinase C δ via the proteoglycan-actin cytoskeleton-ROS generation pathway [29]. These drawbacks could be mitigated by reducing the cationic lipid content in liposomes. Another possibility is to introduce a phospholipid conjugated with a hydrophilic polymer block such as poly(ethylene glycol) (PEG) (PEGylated phospholipid). This forms a hydrophilic brush at the liposome surface that hampers interactions between cationic lipids and the proteoglycan at the cell surface [30]. In addition to reduced toxicity, PEGylated phospholipids can stabilize the fluid liposomal wall by steric hindrance. Cationic liposomes containing PEGylated phospholipid are called sterically stabilized cationic liposomes (SSCL). Unlike conventional sterically stabilized liposomes, or “stealth liposomes”, SSCL are readily recognized by macrophages [30, 31].

Anionic liposomes have also attracted the interest of many researchers for macrophage targeting, particularly those containing negatively charged phospholipids, such as phosphatidylserine and phosphatidylglycerol, which have been shown to be more efficiently taken up by macrophages than neutral liposomes [22]. It is believed that anionic liposomes are

recognized by macrophages as necrotic cells exposing negatively charged phospholipids at their outer surfaces. Hence, anionic liposomes are likely able to interact with scavenger receptors at the macrophage cell membrane and thereby be taken up via a non-opsonic process [32].

In this study, anionic and cationic liposomes were evaluated as potential GSNO delivery systems targeting macrophages. Liposomes were prepared by the solvent-spherule evaporation method, a simple and scalable method that does not require heating or freezing steps that could alter GSNO integrity during preparation. Liposomes were characterized in terms of size, zeta potential, morphology, encapsulation efficiency, *in vitro* drug release profile and cytotoxicity. Their capacity to target macrophages was assessed qualitatively using confocal laser scanning microscopy (CLSM) and transmission electron microscopy and quantitatively by assessing liposomal GSNO internalization. The mechanisms of cellular internalization of anionic and cationic liposomes were investigated by flow cytometry. Finally, the antibacterial activity of liposomal GSNO was determined using two Gram-negative and two Gram-positive bacterial strains.

To our knowledge, no research has been reported to date concerning GSNO encapsulation in liposomes. This is likely due to GSNO stability issues. Short exposures to light or relatively high temperatures or the presence of trace amounts of heavy metals can induce rapid GSNO degradation into oxidized glutathione (GSSG) and NO that oxidizes instantly into nitrite. Accordingly, preparation methods require drastic handling conditions. In addition, GSNO is a small hydrophilic molecule that is subject to leakage during the encapsulation process, leading to low encapsulation efficiencies in biodegradable nanoparticles, as observed in preliminary experiments conducted in our laboratory.

2. Materials and methods

2.1. Materials

S-nitrosoglutathione was synthesized and its purity was determined as previously described [33]. Hydrogenated soybean phosphatidylcholine (HSPC), dipalmitoyl-sn-glycero-3-phospho-rac-glycerol sodium salt (DPPG), and *N*-(carbonyl-methoxypolyethylene glycol-5000)-1,2-dipalmitoyl-*sn*-glycero-3-phosphoethanolamine sodium salt (DPPE-PEG) were purchased from Lipoid AG (Steinhausen, Switzerland). Cholesterol (CH), stearylamine (SA), Triton X-100, osmium tetroxide, tetrasodium ethylenediamine tetraacetate (EDTA), sodium nitrate, sulfanilamide, *N*-1-(naphthyl)ethylenediamine, mercury (II) chloride ($HgCl_2$) and Nile Red (NR) were all purchased from Sigma-Aldrich (Saint Quentin Fallavier, France).

Hoechst 33342 (2'-[4-ethoxyphenyl]-5-[4-methyl-1-piperazinyl]-2,5'-bi-1H-benzimidazole trihydrochloride trihydrate) was purchased from Invitrogen (Val de Reuil, France). Iron (II) chloride tetrahydrate ($FeCl_2$, $4H_2O$), iron (III) chloride hexahydrate ($FeCl_3$, $6H_2O$), hydrochloric acid, acetic acid, ammonia, tetramethyl ammonium hydroxide 1 M, potassium hydroxide, and hexamethylenediamine were purchased from Merck (Fontenay sous Bois, France). DextranT40 was purchased from Amersham Biosciences (Orsay, France). Ultrapure deionized water (>18 $M\Omega.cm^{-1}$) was used in all experiments. Analytical grade chloroform was used (Carlo Erba Reagents, Val de Reuil, France).

2.2. Encapsulation screening

The Bangham method, which requires a heating step for at least 2 h, was evaluated as a strategy for GSNO-loaded liposome preparation by assessing GSNO stability under heating conditions. One milliliter of a 10^{-4} M GSNO aqueous solution was placed in a hermetically sealed 1.5 mL Eppendorf tube and submerged in a 55°C water bath with gentle horizontal stirring. After 1 or 2 h of incubation, tubes were opened and GSNO and nitrite were assayed according to the Griess-Saville and Griess methods [34], respectively. This test was performed in triplicate.

2.3. Preparation of liposomes

Liposomes were prepared according to the solvent-spherule evaporation method introduced by Kim *et al*. [35, 36] with slight modifications. First, a primary water/oil emulsion was prepared from an internal aqueous phase consisting of GSNO dissolved in a 10 mM EDTA solution in ultrapure water and an organic phase composed of phospholipids and cholesterol dissolved in chloroform with a total lipid concentration of 0.11 M. Qualitative and quantitative liposome compositions are shown in Table 1. Emulsification was performed in an ice bath using a 3 mm ultrasonic probe (Vibracell 75022, Bioblock, Illkirch, France) at 40% maximal amplitude for 1 min. The primary emulsion obtained was introduced into an external aqueous phase composed of a 10 mM EDTA solution in ultrapure water. Secondary emulsification was performed in an ice bath using a 6 mm ultrasonic probe at 80% maximal amplitude for 1 min, leading to formation of a double water/oil emulsion. Finally, chloroform and one part water were removed by evaporation under reduced pressure at room temperature using a rotary evaporator (Heidolph 94200, Bioblock, Illkirch, France). The resulting liposomes were recovered by ultracentrifugation for 1 h at 135000 × *g* and re-suspended in an appropriate medium for further investigation.

2.4. Characterization of liposomes

2.4.1. Vesicle size and zeta potential analysis

Mean vesicle size of drug-free and drug-loaded liposomes were determined by photon correlation spectroscopy (PCS) using Malvern Zetasizer 3000E (Malvern Instruments, Worcestershire, UK) after sample dilution in water. Zeta potential was measured by Smoluchowski's equation [37] for electrophoretic mobility of liposomes. All measurements were performed in triplicate at 25°C.

2.4.2. Encapsulation efficiency

Liposome encapsulation efficiency was measured by determining the amount of entrapped drug (E_{drug}) using the ultracentrifugation technique [38]. Briefly, a defined volume of the drug-loaded liposome sample was ultracentrifuged to separate the unloaded drug. The pellet was suspended in a 16 mM Triton X-100 solution and placed in an ultrasonic bath until a limpid solution was obtained. An equal volume of the liposome suspension was used to assess the total amount of the drug (T_{drug}) present in the suspension. Similarly, T_{drug} was measured after liposomes were dissolved and disrupted in a 16 mM Triton X-100 solution using an ultrasonic bath.

Drug encapsulation efficiency (EE %) was expressed as the percentage of encapsulated drug concentration (E_{drug}) relative to the total concentration (T_{drug}), as follows: $EE\% = \frac{E_{drug}}{T_{drug}} \times 100$

Determination of total and encapsulated drug concentration was performed using a colorimetric method according to Griess-Saville [34]. Degradation of GSNO into nitrite during liposome preparation and/or drug extraction was assessed using the Griess assay [34]. Briefly, samples were diluted with acetoacetic buffer (pH 2.5; 1.75 M) to a final volume of 1 mL. Calibration curves were established in the 10^{-6} - 10^{-5} M range using sodium nitrite and GSNO as standards for the Griess and Saville-Griess assays, respectively. Standards were prepared in a 16 mM Triton X-100 solution to which lipids used in liposome preparation were added in the same proportions used in formulation. Standard solutions were then subjected to an ultrasonic bath until clear solutions were obtained.

For the Griess assay, 200 µL of sulfanilamide solution (0.6 % w/v prepared in 0.4 M HCl) was added to the previously diluted sample. After a 3-min incubation in the dark at room temperature (22 ± 2 °C), 50 µL of a *N*-1-(naphthyl)ethylenediamine solution (0.6 % w/v prepared in 0.4 M HCl) was added. After a 5 min incubation, absorbance was read at 540 nm. The same operating conditions were used for the Saville-Griess method, but the sulfanilamide solution included $HgCl_2$ (0.2 % w/v).

All tests were performed in triplicate, and results are expressed as the mean ± standard deviation.

2.4.3. Morphological study by transmission electron microscopy

Liposome suspensions were imaged using a transmission electron microscope (TEM) (Philips CM12, FEI Electron Optics, Eindhoven, The Netherlands). A drop of the liposome suspension was placed onto a carbon-coated copper grid, forming a thin liquid film. Sample excess was removed with filter paper. Liposomes were negatively-stained by exposing the grid to the vapor of a 1% osmium tetroxide solution (w/w) deposited onto filter paper and placed in a sample chamber for 5 min. Finally, the grid was dried at room temperature, and liposome imaging was performed using an accelerating voltage of 80 kV.

2.5. *In vitro* release

GSNO-loaded liposome *in vitro* release studies were performed using a dialysis tube (dialysis tubing cellulose membrane, molecular weight cut-off 10395 Da, Sigma-Aldrich Chemie GmbH PO, Taufkirchen, Germany) at 37 °C in a water bath under gentle horizontal agitation. The dialysis tube was pre-treated for 1 h with phosphate-buffered saline (PBS, pH 7.4) to ensure wetting. A total of 500 microliters of liposome suspension in PBS (pH 7.4) was placed in the dialysis tube. The tube was immersed in 10 mL PBS (pH 7.4). The release medium volume was selected based on sink conditions.

At pre-determined time intervals, aliquot samples of the release medium were withdrawn and replaced with an equal volume of fresh release medium. GSNO concentrations in the release medium were determined using the Griess-Saville assay [34]. Nitrite presence in the release medium at each time interval using the Griess assay was also evaluated. Calibration curves ranging from 10^{-6} - 10^{-5} M were used, with sodium nitrate and GSNO solutions in the release

medium as standards for the Griess and Saville-Griess assays, respectively. All tests were performed in triplicate, and results are expressed as the mean ± standard deviation.

Table I. Physico-chemical characterization of liposomes. Results are expressed as the mean ± standard deviations. Each formulation was performed in triplicate and GSNO and nitrite were assayed thrice in each individual experiment.

Formulation		Constitutive lipids	Vesicle size (nm)	PDI[3]	Zeta potential (mV)	EE[4] (%)	Nitrite content[5] (% w/w)
SSCL[1]	GSNO-loaded liposomes	Mixture of HSPC/ CH/ SA/ DPPE-PEG at a molar ratio [2.4/1/0.7/0.03]	156 ± 10	0.192	16 ± 1	24 ± 2	5 ± 2
	Blank liposomes		155 ± 14	0.186	12 ± 2	-	-
SSAL[2]	GSNO-loaded liposomes	Mixture of HSPC/ CH/ DPPG/ DPPE-PEG at a molar ratio [2.4/1/0.3/0.03]	145 ± 21	0.232	-38 ± 7	22 ± 6	7 ± 3
	Blank liposomes		156 ± 18	0.201	-44 ± 3	-	-

Notes: [1]SSCL = sterically stabilized cationic liposomes; [2]SSAL = sterically stabilized anionic liposomes; [3]PDI = polydispersity index; [4]EE = encapsulation efficiency; [5]The nitrite content represents the percentage of nitrite assayed in harvested liposomes at the end of the preparation process relative to GSNO content.

2.6. Cytotoxicity studies

2.6.1. Cell line and cell culture

The human THP-1 monocyte cell line was obtained from American Type Culture Collection (ATCC, TIB-202TM, Manassas, VA, USA). Cells were grown in RPMI 1640 medium. For complete medium, 10% of heat-inactivated fetal bovine serum, 100 U/mL of penicillin, 100 µg/mL of streptomycin and 0.25 µg/mL of amphotericin B were added. Cells were grown at 37°C in 5% CO_2 and split every 3 days.

2.6.2. Cell viability assessment by trypan blue exclusion

Trypan blue exclusion assays were performed as previously described [39]. Cells were grown on 24-well microplates (Nalgene Nunc International, Rochester, NY) at a density of 1×10^5 cells per well in 0.9 mL of RPMI medium and incubated overnight at 37°C, 5% CO_2 and 95% air. Cells were incubated with 0.1 mL of a GSNO-loaded liposome suspension at predefined concentrations for 4 or 24 h. Three controls were used: cells without any treatment, cells treated with a GSNO aqueous solution (at the same concentration as the most concentrated liposome suspension, *i.e.* 20 µM) and cells treated with blank liposomes (at the same concentration as the most concentrated liposome suspension, *i.e.* 800 µg/mL). Enumeration was performed by immediate microscopic observation using a counting cell (KOVA® Glasstic®, HYCOR Biomedical Inc, California, USA). Numerations per sample were performed in triplicate. Cell viability was expressed as the percentage of living cells that did not incorporate trypan blue, indicating preservation of cell membrane integrity. Results were analyzed using one way ANOVA and Bonferroni post-hoc tests.

2.7. Cell uptake studies

2.7.1. Studies of liposome internalization by confocal laser scanning microscopy

Cell internalization of cationic and anionic liposomes was evaluated by CLSM. Liposomes were labeled by adding a lipophilic fluorescent dye (*i.e.* Nile Red) to the organic phase following the same liposome manufacturing process described in section 2.2.

Cells were seeded on 24-well microplates at a density of 3×10^5 cells/well in 0.9 mL RPMI medium and incubated at 37°C, 5% CO_2 and 95% air overnight. Cells were then incubated with 0.1 mL of the fluorescently-labeled liposome suspension at an equivalent lipid concentration of 4 mg/mL for 1 h.

After incubation with fluorescently-labeled liposomes, THP1 cells were washed thrice with PBS and treated with picric acid-formaldehyde (PAF, 4% v/v in PBS) in the dark at room temperature for 10 min. Cells were washed again with PBS three times and treated with Hoechst 33342 for 10 min in the dark at room temperature. Finally, cells were washed thrice with distilled water, dried at room temperature and stored in the dark at 4°C.

Observations were made using a confocal laser scanning microscope (Leica TCS SP2, Bensheim, Germany) with a 63x/1.32 numerical aperture oil-immersion objective lens.

2.7.2. Liposome internalization by transmission electron microscopy

To visualize cationic and anionic liposome internalization into cellular compartments, TEM was performed according to Eidi *et al.* [40]. Liposomes stained with 20 nm magnetic nanoparticles coated with dextran were used.

Preparation of dextran-coated magnetic nanoparticles consisted of dissolving 2 g of dextran in 7 mL of HCl 1 N and 5 mL of water. This solution was stirred at 60°C for 15 min. Ferrous and ferric chloride salts dissolved in 5 mL of water were added to the dextran solution under vigorous stirring. Ammonium hydroxide solution (10 mL) was then added to the mixture with vigorous stirring at 60 °C for 4 h. The final dispersion was cleaned via centrifugation-redispersion in water.

Magnetic staining of liposomes was achieved by introducing a magnetic nanoparticle aqueous dispersion to the internal aqueous phase following the same manufacturing process described in section 2.2.

Similar to CLSM studies, THP1 cells were incubated with a stained liposome suspension at an equivalent lipid concentration of 4 mg/mL. After a 1 h incubation, cells were fixed with 2.5 % w/v glutaraldehyde solution in cacodylate buffer (0.1 M, pH 7.2) and stored at 4°C. Cells were then treated with 1% w/v OsO_4 solution for 1 h at 4 °C, dehydrated using progressively increasing concentrations of ethanol and resin embedded. Ultrathin sections (70–90 nm) were achieved using an ultra-microtome (Reichert-Yung, Munich, Germany) and examined using a TEM Philips CM12 (FEI Electron Optics, Eindhoven, The Netherlands).

2.7.3. Liposome internalization

To gain insight into the mechanisms of cationic and anionic liposome cell internalization, THP1 cells were seeded on 24-well microplates at a density of 3×10^5 cells/well in 0.89 mL RPMI medium and incubated for 1 h at 37°C, 5% CO_2 and 95% air. Cells were then treated with 10 μL of a metabolic inhibitor solution (20 mM genistein, 0.5 M methyl-β-cyclodextrin

(MβCD), 1 mg/mL chlorpromazine or 2 mM cytochalasin D; Sigma-Aldrich, Saint Quentin Fallavier, France) for 1.5 h. Cells were then incubated with 0.1 mL of fluorescently-labeled liposome suspension at an equivalent lipid concentration of 4 mg/mL for 1 h. In wells treated with MβCD, an intermediate wash step was performed prior to addition of liposomes to the culture medium to avoid liposome interaction with MβCD, which is susceptible to disrupting the liposomal wall.

Cell viability following exposure to metabolic inhibitors was previously evaluated in our laboratory under the same conditions used in the cell uptake studies. Energy dependence internalization was determined by incubating cells with fluorescently-labeled liposomes at 4°C for 1 h.

Flow cytometry measurements from 10000 cells were collected using a FACSCalibur flow cytometer (Becton-Dickinson, Le Pont de Claix, France) equipped with an argon laser tuned to 488 nm. Nile Red fluorescence was analyzed using Cell Quest Pro software. Results from at least three independent biological replicates were averaged and expressed as the percentage of THP-1 control cells treated with fluorescently-labeled liposomes at 37°C. Baseline values were obtained for each data series from untreated control cells and systematically subtracted from the other assays.

2.7.4. Quantitative assessment of liposomal GSNO cell uptake

Quantitative assessment studies were conducted similar to the qualitative studies, with two differences to enhance assay sensitivity. First, cationic and anionic liposomes loaded with GSNO were incubated with THP1 cells for extended periods of time, *i.e.* 4 and 24 h. Second, the cell density was 5×10^5 cells/well/0.9 mL of culture medium. One hundred microliters of a 500 μM solution of free or liposomal GSNO was added to the culture medium. Three control conditions were used: untreated cells and cells incubated with equivalent concentrations of blank cationic or anionic liposomes (SSCL-B and SSAL-B, respectively).

At the end of the incubation period, cells were harvested by centrifugation (1000 × *g* for 10 min at 4°C) and washed with PBS. Cell lysis was performed with 0.25 mL of a Tris buffer (200 mM Tris, pH 7.5) containing 2 M NaCl, 20 mM EDTA and 3.2 mM Triton X-100. The cell suspension was vortexed for 15 min. The cell lysate was stored at 4°C for GSNO (or nitrosated cellular proteins) and sodium nitrite measurements by Saville-Griess and Griess assays, respectively. GSNO and sodium nitrite solutions in the lysis buffer at concentrations ranging from 10^{-6} - 10^{-5} M were used as standards for calibration curves. Sample and standard determination was performed in 96-well microplates, and absorbance was measured at 570 nm using a microplate reader.

Protein concentration in the cell lysate was determined using a bicinchoninic acid assay (BCA, Thermo Scientific, Illkirch, France) according to the manufacturer's specifications. A calibration curve was established using bovine serum albumin (BSA) solutions in the lysis buffer as standards. Absorbance was measured at 570 nm using a microplate reader.

2.8. Liposomal GSNO antibacterial activity assessments

2.8.1. Bacterial strains

Four bacterial strains (*Escherichia coli* ATCC 25922, *Staphylococcus aureus* ATCC 25213, *Enterococcus faecalis* ATCC 29212 and *Pseudomonas aeruginosa* ATCC 27853) were used

as reference strains following the guidelines of the Clinical and Laboratory Standards Institute (CLSI), formerly known as the National Committee for Clinical Laboratory Standards [41].

2.8.2. Minimum inhibiting concentration (MIC) determination

Preliminary studies showed that GSNO-loaded cationic liposomes exhibit higher antibacterial activity than anionic liposomes (data not shown). Hence, antibacterial activity studies were continued only for the former.

A colorimetric method employing a bacterial growth indicator [42] was used. Suspensions were prepared by suspending one isolated colony from Mueller Hinton plates in 5 mL of Mueller Hinton broth. After 24 h of growth at 35°C, the suspensions were diluted in distilled water to obtain a final inoculum of 5×10^5 to 5×10^6 colony forming nits (CFUs)/mL. The purity of the isolates was monitored throughout the study by examination of colony morphology and Gram staining. Two-fold serial dilutions of liposomal GSNO were prepared in Mueller Hinton broth in 96-well plates, starting from a stock solution of 4096 mg/L. Fifty microliters of prepared bacterial inocula were then distributed in each well, except for the negative controls.

After incubation for 24 h at 35°C, each well was treated with 10 µL of 5 mg/mL MTT solution (3-[4,5-dimethylthiazol-2-yl]-2,5-diphenyltetrazolium bromide; Sigma-Aldrich, Saint Quentin Fallavier, France) for 1.5 h. A total of 100 µL of 10% w/v SDS (sodium dodecyl sulfate; Sigma-Aldrich, Saint Quentin Fallavier, France) was added to dissolve formed formazan crystals. Absorbance at 540 nm was measured with an ELISA reader (Multiskan EX, Thermo Electron Corporation, France) and corrected for background noise (absorbance at 690 nm). MICs were determined as the lowest concentration of compound with an absorbance that was comparable to the negative controls (broth only or broth with drug, without inoculum). Results are expressed as the mean of four independent determinations.

MIC determination studies were similarly conducted for free GSNO or blank cationic liposomes as control conditions.

2.9. Statistical analysis

Statistical analysis was performed using the Graphpad Prism 3.0 software package. Differences between groups were analyzed using one way ANOVA and Bonferroni post-hoc tests. $P < 0.05$ was considered statistically significant.

3. Results and discussion

3.1. Screening the liposome manufacturing process

Given that GSNO integrity should be maintained during the preparation process, preliminary experiments were conducted to verify the sensitivity of GSNO to heating, as the Bangham method [43] was intended to be used for liposome elaboration. As a result of these experiments, 90 ± 3% and 48± 5% GSNO was present in the aqueous solution after 1 and 2 h of incubation, respectively, in a 10^{-4} M GSNO aqueous solution in a 55°C water bath with a gentle horizontal stirring. GSNO degradation was accompanied by nitrite formation in the aqueous solution.

Based on these results, the Bangham method for liposome preparation was discarded. The ethanol injection method [44] is an easy, one step process that does not require heating or shearing of the liposome constitutive phases and thus could be the most suitable method for

GSNO encapsulation. Unfortunately, this method could not be used for liposome preparation due to poor solubility of the selected phospholipids in ethanol.

All of the other currently known methods include a heating step and ether injection [45] or remote loading [46] methods. The detergent depletion technique [47] is not suitable for hydrophilic drug encapsulation because of drug leakage during multiple long detergent washing steps. Preliminary experiments conducted in our laboratory using the reverse-phase evaporation method [48] gave rise to micro-sized liposomes, which are beyond the scope of this study.

The solvent-spherule evaporation method [35] was selected for GSNO-loaded liposome manufacturing. This method does not include any heating steps, as the evaporation step can be performed at room temperature under reduced pressure, although it requires two homogenization steps to prepare the double emulsion. Nitrite formation in the final liposome suspension was systematically evaluated at the end of the preparation process (Table 1). The total GSNO concentration was assayed in the prepared liposome suspension and compared with the weighed amount initially introduced in the formulation to assess drug degradation during the preparation process. Results showed that drug degradation into nitrite was not more than 7 ± 3% (Table 1). EDTA was introduced in the formulation to confer enhanced stability of liposomal GSNO. This chelating agent is commonly used in liposome encapsulating drugs that are sensitive to oxidation [49, 50, 51], particularly due to heavy metal traces present in marketed phospholipids, according to the supplier's analysis sheets.

3.2. Physico-chemical characterization of liposomes

Two different formulations were developed for liposomal encapsulation of GSNO; sterically stabilized cationic liposomes (SSCL) and sterically stabilized anionic liposomes (SSAL) (Table 1).

Formulation and process parameters were selected based on preliminary experiments conducted in our laboratory with a goal of obtaining monodiperse nano-sized liposomes. Both formulations were based on phospholipids containing saturated long hydrocarbon chains to obtain liposomes with a rigid structure that are highly resistant to oxidation. All of these lipids have transition temperatures higher than 37°C, making the liposomal wall less fluid and leaky at physiological temperatures.

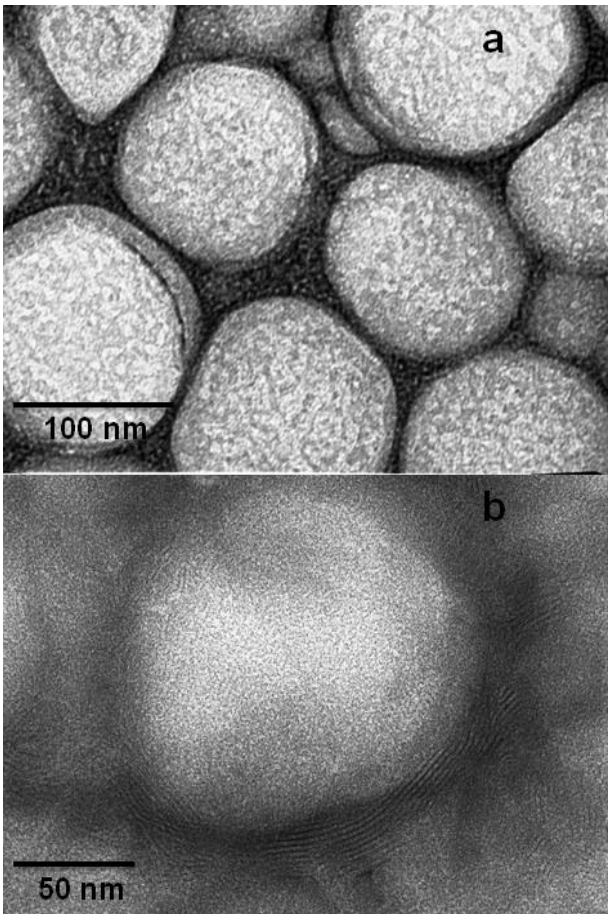

Fig. 1. TEM micrographs of GSNO-loaded sterically stabilized cationic liposomes (SSCL): a) Overview, b) Individual liposome micrograph highlighting the multilamellar structure. Scale bars represent 100 and 50 nm, respectively.

A low percentage of PEGylated phospholipids added to the formulation is thought to reinforce liposomal wall stability and is widely used in liposome design strategy [52]. Sterically stabilized liposomes have steric protection conferred by a PEG brush at the liposome surface, thereby limiting its interaction with proteins and lipoproteins in biological media.
Previously published research has demonstrated that PEGylated phospholipids give rise to increased thermodynamic stability of the liposomal membrane because of decreased hydration of lipid headgroups in conjunction with increased hydration of the outer layer consisting of a PEG brush [53].

Sterically stabilized cationic liposomes
Blank and GSNO-loaded SSCL obtained were monodisperse nanosizing vesicles (155 ± 14 and 156 ± 10 nm, respectively). GSNO encapsulation did not induce an increase in vesicle size. However, a notable difference in zeta potential value between blank and GSNO-loaded SSCL was observed (12 ± 2 and 16 ± 1 mV, respectively). The difference in zeta potential values between blank and loaded liposomes could be explained by interaction between GSNO and the liposomal membrane. GSNO is likely to be encapsulated in both the aqueous cavity and within the phospholipid bilayers. SSCL have been shown to efficiently entrap GSNO, achieving an encapsulation efficiency of 24 ± 2%.
Analysis of SSCL morphology by TEM (Fig. 1) showed that liposomes were spherically-shaped and composed of several phospholipid bilayers (multilamellar) (Fig. 1a). According to TEM images, liposomes were monodisperse in size (100 to 130 nm) (Fig. 1b). Microscopic size results correlated well with the sizes obtained by PCS. These results support previous knowledge about the manufacturing process used, which is known to produce multilamellar vesicles [35]. Liposome lamellarity positively influences drug encapsulation efficiency and liposome stability in storage and has a significant impact on drug fate after cellular uptake [54, 55].

Sterically stabilized anionic liposomes
As expected, SSAL displayed negative zeta potential values (-44 ± 3 and -38 ± 7 mV for blank and GSNO-loaded SSAL, respectively). Vesicle sizes were 156 ± 18 and 145 ± 21 nm for blank and GSNO-loaded SSAL, respectively, which were similar to GSNO-loaded SSCL.
GSNO encapsulation efficiency (22 ± 6%) was similar to SSCL, suggesting that GSNO is primarily encapsulated in aqueous cavities in both types.

3.3. *In vitro* release kinetics
In vitro release studies were performed on SSCL and SSAL (Fig. 2 B and C). A control study was performed using a GSNO solution in PBS at an equivalent amount of encapsulated GSNO to evaluate retention due to drug interaction with the dialysis membrane (Fig. 2 A).
GSNO encapsulation in both SSCL and SSAL resulted in drug retention in the liposomes given that only 28 ± 7% and 21 ± 5% of GSNO was released within 8 h, respectively. Remaining amounts of GSNO in the dialysis bag were evaluated at the end of the release study.
Drug retention in liposomes is of great interest to avoid rapid and early drug release before reaching its target. Hence, improved drug retention could enable selective drug release in

target cells, such as endothelial cells, macrophages, and bacteria, which has already been demonstrated in the literature [56, 31, 27, 18].

The liposomes described in the present study would meet the goal of macrophage targeting.

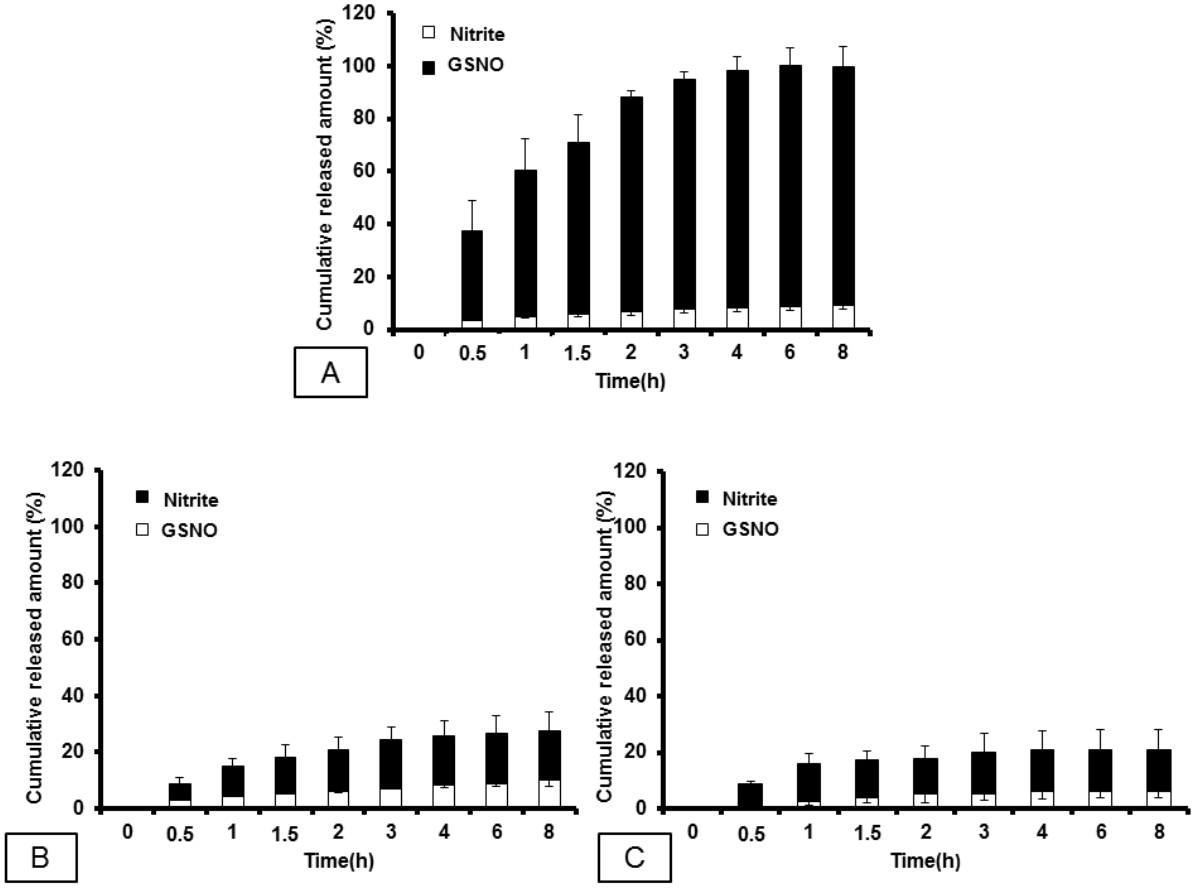

Fig. 2. GSNO release profile through dialysis tubes from a GSNO solution in PBS as the control (A), GSNO-loaded sterically stabilized cationic liposomes (SSCL) (B) and GSNO-loaded sterically stabilized anionic liposomes (SSAL) (C). Results are expressed as the mean ± SD (n=3). One hundred percent of released GSNO corresponds to a concentration of 3.4 × 10 $^{-5}$ M in the release medium.

3.4. Cytotoxicity studies

SSCL cytotoxicity was assessed in this study. To our knowledge, toxicity associated with anionic liposomes, which are composed of endogenously occurring phospholipids, has not been reported. Moreover, previously published research reports have demonstrated the safety of anionic liposomes at the studied concentrations/doses through *in vitro* and *in vivo* studies [57, 58, 59]. As such, toxicity investigations were focused on SSCL.

GSNO-loaded SSCL toxicity was evaluated after 4 and 24 h of incubation and compared to the equivalent amount of free GSNO and blank SSCL at the most concentrated liposome suspension (Fig. 3). After 4 h incubation, drug-loaded or blank liposomes did not show any toxic effects on THP1 cells, nor did the GSNO solution. There was no significant difference in cell viability for non-treated THP1 cells (control) over all of the concentrations evaluated. Cell viability was slightly decreased after 24 h incubation with GSNO-loaded liposomes (SSCL) at lipid concentrations of 800 and 400 µg/mL (81.52 ± 0.48 and 73.30 ± 1.19%, respectively) compared to the control. Under the same exposure conditions using blank

liposomes (SSCL-B), THP1 cell viability was significantly reduced to 36.18 ± 1.2% compared to the control.

No toxicity on THP1 cells after 24 h incubation was observed, as there was no significant difference relative to the control.

In conclusion, according to the toxicity classification proposed by Kong *et al.* [60], GSNO-loaded SSCL were considered non-toxic at lipid concentrations ≤ 400 µg/mL and slightly toxic at concentrations of 800 µg/mL.

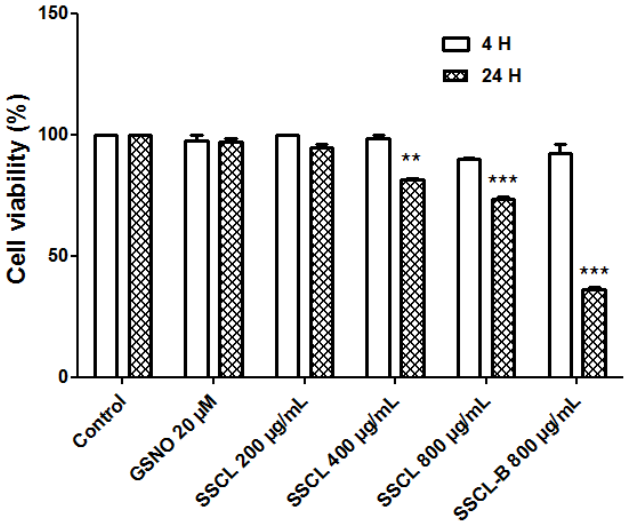

Fig. 3. Viability of human monocyte/macrophage THP1 cells after 4 or 24 h incubation at 37°C with GSNO-loaded sterically stabilized cationic liposomes (SSCL) at lipid concentrations of 200, 400 and 800 µg/mL and loaded-GSNO of 20, 10 and 5 µM, respectively. Three controls were used: cells without any treatment (control), cells treated with a GSNO aqueous solution (at the same concentration as the most concentrated liposome suspension, *i.e.* 20 µM) and cells treated with blank sterically stabilized cationic liposomes (SSCL-B) at the same concentration as the most concentrated liposome suspension, *i.e.* 800 µg/mL). The results are expressed as the average of three independent biological replicates. Error bars indicate standard deviations. **p<0.01 and ***p<0.001 vs. control.

Note: Conditions: 10^5 cells and 0.9 mL culture medium volume per well, 0.1 mL of liposomal suspension at equivalent lipid concentration of 2, 4 or 8 mg/mL.

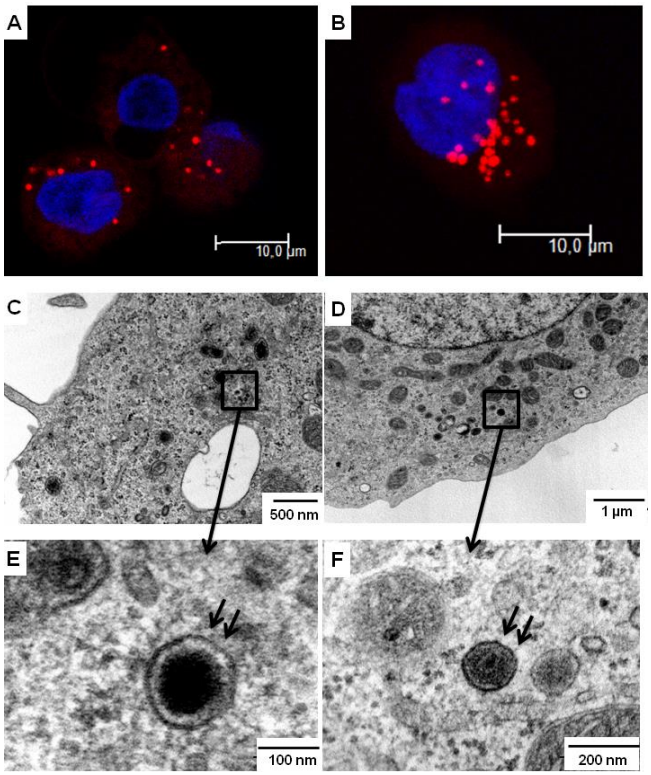

Fig. 4. Cell uptake of liposomes after a 1 h incubation period. A and B represent CLSM images of cell uptake of fluorescently-labeled SSAL and SSCL, respectively. Liposomes were labeled with Nile Red (red), while Hoechst 33342 was used to visualize nuclei (blue). C and D represent TEM images of cell uptake of magnetically-labeled SSAL and SSCL, respectively. E and F are TEM images at a higher magnification.

Note: Conditions: 3×10^5 cells and 0.9 mL culture medium volume per well, 0.1 mL of liposomal suspension at an equivalent lipid concentration of 4 mg/mL. SSCL and SSAL stand for sterically stabilized cationic liposomes and sterically stabilized anionic liposomes, respectively.

3.5. Cell uptake studies

3.5.1. Liposome internalization kinetics

Cell uptake was visualized by CLSM for both SSCL and SSAL after 1 h incubation at a final non-toxic lipid concentration of 400 µg/mL in the culture medium. Liposomes used in this study were labeled with a lipophilic dye, *i.e.* Nile Red (red in Fig. 4 A, B). Nuclei were

labeled by Hoechst 33342 (blue), allowing visualization of fluorescently-labeled liposomes localized in intracellular compartments.

After 1 h incubation, both types of liposomes were internalized and homogenously distributed in the cytoplasm (Fig. 4 A, B). No internalization in the nuclei was detected, which was confirmed by 3D reconstituion of different optic sections (data not shown).

CLSM results were confirmed by TEM (Fig. 4 C, D). No differences in THP1 cell spreading or morphology were observed. This indicates that, at the tested concentration, interactions between liposomes and cells did not result in any damage to cellular organelles or the cytoplasmic membrane, which is consistent with cytotoxicity results. Consequently, cytoplasmic delivery of liposomes could not be explained by a disruption in the cell membrane. In addition, TEM suggests that the liposomal structure was conserved during the internalization process, as shown by isolated spherical electron dense material in the cytoplasm (Fig. 4 E, F).

A 1 h incubation was selected for investigating internalization mechanisms in subsequent experiments.

3.5.2. Liposome internalization mechanism

Before conducting these studies, several investigations were undertaken. First, lack of toxicity of metabolic inhibitors on cells at specific concentrations was verified (data not shown). Second, the inability of Nile Red-free molecules to be taken up by cells was evaluated by CLSM (data not shown). Third, cells were incubated at 37 or 4°C to determine the relative level of liposome internalization by energy-dependent or independent mechanisms, respectively. At 4°C, cell uptake of fluorescently-labeled liposomes was markedly inhibited at 64 ± 2 and 58 ± 4% for SSCL and SSAL, respectively (Fig. 5).

For both type of liposomes, uptake inhibition was not 100%, suggesting that they may interact with cells via energy-independent processes. It is conceivable that the remaining fraction is associated with the plasma membrane or internalized through a fusion process.

Considering the energy-dependent uptake of both SSCL and SSAL and to clarify the mechanisms involved, different inhibitors were screened. Genistein, chlorpromazine and methyl-β-cyclodextrin were used as inhibitors of caveolae-dependent, clathrin-dependent and cholesterol-dependent endocytosis, respectively, whereas cytochalasin D, an inhibitor of actin polymerization, was used as a phagocytosis inhibitor.

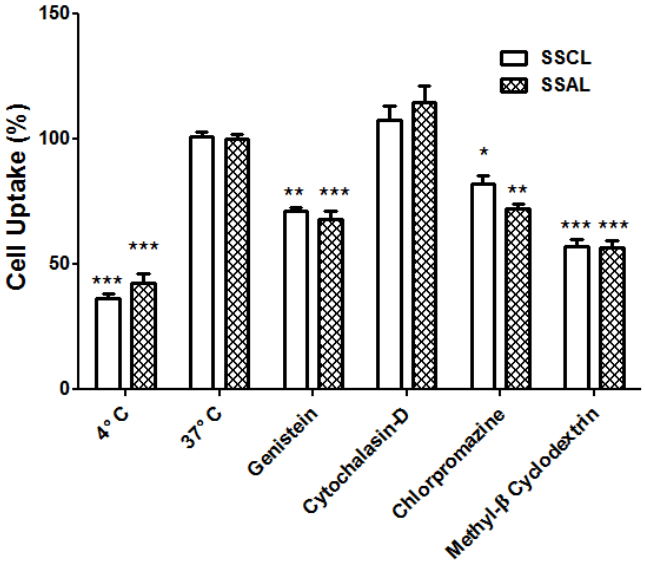

Fig. 5. Effects of different inhibitors on liposome cell uptake. Cell-associated fluorescence was analyzed by flow cytometry. The results are expressed as the average of three independent biological replicates and presented as percentage of the control at 37°C. Error bars indicate standard deviations. *p<0.05, **p<0.01 and *** p<0.001 vs.
Note: Conditions: 3×10^5 cells and 0.9 mL culture medium volume per well, 0.1 mL of liposomal suspension at an equivalent lipid concentration of 4 mg/mL. SSCL and SSAL stand for sterically stabilized cationic liposomes and sterically stabilized anionic liposomes, respectively.

As shown in Fig. 5, genistein significantly reduced the cell uptake of both SSCL and SSAL to 71 ± 2 and 68 ± 3%, respectively.
Similarly, chlorpromazine induced a clear decrease in cell uptake for both SSCL and SSAL to 82 ± 3 and 72 ± 2%, respectively. The highest uptake inhibition was observed for cells treated with methyl-β-cyclodextrin, with uptake reduced to 57 ± 3 and 56 ± 3% for SSCL and SSAL, respectively. Methyl-β-cyclodextrin inhibits cholesterol-dependent endocytic processes by reversibly extracting the steroid out of the plasma membrane. Thus, a large fraction of uptake is dependent on the presence of cholesterol in the plasma membrane. Clathrin-independent endocytosis includes several pathways that share cholesterol dependency, among which caveolin-mediated endocytosis is probably the most thoroughly characterized [61]. Interestingly, cytochalasin D did not induce any inhibition of liposome internalization, irrespective of liposome type. This suggests that phagocytosis is not involved in liposome cell uptake processes.
In conclusion, regardless of liposome type, cell uptake was governed by several endocytic clathrin- and caveolae-dependent mechanisms. These results are in agreement with other published research [62, 63, 64, 65]. However, caveolae-dependent endocytosis seemed to be the most involved mechanism in liposome internalization. This result is of great interest for targeted drug delivery. In fact, the caveolae uptake pathway does not lead to fusion of endosomes with lysosomes in subsequent intracellular trafficking stages in which, due to the highly acidic environment, internalized drug substances could be degraded [66, 67].

3.5.3. Quantitative assessment of liposomal GSNO cell uptake

NO intracellular levels were 9.79 ± 0.38 and 11.23 ± 0.12 µmol/g protein when the cells were incubated with a 50 µM GSNO solution for 4 and 24 h, respectively. These values are not significantly different from NO levels in untreated control cells (7.71 ± 0.66 and 12.08 ± 0.78 µmol/g proteins at 4 and 24 h, respectively) (Fig. 6).

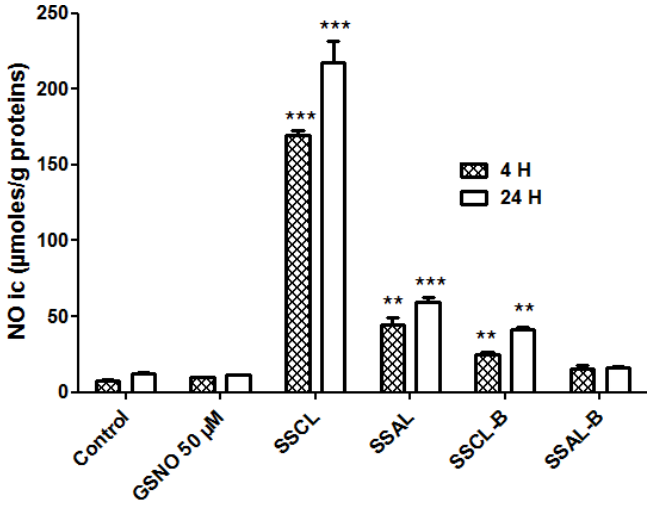

Fig. 6. NO intracellular concentrations in human monocyte/macrophage THP1 cells after 4 or 24 h incubation at 37°C with 50 µM of free or liposomal GSNO. Controls represent the NO intracellular concentration in untreated cells after a 4 or 24 h incubation in the culture medium. Results are expressed as the average of three independent biological replicates. Error bars indicate standard deviations. **p<0.01 and ***p<0.001 vs. control at 4 or 24 h.

Note: Conditions: 5 × 10^5 cells/0.9 mL/well, 0.1 mL of 500 µM of GSNO free or encapsulated in sterically stabilized cationic liposomes (SSCL) or sterically stabilized anionic liposomes (SSAL). Blank SSCL and SSAL (SSCL-B and SSAL-B) were used as controls.

Markedly higher levels of intracellular NO were measured when THP1 cells were incubated with liposomal GSNO. Intracellular NO levels were as high as 169.41 ± 3.28 and 217.75 ± 13.96 µmol/g proteins when THP1 cells were incubated with SSCL-encapsulated GSNO for 4

and 24 h, respectively (Fig. 6). SSAL-encapsulated GSNO cell delivery was also enhanced, as evidenced by NO intracellular levels, which were four-fold higher than levels in the GSNO solution.

These results demonstrate the high efficiency of liposomes, particularly SSCL, regarding macrophage intracellular delivery and their versatility in intracellular infection treatment. For instance, the crucial role of GSNO in controlling intracellular growth of H37Rv, a laboratory strain of *Mycobacterium tuberculosis*, in murine macrophages J774.1 has been demonstrated [68]. A bacteriostatic effect was observed when infected macrophages were treated by either lipopolysaccharide or interferon-γ. This treatment stimulates macrophage NO production and subsequently results in GSNO formation. Addition of an inhibitor of GSH synthesis resulted in significant H37Rv growth and inhibition of the bacteriostatic effect. This study is in agreement with our hypothesis regarding boosting macrophage anti-infectious ability by increasing intracellular GSNO.

3.6. Liposomal GSNO antibacterial activity studies

Due to the high uptake efficiency into monocytes/macrophages and based on preliminary tests, SSCL were selected to investigate antibacterial activity. First, antibacterial GSNO solution activity was evaluated at concentrations ranging from 2048 to 8 mg/L (6 to 0.02 mM). No obvious inhibition of bacterial growth was observed, irrespective of the bacterial strain. According to a recently published study [16], GSNO displayed effective inhibitory and bactericidal effects against Gram-positive and Gram-negative ATCC strains. However, these growth inhibitory effects have been observed at concentrations as high as 4.6 and 12.4 mM for Gram-positive and Gram-negative strains, respectively.

Table II. *In vitro* antibacterial activities of liposomal GSNO and blank liposomes against four laboratory strains: *E. coli, E. faecalis, S. aureus and P. aeruginosa*. No inhibition of growth activity was observed for free GSNO at concentrations ranging from 2048 to 8 mg/L.

	MIC[1] mg/L	
Bacterial strain	GSNO-loaded SSCL[2]	Blank SSCL
E. coli ATCC 25922	256	256
E. faecalis ATCC 29212	64	128
S. aureus ATCC 25213	8	4
P. aeruginosa ATCC 27853	32	64

Note: [1]MIC = minimum inhibiting concentration. Each determination was performed in quadruplicate; [2]SSCL = sterically stabilized cationic liposomes.

SSCL-encapsulated GSNO showed strong growth inhibitory effects on *S. aureus* and *P. aeruginosa* strains (Table 2), as evidenced by MIC values (8 and 32 mg/mL, respectively). The dramatically increased efficiency of liposomal GSNO is likely related to efficient bacterial internalization of GSNO when carried by liposomes. It would be interesting to confirm this hypothesis by imaging studies. A lower effect was observed on *E. faecalis* and even lower effect on *E. coli* strains (Table 2), with higher MIC values observed (64 and 256 mg/mL, respectively). These weak effects on *E. faecalis* and *E. coli* strains could be explained by the presence of compensatory mechanisms, such as denitrosylation. The latter was shown to be a bacterial pathogenesis of *E. coli* and other bacterial species, directly related to expression of nitric oxide reductase [69].

Blank SSCL displayed inhibitory growth effects that remain lower than those observed for SSCL (Table 2). The intrinsic antibacterial activities of cationic liposomes have already been reported in the literature [70]. A synergistic effect between cationic liposomes and their cargo is therefore expected.

We recently analyzed the transcriptome of THP-1 cells exposed to 50 µM of GSNO for 4 h [71]. Our results indicate that GSNO not only displays antibacterial activity, but also acts as a macrophage activator. This activation was possible with the involvement of at least 3 chemokines (CCL4, CCL3 and CCL20) and one cytokine (IL23A). Therefore, next steps in these *in vitro* studies will consist of studying the antibacterial activity of liposomal GSNO in macrophage-bacteria co-cultures.

4. Summary

In this study, GSNO, a small, labile endogenously occurring molecule, was successfully encapsulated in two types of liposomal nanocarriers: cationic and anionic. The nanocarriers met the prefixed objectives, *i.e.* narrowly distributed nanosized liposomes displaying convenient encapsulation efficiencies of up to 24 ± 2% while preserving drug integrity. Moreover, TEM studies showed that the liposomes displayed a multilamellar wall, suggesting a highly stable structure.

In vitro release studies of both types of liposomes confirmed controlled drug-release in which no more than 28 ± 7% and 21 ± 5% was released over 8 h for SSCL and SSAL, respectively. The major part of encapsulated GSNO remained inside the liposomes waiting to be delivered principally to the cellular target. This hypothesis was verified through *in vitro* cell uptake studies in the human monocyte/macrophage cell line THP1. The safety of SSCL was verified and non-toxic concentrations were determined and taken into account in subsequent experiments.

Qualitative uptake studies using CLSM and TEM showed relatively rapid internalization into THP1 cells for both types of liposomes. Over 1 h incubation, the fluorescence signal was detected in the perinuclear cytoplasm. According to TEM images, the integrity of liposomes appeared to be maintained during the internalization process. Flow cytometry studies helped to understand the mechanisms of liposome uptake by THP-1 via several endocytic pathways; caveolae-dependent endocytosis was the predominant mechanism involved. These results are of interest because the caveolae pathway is a unique in that endosomes do not fuse with lysosomes. Consequently, the drug will be protected from degradation in a highly acidic environment.

Quantitative assessment of intracellular NO demonstrated highly efficient uptake of GSNO encapsulated in SSCL and SSAL, which was twenty-fold and four-fold higher than that of GSNO-free molecules, respectively. These results directly confirm the versatility of SSCL and SSAL for macrophage targeting.

Interactions between free or SSCL-encapsulated GSNO and four bacterial strains were studied. According to MIC values obtained, SSCL-encapsulated GSNO showed strong bacteriostatic effects on *S. aureus* and *P. aeruginosa*, which are Gram-positive and Gram-negative bacterial strains, respectively; while no antibacterial activity was observed for free GSNO even at high concentrations (up to 2048 mg/L). In conclusion, SSCL-encapsulated GSNO could be promising for combating *S. aureus* and *P. aeruginosa,* which are among the bacteria involved in nosocomial infections.

These encouraging results suggest that more in-depth investigations should be performed regarding liposome-bacteria interactions.. In addition, it will be interesting to investigate the antibacterial activity of liposomal GSNO on bacteria-macrophage co-cultures. Due to its macrophage targeting capacity and direct antibacterial effects, liposomal GSNO is expected to display a synergistic and hence stronger antibacterial behavior. These studies will be the next steps in this research.

Acknowledgements

S-nitrosoglutathione was synthesized by Dr. F. Aldeek and Pr. R. Schneider in LRGP UPR-CNRS 3349, Université de Lorraine.

We acknowledge Université de Lorraine (UHP_2011_EA3452_BMS_0062), Région Lorraine, and French National Agency for Research (Agence Nationale de la Recherche) (NanoSNO project; ANR-2010-BLANC-1522) for their financial support.

English language editing was performed by BioMed Proofreading.

R e f e r e n c e s

1. P. Allavena, A. Sica, G. Solinas, C. Porta, A. Mantovani, The inflammatory micro-environment in tumor progression: the role of tumor-associated macrophages, Crit. Rev. Oncol. Hematol. 66, 1-9 (**2008**).
2. V. Haine, T. Fischer-Smith, J. Rappaport, Macrophage colony-stimulating factor in the pathogenesis of hiv infection: potential target for therapeutic intervention, J. Neuroimmune Pharmacol. 1, 32-40 (**2006**).
3. J. Li, H. Hsu, J. D. Mountz, Managing macrophages in rheumatoid arthritis by reform or removal, Curr. Rheumatol. Rep. 14, 445-454 (**2012**).
4. J. Bauer, S. R. Ruuls, I. Huitinga, C. D. Dijkstra, The role of macrophage subpopulations in autoimmune disease of the central nervous system, Histochem. J. 28, 83-97 (**1996**).
5. R. L. Tiwari, V. Singh, M. K. Barthwal, Macrophages: an elusive yet emerging therapeutic target of atherosclerosis, Med. Res. Rev. 28, 483-544 (**2008**).
6. P. Bhargava, C. Lee, Role and function of macrophages in the metabolic syndrome, Biochem. J. 442, 253-262 (**2012**).
7. N. K. Jain, V. Mishra, N. K. Mehra, Targeted drug delivery to macrophages, Expert Opin. Drug. Deliv. 10, 353-367 (**2013**).

8. E. Eisele, R. F. Siliciano, Redefining the viral reservoirs that prevent hiv-1 eradication, Immunity 37, 377-388 (**2012**).
9. P. Peyron, J. Vaubourgeix, Y. Poquet, F. Levillain, C. Botanch, F. Bardou, M. Daffé, J. Emile, B. Marchou, P. Cardona, C. de Chastellier, F. Altare, Foamy macrophages from tuberculous patients' granulomas constitute a nutrient-rich reservoir for m. tuberculosis persistence, PLoS Pathog. 4, e1000204 (**2008**).
10. N. Kumar, S. Gupta, A. Dube, S. P. Vyas, Emerging role of vesicular carriers for therapy of visceral leishmaniasis: conventional versus novel, Crit. Rev. Ther. Drug Carrier Syst. 27, 461-507 (**2010**).
11. R. Diab, J. Brillault, A. Bardy, A. V. L. Gontijo, J. C. Olivier, Formulation and in vitro characterization of inhalable polyvinyl alcohol-free rifampicin-loaded PLGA microspheres prepared with sucrose palmitate as stabilizer: efficiency for ex vivo alveolar macrophage targeting, Int. J. Pharmceut. 436, 833-839 (**2012**).
12. S. R. Naik, S. K. Desai, P. D. Shah, S. M. Wala, Liposomes as potential carrier system for targeted delivery of polyene antibiotics, Recent Pat. Inflamm. Allergy Drug Discov. 7, 202-214 (**2013**).
13. P. Vallance, I. Charles, Nitric oxide as an antimicrobial agent: does no always mean no? Gut 42, 313-314 (**1998**).
14. J. Marcinkiewicz, Nitric oxide and antimicrobial activity of reactive oxygen intermediates, Immunopharmacology 37, 35-41 (**1997**).
15. F. C. Fang, Antimicrobial reactive oxygen and nitrogen species: concepts and controversies, Nat. Rev. Microbiol. 2, 820-832 (**2004**).
16. A. J. Cariello, P. J. M. Bispo, G. F. P. de Souza, A. C. C. Pignatari, M. G. de Oliveira, A. L. Hofling-Lima, Bactericidal effect of s-nitrosothiols against clinical isolates from keratitis, Clin. Ophthalmol. 6, 1907-1914 (**2012**).
17. J. S. Stamler, S. Lamas, F. C. Fang, Nitrosylation: The prototypic redox-based signaling mechanism, Cell 106, 675-683 (**2001**).
18. C. Kelly, C. Jefferies, S. Cryan, Targeted liposomal drug delivery to monocytes and macrophages, J. Drug Deliv. 2011, 727241 (**2011**).
19. M. Khan, B. Sekhon, S. Giri, M. Jatana, A. G. Gilg, K. Ayasolla, C. Elango, A. K. Singh, I. Singh, S-nitrosoglutathione reduces inflammation and protects brain against focal cerebral ischemia in a rat model of experimental stroke, J. Cereb. Blood Flow Metab. 25, 177-192 (**2005**).
20. M. Flamant, P. Aubert, M. Rolli-Derkinderen, A. Bourreille, M. R. Neunlist, M. M. Mahé, G. Meurette, B. Marteyn, T. Savidge, J. P. Galmiche, P. J. Sansonetti, M. Neunlist, Enteric glia protect against shigella flexneri invasion in intestinal epithelial cells: a role for s-nitrosoglutathione, Gut 60, 473-484 (**2011**).
21. A. M. A. de Menezes, G. F. P. de Souza, A. S. Gomes, R. F. de Carvalho Leitão, R. D. A. Ribeiro, M. G. de Oliveira, G. A. de Castro Brito, S-nitrosoglutathione decreases inflammation and bone resorption in experimental periodontitis in rats, J. Periodontol. 83, 514-521 (**2012**).
22. F. Ahsan, I. P. Rivas, M. A. Khan, A. I. Torres Suarez, Targeting to macrophages: role of physicochemical properties of particulate carriers-liposomes and microspheres-on the phagocytosis by macrophages, J. Control. Release 79, 29-40 (**2002**).

23. H. Epstein-Barash, D. Gutman, E. Markovsky, G. Mishan-Eisenberg, N. Koroukhov, J. Szebeni, G. Golomb, Physicochemical parameters affecting liposomal bisphosphonates bioactivity for restenosis therapy: internalization, cell inhibition, activation of cytokines and complement, and mechanism of cell death, J. Control. Release 146, 182-195 (**2010**).
24. S. Chono, T. Tanino, T. Seki, K. Morimoto, Influence of particle size on drug delivery to rat alveolar macrophages following pulmonary administration of ciprofloxacin incorporated into liposomes, J. Drug Target 14, 557-566 (**2006**).
25. S. Chono, T. Tanino, T. Seki, K. Morimoto, Uptake characteristics of liposomes by rat alveolar macrophages: influence of particle size and surface mannose modification, J. Pharm. Pharmacol. 59, 75-80 (**2007**).
26. J. Presumey, I. Duroux-Richard, G. Courties, F. Apparailly, Cationic liposome formulations for RNAi-based validation of therapeutic targets in rheumatoid arthritis, Curr. Opin. Mol. Ther. 12, 325-330 (**2010**).
27. J. Wu, A. Lee, Y. Lu, R. J. Lee, Vascular targeting of doxorubicin using cationic liposomes, Int. J. Pharmceut. 337, 329-335 (**2007**).
28. T. Tagami, T. Suzuki, M. Matsunaga, K. Nakamura, N. Moriyoshi, T. Ishida, H. Kiwada, Anti-angiogenic therapy via cationic liposome-mediated systemic sirna delivery, Int. J. Pharmceut. 422, 280-289 (**2012**).
29. K. Takano, K. Sato, Y. Negishi, Y. Aramaki, Involvement of actin cytoskeleton in macrophage apoptosis induced by cationic liposomes, Arch. Biochem. Biophys. 518, 89-94 (**2012**).
30. O. Meyer, D. Kirpotin, K. Hong, B. Sternberg, J. W. Park, M. C. Woodle, D. Papahadjopoulos, Cationic liposomes coated with polyethylene glycol as carriers for oligonucleotides, J. Biol. Chem. 273, 15621-15627 (**1998**).
31. I. Gursel, M. Gursel, K. J. Ishii, D. M. Klinman, Sterically stabilized cationic liposomes improve the uptake and immunostimulatory activity of CPG oligonucleotides, J. Immunol. 167, 3324-3328 (**2001**).
32. S. M. Moghimi, A. C. Hunter, Recognition by macrophages and liver cells of opsonized phospholipid vesicles and phospholipid headgroups, Pharm. Res. 18, 1-8 (**2001**).
33. M. Parent, F. Dahboul, R. Schneider, I. Clarot, P. Maincent, P. Leroy, A. Boudier, A complete physicochemical identity card of s-nitrosoglutathione, Curr. Pharm. Anal. 9, 31-42 (**2013**).
34. N. S. Bryan, M. B. Grisham, Methods to detect nitric oxide and its metabolites in biological samples, Free Radic. Biol. Med. 43, 645-657 (**2007**).
35. S. Kim, M. S. Turker, E. Y. Chi, S. Sela, G. M. Martin, Preparation of multivesicular liposomes, Biochim. Biophys. Acta 728, 339-348 (**1983**).
36. S. Kim, R. E. Jacobs, S. H. White, Preparation of multilamellar vesicles of defined size-distribution by solvent-spherule evaporation, Biochim. Biophys. Acta 812,793-801 (**1985**).
37. A. Sze, D. Erickson, L. Ren, D. Li, Zeta-potential measurement using the Smoluchowski equation and the slope of the current-time relationship in electroosmotic flow, J. Colloid. Interface Sci. 261, 402-410 (**2003**).
38. J. M. Lopez-Pinto, M. L. Gonzalez-Rodriguez, A. M. Rabasco, Effect of cholesterol and ethanol on dermal delivery from DPPC liposomes, Int. J. Pharmceut. 298, 1–12 (**2005**).

39. H. Eidi, O. Joubert, G. Attik, R. E. Duval, M. C. Bottin, A. Hamouia, P. Maincent, B. H. Rihn, Cytotoxicity assessment of heparin nanoparticles in nr8383 macrophages, Int. J. Pharmceut. 396, 156-165 (**2010**).
40. H. Eidi, O. Joubert, C. Némos, S. Grandemange, B. Mograbi, B. Foliguet, J. Tournebize, P. Maincent, A. Le Faou, I. Aboukhamis, B. H. Rihn, Drug delivery by polymeric nanoparticles induces autophagy in macrophages, Int. J. Pharmceut. 422,495-503 (**2012**).
41. NCCLS, National committee for clinical laboratory standards, 2003. methods for dilution antimicrobial susceptibility tests for bacteria that grow aerobically, Approved Standard M7-A6. NCCLS,Wayne, PA, USA , (**2003**).
42. M. Grare, S. Fontanay, C. Cornil, C. Finance, R. E. Duval, Tetrazolium salts for MIC determination in microplates: Why? Which salt to select? How? J. Microbiol. Methods 75, 156-159 (**2008**).
43. A. D. Bangham, M. M. Standish, J. C. Watkins, Diffusion of univalent ions across the lamellae of swollen phospholipids, J. Mol. Biol. 13, 238-252 (**1965**).
44. C. Jaafar-Maalej, R. Diab, V. Andrieu, A. Elaissari, H. Fessi, Ethanol injection method for hydrophilic and lipophilic drug-loaded liposome preparation, J. Liposome Res. 20, 228-243 (**2010**).
45. J. Mathai, V. Sitaramam, Preparation of large uni-lamellar liposomes by the ether injection method and evaluation of the physical integrity by osmometry, Biochem. Educ. 15, 147-149 (**1987**).
46. B. Ceh, D. Lasic, A rigorous theory of remote loading of drugs into liposomes: transmembrane potential and induced pH-gradient loading and leakage of liposomes, J. Colloid. Interface Sci. 185, 9-18 (**1997**).
47. D. D. Lasic, A molecular model for vesicle formation, Biochim. Biophys. Acta 692, 501-502 (**1982**).
48. F. J. Szoka, D. Papahadjopoulos, Procedure for preparation of liposomes with large internal aqueous space and high capture by reverse-phase evaporation, Proc. Natl. Acad. Sci. U.S.A. 75, 4194-4198 (**1978**).
49. M. Jurima-Romet, P. N. Shek, Lung uptake of liposome-entrapped glutathione after intratracheal administration, J. Pharm. Pharmacol. 43, 6-10 (**1991**).
50. M. Jurima-Romet, R. Barber, P. Shek, Liposomes and bronchoalveolar lavage fluid: release of vesicle-entrapped glutathione, Int. J. Pharmceut. 88, 201-210 (**1992**).
51. N. El Kateb, L. Cynober, J. C. Chaumeil, G. Dumortier, L-cysteine encapsulation in liposomes: effect of phospholipids nature on entrapment efficiency and stability, J. Microencapsul. 25, 399-413 (**2008**).
52. K. Yoshino, K. Nakamura, Y. Terajima, A. Kurita, T. Matsuzaki, K. Yamashita, M. Isozaki, H. Kasukawa, Comparative studies of irinotecan-loaded polyethylene glycol-modified liposomes prepared using different PEG-modification methods, Biochim. Biophys. Acta 1818, 2901-2907 (**2012**).
53. O. Tirosh, Y. Barenholz, J. Katzhendler, A. Priev, Hydration of polyethylene glycol-grafted liposomes, Biophys. J. 74, 1371-1379 (**1998**).
54. J. du Plessis, C. Ramachandran, N. Weiner, D. Müller, The influence of lipid composition and lamellarity of liposomes on the physical stability of liposomes upon storage, Int. J. Pharmceut. 127, 273-278 (**1996**).

55. M. Fröhlich, V. Brecht, R. Peschka-Süss, Parameters influencing the determination of liposome lamellarity by ^{31}P-NMR, Chem. Phys. Lipids 109, 103-112 (**2001**).
56. I. A. Bakker-Woudenberg, G. Storm, M. C. Woodle, Liposomes in the treatment of infections, J Drug Target 2, 363-371 (**1994**).
57. S. D. Patil, D. G. Rhodes, D. J. Burgess, Anionic liposomal delivery system for DNA transfection, AAPS J 6, e29 (**2004**).
58. E. Greco, G. Quintiliani, M. B. Santucci, A. Serafino, A. R. Ciccaglione, C. Marcantonio, M. Papi, G. Maulucci, G. Delogu, A. Martino, D. Goletti, L. Sarmati, M. Andreoni, A. Altieri, M. Alma, N. Caccamo, D. Di Liberto, M. De Spirito, N. D. Savage, R. Nisini, F. Dieli, T. H. Ottenhoff, Janus-faced liposomes enhance antimicrobial innate immune response in mycobacterium tuberculosis infection, Proc. Natl. Acad. Sci. U.S.A. 109, E1360-8 (**2012**).
59. M. Alipour, M. G. Smith, K. Pucaj, Z. E. Suntres, Acute toxicity study of liposomal antioxidant formulations containing n-acetylcysteine, α-tocopherol, and γ-tocopherol in rats, J. Liposome Res. 22, 158-167 (**2012**).
60. N. Kong, T. Jiang, Z. Zhou, J. Fu, Cytotoxicity of polymerized resin cements on human dental pulp cells in vitro, Dent Mater 25, 1371-1375 (**2009**).
61. S. Mayor, R. E. Pagano, Pathways of clathrin-independent endocytosis, Nat. Rev. Mol. Cell Biol. 8, 603-612 (**2007**).
62. S. Simões, V. Slepushkin, N. Düzgünes, M. C. Pedroso de Lima, On the mechanisms of internalization and intracellular delivery mediated by pH-sensitive liposomes, Biochim. Biophys. Acta 1515, 23-37 (**2001**).
63. U. S. Huth, R. Schubert, R. Peschka-Süss, Investigating the uptake and intracellular fate of pH-sensitive liposomes by flow cytometry and spectral bio-imaging, J. Control. Release 110, 490-504 (**2006**).
64. A. Homhuan, H. Harashima, I. Yanoc, Cellular attachment and internalization of cationic liposomes containing mycobacterial cell wall, ScienceAsia 34 , 179–185 (**2008**).
65. T. Nakamura, R. Moriguchi, K. Kogure, N. Shastri, H. Harashima, Efficient MHC class I presentation by controlled intracellular trafficking of antigens in octaarginine-modified liposomes, Mol. Ther. 16, 1507-1514 (**2008**).
66. R. G. Parton, K. Simons, The multiple faces of caveolae, Nat. Rev. Mol. Cell Biol. 8, 185-194 (**2007**).
67. S. Cui, B. Wang, Y. Zhao, H. Chen, H. Ding, D. Zhi, S. Zhang, Transmembrane routes of cationic liposome-mediated gene delivery using human throat epidermis cancer cells, Biotechnol. Lett. 36, 1-7 (**2014**).
68. V. Venketaraman, Y. K. Dayaram, M. T. Talaue, N. D. Connell, Glutathione and nitrosoglutathione in macrophage defense against mycobacterium tuberculosis, Infect. Immun. 73, 1886-1889 (**2005**).
69. J. R. Laver, T. M. Stevanin, S. L. Messenger, A. D. Lunn, M. E. Lee, J. W. B. Moir, R. K. Poole, R. C. Read, Bacterial nitric oxide detoxification prevents host cell s-nitrosothiol formation: a novel mechanism of bacterial pathogenesis, FASEB J. 24, 286-295 (**2010**).
70. M. T. Campanhã, E. M. Mamizuka, A. M. Carmona-Ribeiro, Interactions between cationic liposomes and bacteria: the physical-chemistry of the bactericidal action, J. Lipid Res. 40, 1495-1500 (**1999**).

71. C. Ronzani, R. Safar, R. Diab, B. Rihn, O. Joubert, Transcriptome study of THP-1 human monocytes following exposure for 4 h or 24 h to 50 µm s-nitrosoglutathione, 50 and 200 µg/ml *S*-nitrosoglutathione-loaded polymeric and empty Eudragit® RL nanoparticles, GEO NCBI , accession number GSE51186 (**2013**).

Chapitre 3

Microencapsulation de la rifampicine en utilisant le palmitate de saccharose comme tensioactif alternatif à l'alcool polyvinylique pour cibler les macrophages alvéolaires

"Formulation and in vitro characterization of inhalable polyvinyl alcohol-free rifampicin-loaded PLGA microspheres prepared with sucrose palmitate as stabilizer: Efficiency for ex vivo alveolar macrophage targeting"

Ce chapitre représente un travail expérimental sur le développement d'une poudre pour inhalation à base de microsphères polymériques chargées en un antituberculeux, la rifampicine. L'objectif est de viser les macrophages alvéolaires qui sont eux-mêmes des cibles pour *Mycobacterium tuberculosis*.

Ce travail fait l'objet d'une publication scientifique dans l'*International Journal of Pharmaceutics.*

International Journal of Pharmaceutics xxx (2012) xxx–xxx

Contents lists available at SciVerse ScienceDirect

International Journal of Pharmaceutics

journal homepage: www.elsevier.com/locate/ijpharm

Formulation and in vitro characterization of inhalable polyvinyl alcohol-free rifampicin-loaded PLGA microspheres prepared with sucrose palmitate as stabilizer: Efficiency for ex vivo alveolar macrophage targeting

R. Diab[a,b,c], J. Brillault[a,b], A. Bardy[a,b], A.V.L. Gontijo[a,b,d], J.C. Olivier[a,b,*]

[a] INSERM, U1070, 1 rue Georges Bonnet, 86022 Poitiers, France
[b] Université de Poitiers, Faculté de Médecine et de Pharmacie, 6 rue de la Milétrie, 86034 Poitiers, France
[c] Pharmaceutical Technology Group, EA 3452 CITHÉFOR, Faculté de Pharmacie, Université de Lorraine, 5 rue Albert Lebrun, 54001 Nancy Cedex, France
[d] CAPES Foundation, Ministry of Education of Brazil, Caixa Postal 250, Brasília – DF 70040-020, Brazil

ARTICLE INFO

Article history:
Received 26 March 2012
Received in revised form 19 July 2012
Accepted 21 July 2012
Available online xxx

Keywords:
Cell uptake
Alveolar macrophage
PLGA microsphere
Rifampicin
Sucrose palmitate

ABSTRACT

In this work a new formulation of inhalable rifampicin-loaded PLGA microspheres (RIF-MS) is proposed for the management of tuberculosis treatment. For their formulation, the non-biodegradable polyvinyl alcohol surfactant was replaced with a biodegradable and biocompatible sucrose ester, sucrose palmitate. The effects of critical process and formulation parameters have been investigated and the obtained microspheres were characterized in terms of size, morphology, encapsulation efficiencies and RIF release profile. The optimized RIF-MS showed high drug loading (34.2%, w/w), an aerodynamic diameter compliant with deep lung delivery and an in vitro gradual and almost complete drug release over a week. The drug release data fitted well to the Higuchi models suggesting a drug release governed by Fickian diffusion. The RIF-MS uptake qualitative and quantitative studies on ex vivo rat alveolar macrophages (AM) revealed an efficient internalization of RIF-MS and their location in the perinuclear area. RIF intracellular levels were 7-fold higher in AM incubated with RIF-MS than with an equivalent amount of free RIF.

La tuberculose est une infection qui touche un tiers de la population mondiale. Elle a été déclarée par l'OMS comme un problème émergent de santé publique en avril 1993. La microencapsulation de la rifampicine constitue une approche intéressante pour le traitement de la tuberculose dans la phase initiale. En effet, une libération prolongée de la rifampicine dans les macrophages est idéale pour traiter l'infection causée par les bacilles tuberculeux qui ciblent principalement les macrophages pendant les phases précoces.

Il est important de rappeler que le traitement de la tuberculose est un traitement de longue durée et nécessite surtout une bonne observance. Chose qui n'est pas toujours évidente, vu le nombre élevé de comprimés à prendre chaque jour. Une forme inhalée à libération prolongée permettrait donc diminuer le nombre d'administration tout en augmentant l'efficacité du traitement et l'observance du patient.

La première partie de ce travail consiste en la mise au point du procédé d'encapsulation et de caractérisation physico-chimique des microsphères, ainsi que la caractérisation du comportement aérodynamique de la poudre de microsphères. La seconde partie concerne l'évaluation de l'efficacité du ciblage sur un modèle *ex vivo* des macrophages murins. L'innocuité du vecteur a été aussi vérifiée.

Conformément à nos attentes, les microsphères de rifampicine ont permis de réaliser des concentrations intracellulaires supérieures par rapport à la molécule non encapsulée. D'une façon intéressante, nous avons trouvé que les concentrations intracellulaires sont quasi-proportionnelles à la teneur des microsphères en rifampicine.

Formulation and in vitro characterization of inhalable polyvinyl alcohol-free rifampicin-loaded PLGA microspheres prepared with sucrose palmitate as stabilizer: efficiency for *ex vivo* alveolar macrophage targeting

R. Diab[a,b,c], J. Brillault[a,b], A. Bardy[a,b], A. Vidal Lacerda Gontijo[a,b,d], J.C. Olivier[a,b]*

[a]INSERM, U1070, 1 rue Georges Bonnet, 86022 Poitiers, France

[b]Université de Poitiers, Faculté de Médecine et de Pharmacie, 6 rue de la Milétrie, 86034 Poitiers, France

[c]Pharmaceutical Technology Group, EA 3452 CITHÉFOR, Faculté de Pharmacie, Université de Lorraine, 5 rue Albert Lebrun, 54001 Nancy Cedex, France

[d]CAPES Foundation, Ministry of Education of Brazil, Caixa Postal 250, Brasília – DF 70040-020, Brazil

*Corresponding author

Jean-Christophe Olivier, PhD, Professor of Pharmacy

Tel.: +33 5 49 45 45 92; fax: +33 5 49 45 43 78.

E-mail: jean.christophe.olivier@univ-poitiers.fr

A b s t r a c t
In this work a new formulation of inhalable rifampicin-loaded PLGA microspheres (RIF-MS) is proposed for the management of tuberculosis treatment. For their formulation, the non-biodegradable polyvinyl alcohol surfactant was replaced with a biodegradable and biocompatible sucrose ester, sucrose palmitate. The effects of critical process and formulation parameters have been investigated and the obtained microspheres were characterized in terms of size, morphology, encapsulation efficiencies and RIF release profile. The optimized RIF-MS showed high drug loading (34.2% w/w), an aerodynamic diameter compliant with deep lung delivery and an *in vitro* gradual and almost complete drug release over a week. The drug release data fitted well to the Higuchi models suggesting a drug release governed by Fickian diffusion. The RIF-MS uptake qualitative and quantitative studies on *ex vivo* rat alveolar macrophages (AM) revealed an efficient internalization of RIF-MS and their location in the perinuclear area. RIF intracellular levels were 7-fold higher in AM incubated with RIF-MS than with an equivalent amount of free RIF.

Keywords: Cell uptake, alveolar macrophage, PLGA microsphere, rifampicin, sucrose palmitate.

Abbreviations
AM: Alveolar macrophages, RIF: rifampicin, RIF-MS: rifampicin loaded-microspheres.

1. Introduction

The last few decades have witnessed a growing clinicians' interest in the pulmonary route for drug administration aiming to target local diseases (e.g., respiratory infections (Dudley *et al.*, 2008), pulmonary hypertension (Leuchte *et al.*, 2004) and lung metastasis (Koshkina *et al.*, 2001), (Gagnadoux *et al.*, 2006)). Using aerosol therapy, high drug concentrations in the lungs and low systemic drug exposure are expected leading to enhanced therapeutic outcomes. The first-line antitubercular drug rifampicin (RIF) may benefit from innovative aerosol based on inhalable nanoparticles and microspheres (Muttil *et al.*, 2009). Indeed, mycobacteria are facultative intracellular pathogens and are located in lung macrophages at the acute stage of the disease and in both–macrophages and granulomas (*i.e.* extracellular location) at the chronic stage. Microspheres of 1 to 3 µm diameter have been shown to be phagocytosed by alveolar macrophages (AM) (Makino *et al.*, 2003) and could be used to target alveolar macrophages. In addition, the gradual release of RIF from both extracellular and phagocytosed microspheres is expected to increase RIF's activity against mycobacteria and to improve treatment efficiency, while reducing the dosing frequency.

The development of inhaled microparticulate delivery systems involves three requirements: (1) a biocompatibility and a relatively rapid biodegradability of the constituting polymer in order to avoid toxic accumulation of materials within the lungs, especially in the case of long-term treatments such as tuberculosis chemotherapy, (2) a high drug loading in order to minimize the administration of inert materials, and (3) particle aerodynamic diameters between 1 and 5 µm when a deep deposition in the respiratory tract is aimed.

PLGA are biodegradable and biocompatible polymers (Shive and Anderson, 1997) and the relatively fast degradation rate of low molecular weight PLGA 50:50 complies well with biodegradability requirement for polymers destined for pulmonary delivery. Indeed, it was

previously shown that microspheres made from Resomer® RG 502 H are extensively degraded within one week (Díez and Tros de Ilarduya, 2006).
RIF-loaded PLGA microspheres are generally prepared by the solvent evaporation emulsion process using the non-biodegradable polyvinyl alcohol (PVA) polymer as an emulsion stabilizing agent. Little is known about PVA's elimination rate and toxicity, in particular in the lung keeping in mind that PVA residues remain in microspheres despite the multiple post-manufacturing purification steps. Furthermore, the RIF loading that has been achieved so far in microspheres of diameter compatible with lung administration (i.e., 1 to 5 µm diameter) that were prepared by the solvent evaporation emulsion process hardly reaches 15% (w/w) (Makino *et al.*, 2004), which implies that most materials to be administered to the lungs are non-active excipients.
The aim of the present work was to prepare RIF-loaded microspheres (RIF-MS) with high RIF payload and sustained release properties and that meet lung delivery requirements. For this purpose, PVA was replaced with a biodegradable and biocompatible sucrose ester surfactant, sucrose palmitate. Various microsphere batches have been prepared by varying the process and formulation parameters and then characterized in terms of size and encapsulation efficiencies. Further investigations have been performed on the optimized formula such as morphology and *in vitro* drug release studies. Aerodynamic aerosol behaviour and *ex vivo* rat AM uptake of RIF-MS have been studied in order to assess the suitability of elaborated microspheres to target AM deeply in the lungs.

2. Materials and methods

2.1. Materials

Resomer® RG 502 H (poly(d,l-lactide-co-glycolide) 50:50 (PLGA), inherent viscosity of 0.19 dl/g (25° C, 0.1% in chloroform), Mw 10500, Mn 6100 (Mw/n = 1.71)) was purchased from Boehringer Ingelheim (Ingelheim, Germany). Rifampicin, Chloroform (HCl_3), dichloromethane (DCM), dimethyl sulfoxide (DMSO) and HPLC analytical grade acetonitrile were obtained from Sigma (Saint Quentin Fallavier, France). Sucrose palmitate (Stelliester DUB SE 15P, 70% monoester, HLB = 15) was a gift from Stéarinerie Dubois (Grenoble, France). Purified water was produced using a MilliQ gradient® Plus Millipore system.

2.2. Microsphere preparation

RIF-MS were prepared by the oil-in-water (O/W) emulsion-solvent evaporation method as previously described by (Barrow *et al.*, 1998) with slight modifications. Briefly, according to formulae listed in Table 1, the solutions of RIF and PLGA in dichloromethane, chloroform or a chloroform-dichloromethane 1:5 mixture constituting the organic phase were emulsified in 50 mL sucrose palmitate aqueous solution for 5 min using a Polytron® Homogenizer PT 3100D set at 10000 rpm and equipped with a 12 mm-diameter aggregate-dispersing rotor-stator. After the O/W emulsion formation, the organic solvent was removed by evaporation either in a rotary evaporator under reduced pressure (room temperature (RT), 40 mbar) for 15 min or under magnetic stirring at 500 rpm at atmospheric pressure for 3 hours. RIF-MS were then separated by centrifugation at 280 g for 15 min and then washed thrice with purified water in order to remove residual surfactant and free drug. Finally, the recovered RIF-MS were freeze-dried with a Labconco FreeZone Triad™ freeze-drier (Serlabo, France).

Formulation and process parameters, such as RIF:PLGA weight ratios, the organic solvents, the sucrose palmitate concentrations and the solvent evaporation rate, were investigated for their effects on RIF-MS size and RIF loading and for selecting the optimal formula and process parameters.

2.3. Microsphere characterization

2.3.1. Size

The volume-averaged diameter of RIF-MS was measured by laser light diffraction using a Microtrac® X100 particle size analyzer.

2.3.2. RIF loading and encapsulation efficiencies

The amount of the RIF entrapped within RIF-MS, i.e. RIF loading, was determined as described previously (Doan and Olivier, 2009). Briefly, freeze-dried RIF-MS were dissolved in DMSO and RIF concentrations were determined at 485 nm using a Varian Cary 50 UV-Visible spectrophotometer, with a RIF calibration curve (0.004–0.050 mg/mL concentration range in DMSO). RIF loading was expressed as mg drug per 100 mg of RIF-MS (% w/w).
RIF entrapment efficiencies (%) were calculated as the percent ratio of the determined loading to the theoretical loading that should be obtained in case of a 100% entrapment efficiency.

2.4. Morphology analysis

Microsphere morphology was examined using a JSM-840A JEOL scanning electron microscope at 15 kV, after gold-sputtering the microspheres in argon atmosphere.

2.5. *In vitro* RIF release studies

An amount of RIF-MS corresponding to 2 mg of RIF was dispersed in 4 mL of a release medium consisting of phosphate buffer saline (PBS), pH 7.4, containing 1% (w/v) ascorbic acid as antioxidant to prevent RIF oxidative degradation. The RIF-MS dispersion was incubated at 37°C under magnetic stirring at 90 rpm and protected from light. At predetermined time points, it was centrifuged (280 g, 5 min) and the supernatants were collected and replaced with a fresh release medium, in order to maintain sink conditions. RIF was assayed in the recovered supernatant by spectrophotometry measurements at 485 nm and concentrations calculated using a calibration curve prepared in PBS containing 1% (m/v) ascorbic acid (0.010 to 0.050 mg RIF per mL, r^2 = 0.9996). The release studies were triplicated.
RIF release kinetics were analyzed using the Higuchi model (equation 1), in order to clarify the RIF release mechanism from RIF-MS (Costa and Sousa Lobo, 2001) :

$$Q_t = K_H \cdot t^{0.5} \qquad \text{Equation 1}$$

Where Q_t is the amount of drug released at time t, the release time, K_H the Higuchi diffusion constant. The correlation between experimental data and the Higuchi model was evaluated using the determination coefficient r^2.

Table 1. Preparation and physico-chemical characterization of PLGA microspheres prepared from different formulae using the solvent emulsion-evaporation method (mean ± SD, n=3).

Formula	Rifampicin mass (mg)	PLGA mass (mg)	[SP] (% w/w)	Organic solvents	Organic solvent volume (mL)	Solvent evaporation rate	RIF loading (mg/100mg)	Encapsulation efficiency (%)	Size (µm)
MS1	12.5	25	0.1	DCM	2.5	high[a]	7.0 ± 0.2	21.1 ± 0.4	1.5 ± 0.2
MS2	100	100	0.5	DCM: HCl_3 (1:5)	2.5	low[b]	17.4 ± 0.5	34.7 ± 0.4	2.5 ± 0.1
MS3	100	100	0.5	DCM: HCl_3 (1:5)	2.5	high[a]	34.2 ± 4.0	68.5 ± 7.2	2.7 ± 0.2
MS4	100	25	0.1	HCl_3	1	high[a]	14.8 ± 1.1	18.6 ± 1.0	5.2 ± 0.7
MS5	100	25	0.1	DCM: HCl_3 (1:5)	1	high[a]	15.2 ± 1.7	18.8 ± 0.8	7.0 ± 0.8
MS6	100	50	0.1	HCl_3	1	high[a]	26.5 ± 1.2	39.6 ± 0.5	6.1 ± 1.3
MS7	100	50	0.5	HCl_3	1	high[a]	33.9 ± 1.7	50.6 ± 1.6	6.5 ± 0.3
MS8	50	25	0.1	HCl_3	2.5	high[a]	29.6 ± 1.5	44.2 ± 1.8	1,6 ± 0.1
MS9	25	25	0.1	HCl_3	2.5	high[a]	22.2 ± 1.1	44.4 ± 2.2	1.5 ± 0.3
MS10	12.5	25	0.1	HCl_3	2.5	high[a]	10.5 ± 2.3	31.9 ± 5.5	2.4 ± 0.9
MS11	100	50	1	HCl_3	1	high[a]	42.4 ± 2.2	63.5 ± 2.1	5.1 ± 1.1
MS12	50	50	0.5	DCM: HCl_3 (1:5)	2.5	high[a]	28.7 ± 0.7	57.4 ± 0.6	2.2 ± 0.4

[a] solvent evaporation performed at RT and 40 mBar for 15 min

[b] solvent evaporation performed at RT and atmospheric pressure for 3 h.

2.6. Aerodynamic evaluations

A Next Generation Impactor NGI (Copley Scientific Limited, Nottingham, UK) equipped with a preseparator and connected to a Copley HCPS pump was used to investigate the aerodynamic behavior of the RIF-MS dry powder as per the guidelines of European Pharmacopoeia 7.5 edition, as previously described (Doan and Olivier, 2009). RIF-MS dry powder was aerosolized into the NGI induction port using a Model DP-4 dry powder insufflator^{TM} for rat (Penn Century Inc., USA) by actuating a syringe filled with 2.5 mL air. The RIF-MS aerosol was drawn into the NGI by the air flow at a 30 L/min rate for 10 seconds. Several insufflations were carried out in order to deliver approximately 20 mg of RIF-MS. The RIF-MS deposited on each NGI cup coated with silicon oil were afterwards dissolved with 1 mL DMSO for RIF determination by UV-Visible spectrophotometry at 485 nm as described above. The mass median aerodynamic diameter (MMAD) was calculated from the curve of the cumulative mass distribution versus log aerodynamic diameters (AED) (Jaafar-Maalej *et al.*, 2010). Respirable fraction or fine particle fraction (FPF) was the mass fraction of RIF-MS with an aerodynamic diameters from 1 to 5 µm (Sung *et al.*, 2009).

2.7. Alveolar macrophage cells

Male Sprague-Dawley rats from Janvier Laboratories (Le Genest-St-Isle, France) weighing between 450 and 560 g were used for these investigations. Rats were deeply anesthetized via intraperitoneal injection of pentobarbital sodium (27 mg/kg body wt). The trachea was cannulated and the rib cage opened. Lungs were lavaged with ten separate 10-ml volumes of phosphate buffered saline solution containing 1% (w/v) penicillin and streptomycin. The lavage fluid was centrifuged at 1,000 g at 4°C for 5 min, and the pellet was resuspended in culture media (DMEM/Ham's F12 (1/1) supplemented with L-glutamine (2 mM), foetal calf serum (10% v/v) and 1% (w/v) penicillin and streptomycin). Purity of AM was assessed by May-Grunwald and Giemsa staining and was about 95%.

2.8. RIF uptake by alveolar macrophage

For cell uptake and cell viability studies, three batches of RIF-MS were prepared according to MS1, MS2 and MS3 formulae (Table 1). RIF loading values were determined to be 6.8, 17.2 and 38.8% (w/w), respectively. AM were seeded as $2.5x10^5$ cells per well in 24-well plates (Nalgene Nunc International, Rochester, NY) and incubated at 37°C under 90-95% relative humidity and 5% (v/v) CO_2 atmosphere for one hour in order to let them attach to the wells, before performing RIF uptake experiments according to (Makino *et al.*, 2004). A RIF solution corresponding to 78 µg RIF or a suspension of 200 µg of RIF-MS corresponding to a RIF amount of 14 µg (MS1), 34 µg (MS2) and 78 µg (MS3) were incubated with AM for 4 hrs (1mL cell culture medium per well). AM were then washed twice with PBS and 400 µl of a 0.25% trypsin solution was added for 5 to 10 min at 37°C. Once the cells detached, 100 µl of culture medium was added to stop the trypsin reaction. Free RIF-MS and cells were separated using a Percoll gradient at 4°C: 500 µl of 80% Percoll was mixed to the cell suspension and the resulting 40% Percoll was layered above 500 µl of 70% Percoll solution. After centrifugation (10 min at 8,000 g at 4°C), the upper AM-containing layer was collected and AM were washed with 10 ml of ice-cold PBS. After centrifugation (10 min at 1,000 g at 4°C) and discard of the supernatants, the cell pellets were stored at -20°C until RIF assay. To

evaluate the efficacy of the Percoll gradient method to separate AM from free MS, RIF-MS (MS3 formula) were added to cells at 4°C and immediately processed to separation on Percoll gradient. In these conditions, the RIF amount retrieved from the cell pellet was determined to be below 0.07 µg/10^5cells.

For RIF assay, cell pellets were thawed and the remaining water was evaporated under N_2 flux at 45°C. One ml of dichloromethane (DCM) and 50 µl of water were added to the samples. After vortexing and centrifugation, 800 µl of the DCM phase was collected, evaporated under N_2 flux and 1 ml of the mobile phase for the "RIF-MS" samples and 100 µl for the "RIF-solution" samples were added. Samples were analyzed by reversed-phase HPLC with UV detection (333 nm wavelength). RIF standards were prepared in 1 mL DCM, evaporated under N_2 flux and reconstituted with 1 ml of the mobile phase. Calibration curves were linear ($r^2 > 0.995$) within the 0.25 to 8 µg/ml RIF concentration range. The chromatographic system consisted of Waters 717 Autosampler (Waters Millipore, Milford, MA, USA), Lachrom 7110 solvent delivery pump (Merck, Darmstadt, Germany) and Shimadzu SPD-10A UV detector (Shimadzu France, Champs-sur-Marne, France). The flow-rate was 0.25 ml/min. Chromatography was carried out using an Xbridge C18 (150 x 2.1 mm i.d., 5 µm of particle size, Waters Millipore) analytical column, protected by an Interchrom C18 guard column (10 x 4 mm i.d., 5 µm of particle size). Following the injection (20 µl), samples were recorded and analyzed by EZChrom Elite system (Agilent Technologies, Massy, France). The mobile phase consisted of aqueous formic acid solution (0.1 %) containing 50% acetonitrile (v/v). Results were analyzed using one way ANOVA and Bonferroni post-hoc tests.

2.9. Toxicity assay

AM were seeded in 96 well plates as 10^5 cells/well in culture media. After 1 hr at 37°C under 90-95% relative humidity and 5% (v/v) CO_2 atmosphere, 80 µg of blank microspheres, of RIF-MS (MS1, MS2, MS3) or of their equivalent amount of RIF (5.6, 13.6 and 31.2 µg respectively) were added to the cells for 4 hrs. Cell viability was then assessed using the Celltiter 96 aqueous solution from Promega (Lyon, France) according to manufacturer's protocol. Results were analyzed using one way ANOVA and Bonferroni post-hoc tests.

3. Results and discussion

3.1. Preparation and characterization of RIF-loaded microspheres

RIF-MS were prepared by the simple emulsion solvent evaporation method using as constitutive polymer, PLGA Resomer® RG 502 H with the 50:50 ratio of PGA:PLA and low molecular weight. It was selected for its well-known biocompatibility (Shive and Anderson, 1997) and its fastest degradation rate among Resomer® PLGA grades. Microspheres of 1.6 µm diameter made from Resomer® RG 502 H were shown by SEM to be extensively degraded within one week in vitro at 37°C in buffer, pH 7.4 (Díez and Tros de Ilarduya, 2006), which should avoid lung accumulation on the basis of 2 or 3 administrations a week for several months. Sucrose palmitate was used as a surfactant as an alternative to non-biodegradable PVA. Sucrose esters, a group of non-ionic surfactants of low toxicity and good biodegradability and biocompatibility, are increasingly used in the formulation of biodegradable and biocompatible drug delivery nanosystems (Li *et al.*, 2011) (Uchino *et al.*,

2011) and microparticles (Youan *et al.*, 2003). Sucrose palmitate was selected because its high HLB value (i.e. 15) permits the preparation of O/W emulsions. Oil-in-water emulsions were obtained using a mechanical homogenizer and preliminary experiments showed that a homogenization rate of 10,000 rpm was a good compromise to obtain RIF-MS in the micrometer range, while limiting the formation of nanoparticles. Manufacturing formulae and solvent evaporation rates were investigated in order to identify relevant parameters leading to RIF-MS suitable for lung delivery as aerosols, i.e. in term of aerodynamic diameter, drug loading and drug release rate (Table 1). In a previous work we showed that in order to comply with aerodynamic requirements for lung delivery, i.e. aerodynamic diameters ranging from 1 to 5 µm, the target hydrodynamic diameter had to be set at 1 to 3 µm (Doan *et al.*, 2011). Such a target was therefore kept in the present work. Minimal RIF loading target was set at 30 mg RIF per 100 mg (30% (w/w)) RIF-MS. Overall (Table 1), the prepared RIF-MS exhibited RIF loadings ranging from 7.0 ± 0.2 to 42.4 ± 2.2 % (w/w), encapsulation efficiencies from 21.1 ± 0.4 to 63.5 ± 2.1 % and RIF-MS sizes from 1.5 ± 0.2 to 7.0 ± 0.8 µm.

Effect of the organic solvent evaporation rate

The shorter time for evaporation under low pressure of the organic solvent (15 min) compared to evaporation time under atmospheric pressure (3 hours) nearly doubled RIF loadings (Table 1, MS3 and MS2, respectively), limiting RIF loss by diffusion into the aqueous phase due to rapid solidification of the PLGA polymer matrix. Similar observations have been reviewed previously (O'Donnell and McGinity, 1997). As expected, the organic solvent evaporation rate did not have any impact on RIF-MS diameters, which were within targets.

Effect of the organic phase : aqueous phase volume ratio and of the solvent types

The volume of organic solvent, independently of other parameters, seemed to have the main impact on RIF-MS size. All the RIF-MS prepared with 1 mL organic solvent (for 50 mL aqueous phase) were of diameters (from 5.1 ± 0.2 to 7.0 ± 0.8 µm) beyond the 3 µm diameter upper target limit, whereas RIF-MS prepared with 2.5 mL were within targets. This was independent of the PLGA polymer concentration, therefore of the viscosity of the organic phase, since RIF-MS obtained from MS2 and MS3 formulae were smaller in diameter than those from MS4 and MS5 formulae. The dependence of the RIF-MS diameter to the organic phase: water phase volume ratio may be attributed to the dynamic attributes of the homogenization process, which probably requires a minimal volume of dispersed phase for efficiency.

Replacing chloroform with a mixture of dichloromethane and chloroform as organic phase, while keeping other parameters fixed (Table 1, MS4 and MS5 formulae), had no influence on RIF loading, but resulted in slightly larger microspheres. This was attributed to the more rapid evaporation rate of DCM compared with chloroform (respective boiling points under atmospheric pressure: 40°C and 61°C), which may have resulted in earlier solidification of the PLGA matrix, thus in a lower shrinkage factor (Rosca *et al.*, 2004).

Influence of sucrose palmitate concentration

Considering formulae MS6, MS7 and MS11 (all parameters, but sucrose palmitate concentration, kept constant), sucrose palmitate concentration in the 0.1 to 1% range had little

impact on RIF-MS mean diameter. Similar observations have been reported by (Yüksel and Baykara, 1997) who observed no correlation between the sucrose ester concentration and microsphere diameters. However, a noticeable increase in RIF loading and entrapment efficiencies was observed with increasing surfactant concentrations. This might result from increased emulsion droplet inter-phase stabilization, thus decreasing drug diffusion from the dispersed phase to the aqueous phase during microsphere preparation (Sansdrapa and Moës, 1993).

Influence of RIF input

As expected (see formulae MS8 to 10 and MS3, Table 1), the higher the drug amount (RIF input) used in formula, the higher the drug loading in RIF-MS. Encapsulation efficiencies increased with the RIF input, with no significant impact on the RIF-MS diameters which were within the diameter target. The highest loading and the highest encapsulation efficiency were obtained with the MS3 formula, i.e. at the highest RIF input used in this study and with the DCM:chloroform mixture, probably because the presence of DCM accelerated the solvent evaporation, hence the PLGA matrix solidification, compared to pure chloroform.

From the above results, MS3 was considered to be the most suitable formulation, presenting high encapsulation efficiency, a loading value above the 30% (w/w) target and mean particle size suitable for deep lung delivery of RIF by aerosolization. Considering a dosing of 1 to 2 mg RIF per kg in rats for therapeutic activity (Suarez *et al.*, 2001), the amount of microspheres to be administered into the lungs of a 250 g-rat would be 2.9 to 5.9 mg, which is acceptable. Therefore, MS3 was selected for further characterisations.

3.2. Morphology analysis

Under SEM (Figure 1), RIF-MS (MS3 formula) have a spherical shape and a smooth surface, most of them having a few pores. The surface porosity of RIF-MS could be explained by gas bubble formation during the organic solvent evaporation step carried out under reduced pressure.

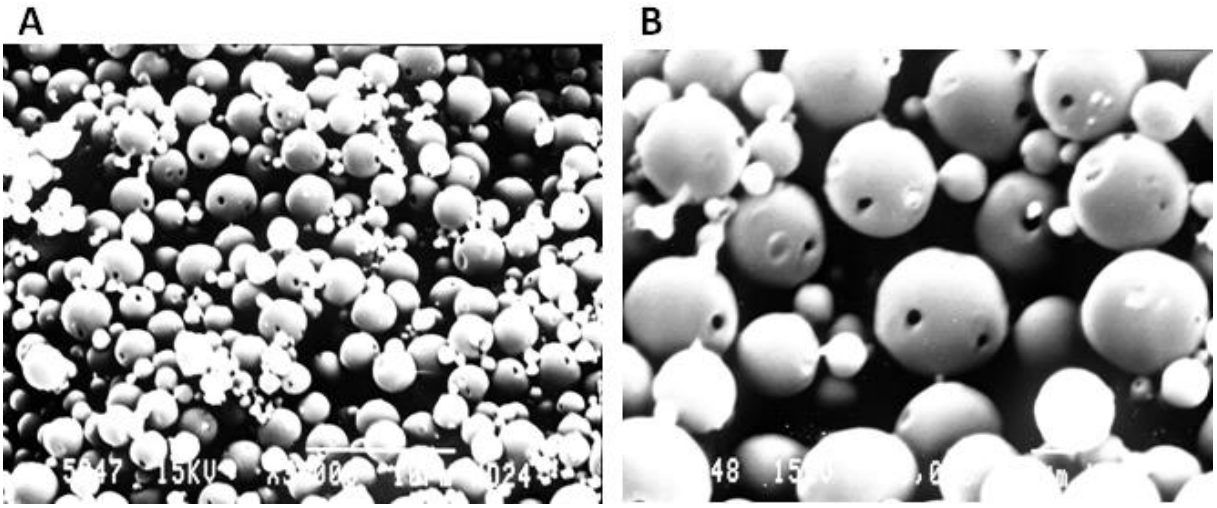

Figure 1. Scanning electron micrographs of MS3 rifampicin-loaded microspheres. The scale bars represent 10 µm and 1 µm for 1A and 1B, respectively.

3.3. In vitro RIF release studies

The profile of RIF release from MS3 RIF-MS in pH 7.4 phosphate buffer is presented on Figure 2. The sink conditions were maintained over the release period, as the measured concentrations never exceeded 0.05 mg/mL, value to be compared to the RIF solubility of 3.35 mg/mL in pH 7.4 phosphate buffer (Becker *et al.* 2009). According to Figure 2, RIF was sustainably released from RIF-MS, with 71% of RIF released over a week. No initial burst release was observed, since around 10% RIF was released during the first three hours. Data fitting to the Higuchi model showed a good correlation (Figure 3, $r^2 > 0.98$), indicating that RIF release was governed by Fickian diffusion from the polymer matrix (Costa and Sousa Lobo, 2001).

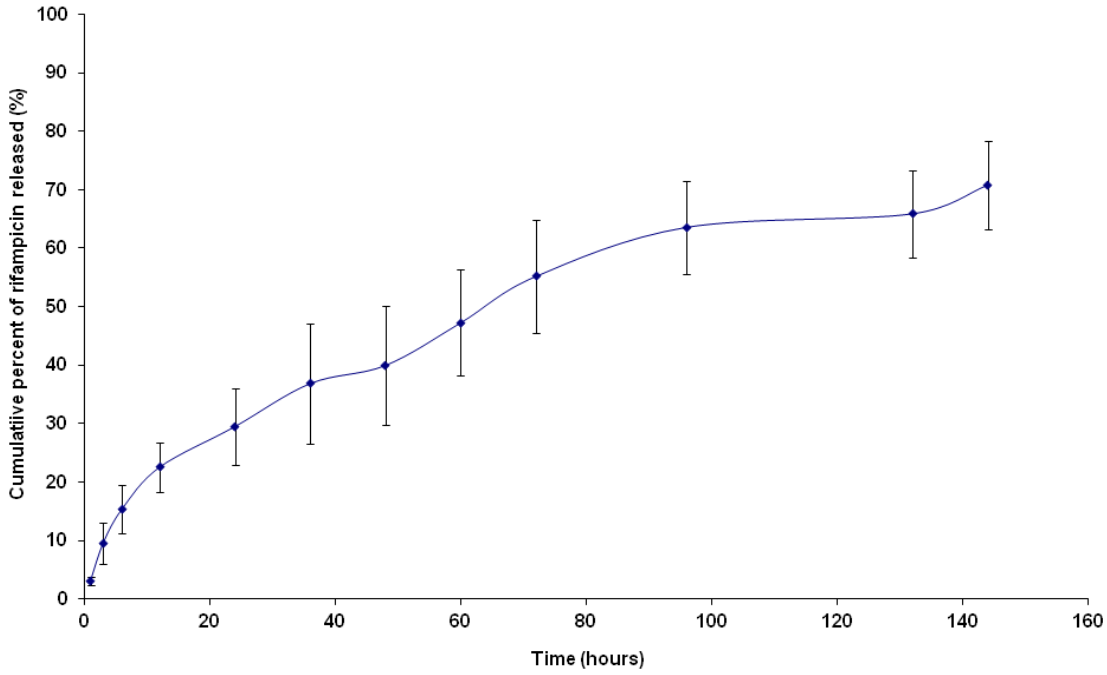

Figure 2. In vitro RIF release in PBS, pH 7.4, 37°C, from MS3 RIF-loaded microspheres (n = 3).

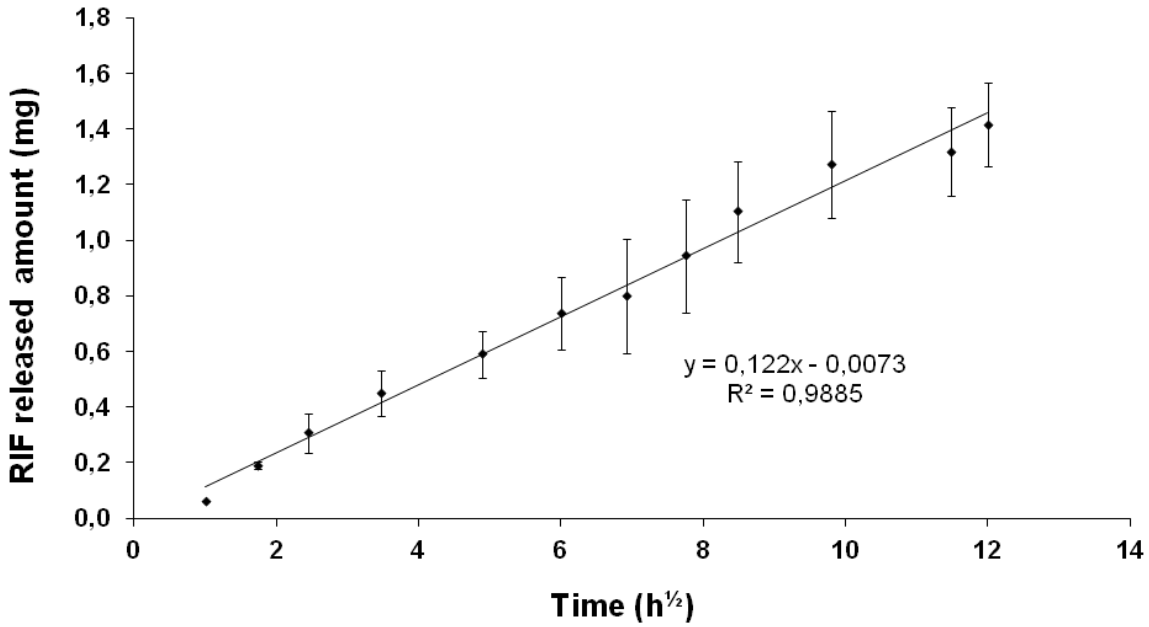

Figure 3. Higuchi plot of in vitro RIF release in PBS, pH 7.4, 37°C, from MS3 RIF-loaded microspheres (same data as in Fig. 2).

3.4. Aerodynamic behavior assessment of RIF-loaded microspheres

MMAD is a key factor of the aerosol lung deposition. An aerosolized particle of a diameter < 5 µm can reach deep lung (Suarez and Hickey, 2000). FPF therefore informs about respirable fraction, which is directly related to the amount of drug able to reach the deep lung (Sebti and Amighi, 2006). For RIF-MS prepared according to MS3 formula, MMAD and FPF values were found to be 4.5 µm and 52%, respectively. Despite an apparent porous structure which should reduce microsphere density and impact their aerodynamic properties (Rawat *et al.*, 2008), the MMAD was larger than the mean volume diameter (2.7±0.2 µm). This was attributed to an inefficient disaggregation of the RIF-MS during aerosolization.

3.5. Rifampicin uptake by alveolar macrophage

The RIF-MS uptake by *ex vivo* rat AM was evaluated after a 4-incubation qualitatively by imaging cells using optic microscope and quantitatively by internalized RIF amount determination using HPLC assay. Figure 4 is a representative micrograph of MS internalized into AM showing that MS3 RIF-MS were located in the perinuclear area of the cells, in agreement with an internalization of the MS into the cells. AM intracellular levels of RIF were 0.17 ± 0.06 µg/10^5cells when the cells were incubated for 4 hrs with a RIF solution (78 µg of free RIF equivalent amount), which was similar to the uptake obtained with 200 µg of MS1 RIF-MS loaded with a 6.8% (w/w) RIF (i.e. carrying 14 µg RIF) (Figure 5). At a constant microsphere added amount, cell RIF uptake increased with RIF-MS drug loading, almost proportionally to the RIF loading. This trend was in agreement with the previous works of (Makino *et al.*, 2004). With MS3 RIF-MS (with 38.8% w/w of RIF load), intracellular levels of RIF were 1.21 ± 0.16 µg/10^5cells, which was 7-fold higher than with an equivalent amount of RIF brought as a solution, demonstrating the high efficiency of these microspheres to delivering RIF into AM. Finally, in order to differentiate between active cell internalization of RIF-MS and their passive adhesion onto the outer cell membrane, incubation of the cells with RIF-MS (MS3 formula) was carried out at 4°C for 4 hrs. The level of RIF uptake was found to be 0.15 ± 0.07 µg/10^5cells, which was 8 times lower than when cells where incubated at 37°C.

3.6. Cell toxicity

Toxicity of the RIF-MS (MS1, MS2 and MS3 formulae) was evaluated after 4 hrs incubation and compared to their equivalent amount of free RIF and to blank microspheres (Figure 6). Incubation with blank microspheres or with the three different RIF-MS resulted in a significant decrease in viability compared to control. RIF decreased the viability according to a concentration-dependant effect. There was no significant difference between RIF-MS and blank microspheres. There was no significant difference either between the two higher RIF concentrations and the RIF-MS or blank microspheres. This apparent absence of synergistic effect between RIF and microspheres may be attributed to the slow rate of RIF release from the RIF-MS (Figure 2), which probably maintained level of concentration of free RIF below the RIF toxic threshold within AM despite high RIF uptake (Figure 5). In other experimental conditions, surfactant-free or PVA-stabilized RIF-loaded PLGA microspheres were shown to have no apparent effect on viability of various macrophage cell lines over at least 4 hours (Hirota *et al*. 2010, 2007). The present viability results therefore calls for deeper toxicological investigations to assess safety of using sucrose palmitate as a microsphere-stabilizing agent.

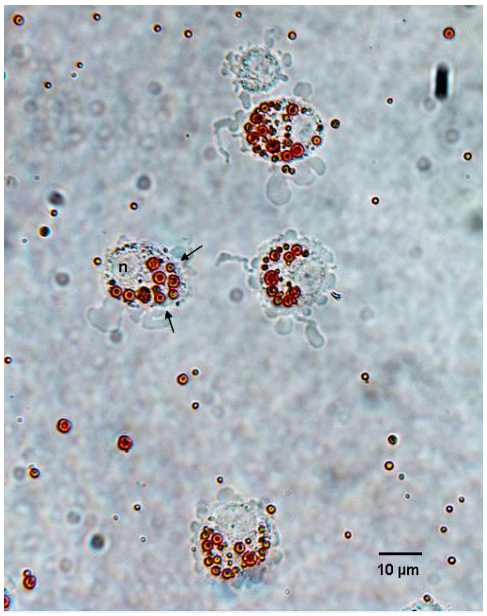

Figure 4. Bright field micrograph of MS3 RIF-loaded microspheres (arrows) internalized into alveolar macrophages (n: nucleus).

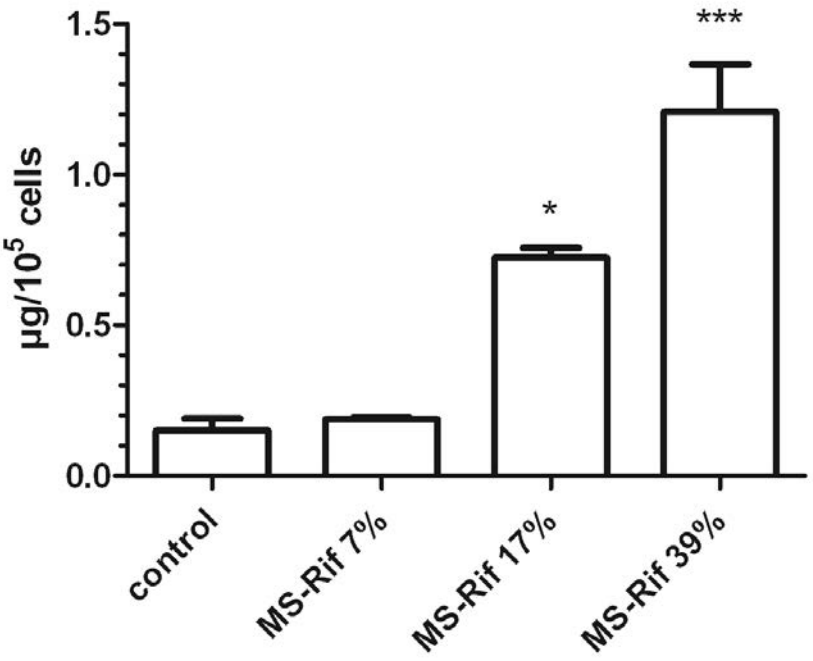

Figure 5. Alveolar macrophage intracellular concentrations of rifampicin after 4 hr incubation at 37°C with 78 µg of free RIF brought as a solution (Control) or with RIF-loaded microspheres (200 µg RIF-loaded microspheres MS1, MS2 or MS3 with respective RIF loading of of 6.8, 17.2 and 38.8% (m/m), i.e. 13.6, 34.4 and 77.6 µg). Conditions: $2.5x10^5$ cells/well, 1 mL culture medium volume per well. *p<0.05, ***p<0.001 vs. control.

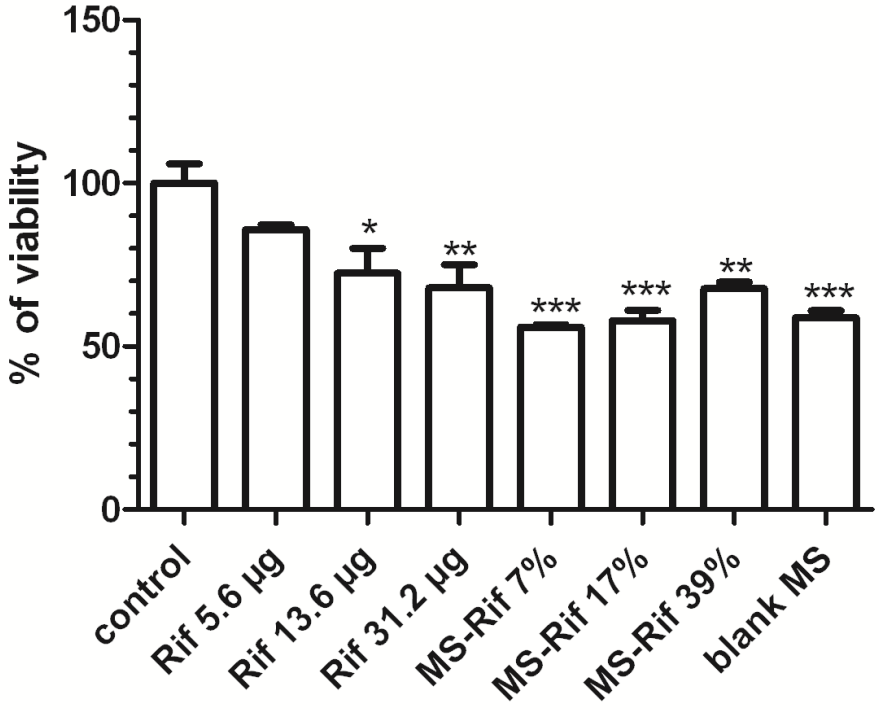

Figure 6. Viability of the alveolar macrophages after 4 hr incubation at 37°C with the culture medium alone (control), blank microspheres (blank-MS), RIF-loaded microspheres MS1, MS2 or MS3 (with respective RIF loading of 6.8, 17.2 and 38.8% (w/w)), or their equivalent amount of free RIF brought as a solution. Results are given as a percentage to the control which corresponds to the AM viability after a 4 hr-incubation alone. Conditions: 105 cells and 100 µl culture medium volume per well, 80 µg of blank or RIF-loaded microspheres. * p<0.1 vs. control.

4. Conclusion

Sucrose palmitate permitted to prepare sustained-release RIF-MS with high RIF loading and aerodynamic diameter adequate for lung administration as aerosols. RIF-MS were efficiently phagocytosed by *ex vivo* rat alveolar macrophages. Further toxicological studies are required for assessing safety of sucrose palmitate, before using this surfactant as a stabilizer alternative to PVA in the preparation of PLGA microspheres for lung delivery.

Acknowledgment

The authors wish to thank Mr. Emile Béré from ImageUP, University of Poitiers, for his technical assistance in electron microscopy.

References

Barrow, E.L., Winchester, G.A., Staas, J.K., Quenelle, D.C., Barrow, W.W., 1998. Use of microsphere technology for targeted delivery of rifampin to mycobacterium tuberculosis-infected macrophages. Antimicrob. Agents Chemother. 42, 2682-2689.

Becker, C., Dressman, J.B., Junginger, H.E., Kopp, S., Midha, K.K., Shah, V.P., Stavchansky, S., Barends, D.M., 2009. Biowaiver monographs for immediate release solid oral dosage forms: rifampicin. J. Pharm. Sci. 98, 2252-2267.

Costa, P., Sousa Lobo, J.M., 2001. Modeling and comparison of dissolution profiles. Eur. J. Pharm. Sci. 13, 123-133.

Doan, T.V.P., Couet, W., Olivier, J.C., 2011. Formulation and in vitro characterization of inhalable rifampicin-loaded plga microspheres for sustained lung delivery. Int. J. Pharm. 414, 112-117.

Doan, T.V.P., Olivier, J.C., 2009. Preparation of rifampicin-loaded plga microspheres for lung delivery as aerosol by premix membrane homogenization. Int. J. Pharm. 382, 61-66.

Dudley, M.N., Loutit, J., Griffith, D.C., 2008. Aerosol antibiotics: considerations in pharmacological and clinical evaluation. Curr. Opin. Biotechnol. 19, 637-643.

Díez, S., Tros de Ilarduya, C., 2006. Versatility of biodegradable poly(d,l-lactic-co-glycolic acid) microspheres for plasmid dna delivery. Eur. J. Pharm. Biopharm. 63, 188-197.

Gagnadoux, F., Leblond, V., Vecellio, L., Hureaux, J., Le Pape, A., Boisdron-Celle, M., Montharu, J., Majoral, C., Fournier, J., Urban, T., Diot, P., Racineux, J., Lemarié, E., 2006. Gemcitabine aerosol: in vitro antitumor activity and deposition imaging for preclinical safety assessment in baboons. Cancer Chemother. Pharmacol. 58, 237-244.

Higuchi, T., 1963. Mechanism of sustained-action medication. theoretical analysis of rate of release of solid drugs dispersed in solid matrices. J. Pharm. Sci. 52, 1145-1149.

Hirota, K., Hasegawa, T., Nakajima, T., Inagawa, H., Kohchi, C., Soma, G., Makino, K., Terada H., 2010. Delivery of rifampicin-PLGA microspheres into alveolar macrophages is promising for treatment of tuberculosis. J. Control. Release. 142, 339-346.

Hirota, K., Hasegawa, T., Hinata, H., Ito F., Inagawa, H., Kochi, C., Soma, G., Makino, K., Terada H., 2007. Optimum conditions for efficient phagocytosis of rifampicin-loaded PLGA microspheres by alveolar macrophages. J. Control. Release. 119, 69-76.

Jaafar-Maalej, C., Diab, R., Andrieu, V., Elaissari, A., Fessi, H., 2010. Ethanol injection method for hydrophilic and lipophilic drug-loaded liposome preparation. J. Liposome Res. 20, 228-243.

Koshkina, N.V., Waldrep, J.C., Roberts, L.E., Golunski, E., Melton, S., Knight, V., 2001. Paclitaxel liposome aerosol treatment induces inhibition of pulmonary metastases in murine renal carcinoma model. Clin. Cancer Res. 7, 3258-3262.

Leuchte, H.H., Schwaiblmair, M., Baumgartner, R.A., Neurohr, C.F., Kolbe, T., Behr, J., 2004. Hemodynamic response to sildenafil, nitric oxide, and iloprost in primary pulmonary hypertension. Chest. 125, 580-586.

Li, W., Das, S., Ng, K., Heng, P.W.S., 2011. Formulation, biological and pharmacokinetic studies of sucrose ester-stabilized nanosuspensions of oleanolic acid. Pharm. Res. 28, 2020-2033.

Makino, K., Nakajima, T., Shikamura, M., Ito, F., Ando, S., Kochi, C., Inagawa, H., Soma, G., Terada, H., 2004. Efficient intracellular delivery of rifampicin to alveolar macrophages using rifampicin-loaded PLGA microspheres: effects of molecular weight and composition of plga on release of rifampicin. Colloids Surf. B Biointerfaces. 36, 35-42.

Makino, K., Yamamoto, N., Higuchi, K., Harada, N., Ohshima, H., Terada, H., 2003. Phagocytic uptake of polystyrene microspheres by alveolar macrophages: effects of the size and surface properties of the microspheres. Colloids Surf. B Biointerfaces. 27, 33-39.

Meng, X., Yang, D., Keyvan, G., Michniak-Kohn, B., Mitra, S., 2011. Synthesis and immobilization of micro-scale drug particles in cellulosic films. Colloids Surf. B Biointerfaces. 86, 181-188.

Muttil, P., Wang, C., Hickey, A.J., 2009. Inhaled drug delivery for tuberculosis therapy. Pharm. Res. 26, 2401-2416.

O'Donnell, P., McGinity, J., 1997. Preparation of microspheres by the solvent evaporation technique. Adv. Drug Deliv. Rev. 28, 25-42.

Rawat, A., Majumder, Q.H., Ahsan, F., 2008. Inhalable large porous microspheres of low molecular weight heparin: in vitro and in vivo evaluation. J. Control. Release. 128, 224-232.

Rosca, I.D., Watari, F., Uo, M., 2004. Microparticle formation and its mechanism in single and double emulsion solvent evaporation. J. Control. Release. 99, 271-280.

Sansdrapa, P., Moës, A.J., 1993. Influence of manufacturing parameters on the size characteristics and the release profiles of nifedipine from poly(dl-lactide-co-glycolide) microspheres. Int. J. Pharm. 98, 157-164.

Sebti, T., Amighi, K., 2006. Preparation and in vitro evaluation of lipidic carriers and fillers for inhalation. Eur. J. Pharm Biopharm. 63, 51-58.

Shive, M., Anderson, J., 1997. Biodegradation and biocompatibility of pla and plga microspheres. Adv. Drug Deliv. Rev. 28, 5-24.

Suarez, S., Hickey, A.J., 2000. Drug properties affecting aerosol behavior. Respir. Care. 45, 652-666.

Suarez, S., O'Hara, P., Kazantseva, M., Newcomer, C.E., Hopfer, R., McMurray, D.N., Hickey, A.J., 2001. Respirable plga microspheres containing rifampicin for the

treatment of tuberculosis: screening in an infectious disease model. Pharm. Res. 18, 1315-1319.

Sung, J.C., Padilla, D.J., Garcia-Contreras, L., Verberkmoes, J.L., Durbin, D., Peloquin, C.A., Elbert, K.J., Hickey, A.J., Edwards, D.A., 2009. Formulation and pharmacokinetics of self-assembled rifampicin nanoparticle systems for pulmonary delivery. Pharm. Res. 26, 1847-1855.

Uchino, T., Lefeber, F., Gooris, G., Bouwstra, J., 2011. Physicochemical characterization of drug-loaded rigid and elastic vesicles. Int. J. Pharm. 412, 142-147.

Youan, B.C., Hussain, A., Nguyen, N.T., 2003. Evaluation of sucrose esters as alternative surfactants in microencapsulation of proteins by the solvent evaporation method. AAPS PharmSci. 5, E22.

Yüksel, N., Baykara, T., 1997. Preparation of polymeric microspheres by the solvent evaporation method using sucrose stearate as a droplet stabilizer. J. Microencapsul. 14, 725-733.

Conclusion générale

Dans cette thèse, nous avons projeté la lumière sur les récentes avancées de la nanotechnologie dans le domaine de l'antibiothérapie. Nous avons également contribué par des travaux de recherche originaux sur la vectorisation d'antibiotiques.

Les données récentes de la littérature scientifique montrent la supériorité des « nano-antibiotiques » par rapport aux antibiotiques non vectorisés. Grâce à la nanotechnologie, il serait possible de submerger, inhiber ou contourner la résistance bactérienne. Cette dernière se manifeste par de multiples stratégies, telle que la sécrétion d'une matrice extracellulaire complexe appelée « biofilm ». Dans cette matrice, les cellules bactériennes sont camouflées et protégées de l'action d'antibiotiques. Les nanoparticules peuvent faciliter la pénétration de l'antibiotique transporté à travers le biofilm pour accéder finalement à la cellule bactérienne. Certains types de nanoparticules, comme celles libérant de l'oxyde nitrique, exercent une activité « antibiofilm » propre.

L'imperméabilité de la membrane bactérienne et/ou l'efflux actif d'antibiotiques constituent d'autres stratégies de résistance que les nanoparticules se sont montrées capables de déjouer. La sécrétion d'enzymes destructrices qui désactivent les antibiotiques les plus efficaces est aussi une stratégie de résistance contre laquelle les antibiotiques peuvent être protégés grâce à la barrière physique que leur offrent les nanoparticules.

Les infections intracellulaires peuvent être considérées comme une forme de résistance où la bactérie se confine à l'intérieur des macrophages, à l'abri des « regards » du système immunitaire mais aussi loin de l'action des antibiotiques. Les nanoparticules, étant facilement repérables par le système immunitaire, peuvent être utilisées pour cibler les macrophages afin d'agir sur les bactéries intracellulaires. Nous avons vérifié cette hypothèse à travers nos travaux de recherche présentés dans cette thèse. Les nanoliposomes chargés en *S*-nitrosoglutathion se sont montrés capables de cibler les macrophages et d'y réaliser une concentration intracellulaire en NO 20 fois plus élevées par rapport à la molécule libre (non encapsulée). D'une façon similaire, les microsphères de rifampicine ont permis de réaliser des concentrations intracellulaires supérieures par rapport à la molécule non encapsulée et d'une manière quasi-proportionnelle à la teneur des microsphères en rifampicine.

Toutefois, l'évaluation des vecteurs développés sur une co-culture macrophages-bactéries n'a pas été réalisée. Cela constituera donc la suite logique de ces travaux.

N° d'identification :8010

TITRE

Apport de la nanotechnologie dans le domaine de l'antibiothérapie

Thèse soutenue le 02 octobre 2015

Par Roudayna DIAB

RESUME :

Le développement de vecteurs non viraux capables de piloter l'antibiotique et de franchir les barrières biologiques bactériennes ou celles de l'hôte, est une approche qui séduit de plus en plus de chercheurs dans le monde. Cette thèse associe une analyse des données de la littérature et des travaux de recherche originaux dans le but d'aborder quelques aspects de l'apport considérable de la nanotechnologie dans le domaine de l'antibiothérapie.

Le premier chapitre constitue une synthèse de 98 articles scientifiques traitant l'encapsulation d'antibiotiques dans des vecteurs non viraux, leurs mécanismes d'interactions avec les bactéries et leurs modes d'action pour contourner la résistance bactérienne. Le deuxième chapitre présente un travail original concernant l'élaboration des nanoliposomes chargés en *S*-nitrosoglutathion (GSNO), un donneur endogène de l'oxyde nitrique, comme une nouvelle thérapeutique antibactérienne. L'objectif principal de l'encapsulation est de réaliser une libération sélective du GSNO dans les macrophages afin de renforcer ses capacités de défense. Le troisième chapitre est aussi un travail original traitant le développement d'une poudre inhalable à base de microsphères polymériques chargées en rifampicine. L'objectif étant de cibler les macrophages, siège de l'infection intracellulaire causée par les mycobactéries.

MOTS CLES :

Antibiotiques, bactéries, barrières biologiques, ciblage, interactions, microsphères, nanoliposomes, nanoparticules, oxyde nitrique, résistance, rifampicine, vecteurs.

Directeur de thèse	Intitulé du laboratoire	Nature	
Professeur Raphaël DUVAL	**2 MIC Group, UMR CNRS 7565 SRSMC**	**Expérimentale**	**X**
		Bibliographique	☐
		Thème	**3**

Thèmes **1 – Sciences fondamentales** **2 – Hygiène/Environnement**
3 – Médicament **4 – Alimentation – Nutrition**
5 - Biologie **6 – Pratique professionnelle**